UNIVERSIDADE
BEIRA INTERIOR

Performance Optimisation of a Geared Turbofan with Intercooler and Regenerator

Liliana da Fonte Domingues

Dissertação para obtenção do Grau de Mestre em
Engenharia Aeronáutica
(mestrado integrado)

Orientador: Prof. Doutor Francisco Miguel Ribeiro Proença Brójo

janeiro de 2022

Dedicatória

To my parents, Luciano and Maria da Conceição, my brother, Ricardo, and especially to my grandmother, Maria Domingas, who saw me start this journey of my life, but with great sorrow, she is not here physically to watch me end it.

"Our doubts are traitors, and make us lose the good we oft might win, by fearing to attempt."

William Shakespeare

Acknowledgements

Firstly, I would like to express my sincere gratitude to my supervisor, Professor Francisco Miguel Ribeiro Proença Brójo, for the valuable support, guidance and availability showed since the first day.

I would like to thank my friends, who over these years shared and experienced with me unforgettable moments, for their friendship and support. Moreover, I would like to thank especially to my dearest friend, Filipa Balça, for always being there for me.

Last but not least, I would like to thank my parents and my brother for their unconditional support, encouragement and dedication throughout this journey.

Resumo

Com o enorme crescimento do tráfego aéreo mundial, muitas vozes se erguem a exigir medidas urgentes contra as alterações climáticas. Portanto, as preocupações ambientais estão a desafiar e impulsionar o setor da aviação a adotar estratégias inovadoras e desenvolvimentos promissores. Alguns desses avanços, no campo da propulsão, visam motores mais eficientes, com menor consumo de combustível, menores emissões de gases poluentes e menor ruído.

Dito isto, a contínua evolução por motores aeronáuticos mais amigos do ambiente, poderá passar pela introdução de permutadores de calor, de modo a responder aos desafios do futuro. Assim sendo, esta dissertação tem como principal objetivo a implementação de um intercooler e/ou regenerador num turbofan, para entender o comportamento do motor, bem como a influência destes dois componentes nos parâmetros de desempenho. Mais concretamente, pretende-se avaliar a possibilidade de diminuir o consumo do combustível sem comprometer a tração. Para que isto seja possível, um motor moderno turbofan com caixa redutora (GTF) é utilizado como motor base, pois este tipo de motor permite atingir valores de razão de bypass elevados, bem como melhorar a eficiência dos componentes e pesar menos que um turbofan convencional, o que implica que o peso extra dos permutadores de calor tenha menos impacto.

Nesta dissertação vários parâmetros do motor, como razão de bypass, razão de pressão da fan, razão de pressão do compressor e temperatura de entrada da turbina, são variados e seus impactos nos parâmetros de desempenho analisados (tração específica e consumo específico de tração) para cada configuração. Para além deste estudo paramétrico, realiza-se também a otimização do desempenho de todas as configurações - GTF convencional, GTF com intercooler, GTF com regenerador e GTF com intercooler e regenerador – com o auxílio de um algoritmo genético disponível no software MATLAB.

Os resultados revelaram que a configuração convencional é a melhor opção, na medida em que é a que apresenta os valores mais baixos de TSFC para um dado valor de tração especifica. No entanto, se a principal preocupação é produção de energia e custos associados com a produção e a manutenção, do que custos de combustível então a configuração com apenas o intercooler apresenta-se como uma escolha interessante, pois permite trações específicas elevadas a baixas temperaturas de entrada na turbina. Por fim, caso se verifique

uma tendência no aumento da temperatura de entrada na turbina, então o efeito do regenerador é mais significativo, o que muito provavelmente conduzirá a configuração com regenerador a ter valores de TSFC inferiores aos da configuração convencional para o mesmo valor de tração específica.

Palavras-chave

Motor de aeronave, turbofan com caixa redutora, bypass, ciclo termodinâmico, intercooler, regenerador, estudo paramétrico, otimização, desempenho

Abstract

With the enormous growth of the worldwide air traffic, many voices rise demanding urgent measures against climate changes. Therefore, the environmental and climate concerns are challenging and promoting the aviation sector to adopt innovative strategies and promising developments. Some of these advances, in the propulsion field, aim for more efficient engines that are less fuel dependent and that pollute less (noise and emissions).

In this context, the continuous evolution for even more eco-friendly aeroengines, includes the proposal of introducing heat exchangers to meet the challenges of the future. Thus, this dissertation focuses on implementing an intercooler and/or a regenerator in a turbofan to understand the engine's behaviour, as well as the influence of these two components in the performance parameters, more accurately, to assess the possibility of decreasing fuel consumption without jeopardizing thrust. To accomplish all this, a modern geared turbofan is used as the baseline engine, because this type of engine allows to reach high values of bypass ratios, as well as improves component efficiency and it weighs less than a conventional turbofan, so the extra weight from the heat exchangers have less impact.

Furthermore, several engine parameters, such as bypass ratio, fan pressure ratio, compressor pressure ratio and turbine inlet temperature, are varied and theirs impacts on the performance parameters analysed (specific thrust and thrust specific fuel consumption) for each configuration. Besides the parametric study, a performance optimisation of all the four configurations – conventional GTF (Geared Turbofan), GTF with intercooler, GTF with regenerator and GTF with intercooler and regenerator - is done with the help of a genetic algorithm provided by the MATLAB software.

The results showed that the conventional configuration is the best option, because it was the configuration with the lowest values of TSFC for a given specific thrust. Nevertheless, if the main concern is power production, production and maintenance costs than fuel costs, then the configuration with only the intercooler might be an interesting option, because it reached high values of specific thrust at lower turbine inlet temperatures. Additionally, if the turbine inlet temperature increases, then the regenerator effect is more pronounced, which might result in lower values of TSFC than the ones of the conventional configuration for the same amount of specific thrust.

Keywords

Aircraft engine, geared turbofan, bypass, thermodynamic cycle, intercooler, regenerator, parametric study, optimisation, performance

Contents

List of Figures

List of Tables

Nomenclature

C	Velocity	m/s
C_0	Flight velocity	m/s
c_{p_c}	Specific heat at constant pressure for cold air	$J/(kg \cdot K)$
c_{p_h}	Specific heat at constant pressure for hot gases	$J/(kg \cdot K)$
F	Thrust	N
F_s	Specific thrust	$(N \cdot s)/kg$
f	Fuel to air ratio	
$\dot{m}$	Mass flow rate	m/s
P	Pressure	N/m^2
Q_{hv}	Fuel lower heating value	J/kg
R	Specific gas constant	$J/(kg \cdot K)$
s	Specific entropy	$J/(kg \cdot K)$
T	Temperature	K
TIT	Turbine Inlet Temperature	K
$TSFC$	Thrust specific fuel consumption	$Kg/(N \cdot h)$
v	Specific volume	m^3/kg
$\dot{W}$	Work	J

Greek Symbols

β	Bypass ratio
γ	Specific heat ratio
Γ	Data type of elements
Δ	Variation

η	Efficiency
π	Pressure ratio
Υ	Scaling function
Φ	Chromosome decoding function
Ψ	Objective Function

Subscripts

a	Air
c	Cold air
CC	Combustion chamber
d	Admission
f	Fuel
F	Fan
gb	Gearbox
h	Burned gases
HPC	High-pressure compressor
HPT	High-pressure turbine
hv	Heating value
LPC	Low-pressure compressor
LPT	Low-pressure turbine
m	Mechanical spool
n	Nozzle
O	Overall
p	Constant pressure
s	Specific

0	Free stream
2	Admission
3	Fan outlet
3.1	Intercooler exit
4	LPC outlet
4.1	HPC inlet
5	HPC outlet
5.1	Combustion chamber inlet
6	Combustion chamber outlet
7	HPT outlet
8	Hot nozzle duct
8.1	Regenerator exit
9	Hot nozzle outlet
10	Cold nozzle outlet

Acronyms and abbreviations

ACARE	Advisory Council for Aviation Research and Innovation in Europe
ADP	Aerodynamic Design Point
BPR	Bypass Ratio
CAEP	Committee on Aviation Environmental Protection
CC	Combustion Chamber
CMC	Ceramic Matrix Composite
CPR	Compressor Pressure Ratio
CROR	Counter Rotating Open Rotor
CRTF	Contra Rotating Turbo Fan

DDTF	Direct Drive Turbofan
DOC	Direct Operating Cost
EA	Evolutionary Algorithm
EC	Evolutionary Computation
EI	Emission Index
EIS	Entry In Service
EVA	EnVironmental Assessment
FPR	Fan Pressure Ratio
GAs	Genetic Algorithms
GESTPAN	GEneral Stationary and Transient Propulsion ANalsysis
GOR	Geared Open Rotor
GTF	Geared Turbofan
HPC	High-pressure compressor
HPT	High-pressure turbine
IC	Intercooler
ICAO	International Civil Aviation Organization
IPC	Intermediate Pressure Compressor
IR	Intercooled Regenerative
IRA	Intercooled Recuperative Aeroengine
ISA	International Standard Atmosphere
JAEC	Japanese Aero Engines Corporation
LEAP	Leading Edge Aviation Propulsion
LP	Low Pressure
LPC	Low-pressure compressor
LPT	Low-pressure turbine
LTO	Landing and Take Off
MATLAB	Matrix Laboratory

MOO	Multi Objective Optimisation
MOP	Multi Objective Problem
MTOW	Maximum Take-Off Weight
MTU	Motoren und Turbinen Union
NEO	New Engine Option
NEWAC	New Aero Engine Core concepts
NPSS	Numerical Propulsion System Simulation
OPR	Overall Pressure Ratio
PW	Pratt & Whitney
SAGE	Sustainable and Green Engines
SFC	Specific Fuel Consumption
SLS	Sea Level Static
TBC	Thermal Barrier Coating
TIT	Turbine Inlet Temperature
TSFC	Thrust Specific Fuel Consumption
UHBR	Ultra High Bypass Ratio
VHBR	Very High Bypass Ratio
VITAL	EnVIronmenTALly aero-engine
WATE	Weight Analysis of Turbine Engines
WeiCo	Weight and Cost

Chapter 1

Introduction

The present dissertation focuses on analysing the viability, in terms of performance, of incorporating different heat exchangers in a modern geared turbofan at cruise phase. Therefore, the current chapter gives an initial introduction to this subject.

The first section enlightens the reader towards the reasons behind the choice of such subject, the second section exposes the objectives established for this work and the third and last section displays the summarized structure of this document.

1.1 Background and Motivation

Since the first turbofan entered service in the fifties, it has shown to be the most reliable engine ever developed [1]. Nowadays, most modern military and civil aircrafts are powered by some form of turbofan engine, because such engine is more efficient (propulsively) than a turboprop or turbojet engine for high subsonic flight speed [2].

The aviation industry underwent a rapid development in recent decades, and it is currently showing no signs of stopping. In a projection done by ICAO about the expected number of commercial aircrafts flying in 2036, the number 47500 was pointed out, and more than 44000 (94%) aircraft will be new generation technology [3].

It is well established that due to the high growth in air traffic, public environmental awareness increased, mainly because the exhaust gases that leave the gas turbine have a serious negative impact on the environment. To diminish the ecological footprint left by the aviation industry, stringent environmental measures demanding emissions, noise and fuel consumption reduction have been put in action [4]. Although, the fuel consumption must be reduced because of its impact on the environment, it is also desirable from the airline companies' perspective, because they want to minimise the direct operating costs in order to be more profitable.

Thus, engine manufacturers have been searching for innovative techniques that result in more reliable, lightweight and fuel efficient, as well as environmentally friendly (low NO_x and CO_2 emissions and low noise) engines [5]. Therefore, next generation of turbofan

engines will burn less fuel. This can be achieved by reducing engine weight, size, and thrust specific fuel consumption (TSFC) [6, 7]. This last one, TSFC, is an efficiency factor used by engineers to identify if an engine is fuel efficient, i.e., a low value of TSFC means that the engine is fuel efficient. A reduction in TSFC could be obtained by improving thermal and propulsive efficiencies and components efficiencies [6, 7].

On one hand, to improve thermal efficiency, the basic thermodynamic cycle needs to be altered or the overall pressure ratio (OPR) and turbine inlet temperature (TIT) increased [7]. Nevertheless, a further increase of OPR and TIT is limited by maximum material temperatures and increasing NO_X emissions.

On the other hand, to achieve a higher propulsive efficiency, the exhaust velocity has to reduce, which means that the bypass ratio needs to increase, as well as the fan diameter. This latter aspect leads to a heavier and sizeable engine that produces more drag and to problems related with ground clearance. So, an improvement on the propulsive efficiency needs to be accompanied by a development on lightweight fan and downsizing of the core [8].

By increasing the bypass ratio (BPR), the speed incompatibility between the fan and the low-pressure spool aggravates, because the fan is more efficient operating at a lower speed, whereas the LPC and the LPT prefer to operate at higher speeds [8]. This contradiction uncovers the problem of incompatibility of spool speed that becomes unfavourable for BPR above 10 [9]. To deal with this issue, a change in the conventional turbofan engine design was done. This consisted of a fan drive gear system that de-couples the fan from the rest of the low-pressure spool, which allows for the fan and the rest of the low-pressure spool to revolve at optimum rotational speeds. This engine is called geared turbofan [6, 8]. Moreover, the introduction of a gearbox on a turbofan allows for the future aeroengines to have a BPR above 10, which results in lower fan noise, higher propulsive and component efficiencies, and reduction of engine weight [8].

Besides the reduction gear system, that allows a UHBR, there are new proposals aiming to meet the challenges of the future aeroengines. Some of these proposals consist in introducing changes on the basic thermodynamic cycle by adding an intercooler and/or regenerator. The integration of heat exchangers will theoretically lead to a higher thermal efficiency and, therefore, a reduction in fuel consumption.

In this context, this dissertation is focused on incorporating on a modern geared turbofan engine different heat exchangers (intercooler and regenerator) and evaluate whether the

new configurations are viable, in terms of fuel consumption and thrust production, when compared with each other and with the conventional geared turbofan.

1.2 Objectives

The main goal of the present dissertation is to assess the viability of incorporating on a two-spool geared turbofan with high bypass ratio, in current operation, an intercooler and/or a recuperator. In this sense, these new configurations (with heat exchangers) and the conventional one are evaluated and compared, in order to verify if they bring advantages, in terms of fuel consumption reduction without jeopardizing the amount of produced thrust.

1.3 Overview

The present dissertation is organized in eight chapters, including this one, which provides the context and the motivation, with a view in the current and future trend of aeroengines, the objectives that served as base for the subject addressed, and the overview, which refers to how this dissertation is organized.

The second chapter is dedicated to the review of the bibliography regarding geared turbofans, heat exchangers applied in turbofans and to several environmentally friendly programmes that use these technologies.

The third chapter exhibits the scientific and theoretical foundations that sustain this study. Firstly, the gas turbine concept is introduced, followed by its ideal and real thermodynamic cycle. Then, the alternative thermodynamic cycles (intercooling and regeneration) are described and a bridge with the gas turbine is established. Additionally, a review about the turbofan engine is presented, which includes its evolution, its operation method, and the different types of turbofan engines there are. To finish, the importance of the bypass ratio in the aeronautical sector is discussed.

The fourth chapter gives an overview related to the geared turbofan history, evolution and advantages. Moreover, the engine that serves as baseline in this dissertation is also presented, followed by its specifications and the conditions, in which this study is conducted.

The fifth chapter is dedicated to the parametric study, where the assumptions made are presented, as well as the mathematical models for all the four engine configurations. Additionally, the results obtained in this study are showed.

In the sixth chapter, the second part of this dissertation is for the first time addressed. Therefore, a theoretical overview of the evolutionary computational theory is given. Furthermore, is also presented the type of algorithm used in the optimisation study.

The seventh chapter introduces the concepts associated with the multi objective optimisation performed. Additionally, the chosen setup is presented, followed by the optimisation results.

Finally, the last chapter (Chapter 8) summarizes the main conclusions of this dissertation and presents future work suggestions.

Chapter 2

Literature Review

This chapter is dedicated to the review of some studies concerning turbofan engines, with particular emphasis on geared turbofan engines and on heat exchangers applied in aeroengines. Moreover, are also presented some eco-friendly programmes that developed technologies to diminish the environmental impact of air traffic, with special focus on the technologies previously mentioned.

2.1 The Geared Turbofan

For the last 55 years turbofan engines proved their powerful contribution in making the commercial aviation a success. The responsible for this was the constant evolution that these underwent throughout the years to satisfy the market needs. In this context, technical innovations to the turbofan engine were accomplished in the sense of improving its performance, reliability, safety, and of course, noise and emissions [10].

In the pursuit for cleaner engines, the manufacturers are recovering and upgrading an old technology, gearbox, which was only used until a few years ago in business jets.

2.1.1 Relevant Studies

To highlight the advantages and limitations of a geared turbofan versus other engines architectures several works were conducted throughout the years, and some of them are here presented.

Humhauser et al. (2005) [10] stated that in the future, it is expected engines with better values of thermal, propulsive and components efficiencies and noise, since all developments point in that direction. To enhance the propulsive efficiency and reduce the engine noise, the jet velocity and fan tip speed needs to be reduced, which can be achieved by increasing the bypass ratio. To augment the thermal efficiency, Humhauser et al. (2005) [10] implies increasing the overall pressure ratio and turbine inlet temperature. This enhances an even

more compact engine core, which in terms of weight translates into a reduction that can counteract the weight penalties inflicted by enlarging BPR and fan diameter.

In order to achieve such high values of BPR and OPR, the authors (2005) [10] suggest the introduction of a fan drive gear system, since the reduction gear allows the fan to revolve at a lower speed (optimum speed), which translates into less noise produced by the fan (Figure 2.1). Moreover, the low-pressure spool also rotates at his optimum speed (higher speeds), which means that the number of stages for the LPT and the LPC are less (Figure 2.1).

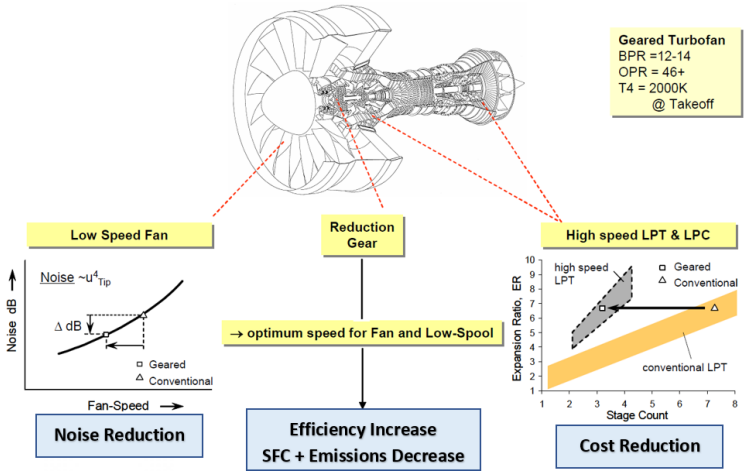

Figure 2.1: The Geared Turbofan concept [10].

Larsson et al. (2011) [11] optimised a conventional (DDTF) and a geared turbofan engine by minimising CO_2 emissions for a certain aircraft mission (take off and cruise).

In order to learn which engine configuration during the mission had the lowest fuel consumption, a multidisciplinary preliminary design process was performed. Thus, a preliminary design and a performance analysis of both the aircraft and the engines were conducted using a selection of various generic tools (GESTPAN, WeiCo and Isight). This led to results of nacelle drag, engine dimensions and weight.

After the preliminary design of the engines, the optimisations were done by changing different parameters: BPR, FPR and OPR.

Although the optimal bypass ratio between the two engines did not differ a lot and the OPR was the same (Table 2.1), the optimisation results showed a 3.0% reduction of fuel burn for the GTF.

Table 2.1: Performance values of final engine configurations [11].

Parameters	DDTF	GTF
BPR	12.5	13.5
TIT [K]	1850	1850
FPR	1.47	1.45
LPC pressure ratio	1.45	2.5
HPC pressure ratio	18.76	11.03
OPR	40	40
Mission fuel burn [%]	Ref.	-3.0

By examining Table 2.1, more concretely the DDTF, the authors realized that since the LPC was not rotating at its optimum speed, it did not contribute significantly to the OPR. So, the pressure ratio for the HPC had to be higher, which translated on a HPC with more stages and heavier.

Regarding the engine weight and its dimension (Table 2.2), Larsson et al. (2011) [11] concluded that the main contributor for the difference between these two engines physic characteristics was stage count (Table 2.2), which, in practical terms, translated into a DDTF 0.40 m longer and 220 kg heavier than the GTF.

Table 2.2: Dimensions, weight and number of stages of the optimised engines [11].

Parameters	DDTF	GTF
Fan diameter [m]	1.84	1.87
Fan weight [kg]	888	906
LPC stages	4	3

(continued on next page…)

Table 2.2: (continued)

Parameters	DDTF	GTF
LPC weight [kg]	66	55
HPC stages	9	6
HPC weight [kg]	87	48
HPT stages	2	2
HPT weight [kg]	66	78
LPT stages	8	3
LPT weight [kg]	555	221
LP spool weight [kg]	44	18
Gearbox weight [kg]	N/A	170
Total engine weight [kg]	3100	2880
Nacelle length [m]	3.8	3.4

The authors (2011) [11] noticed that as the BPR increased, the fuel consumption decreased. However, this had a negative effect on the number of LPT stages, which increased. This growth of LPT stages was more noticeable for the DDTF. So, this scenario led the authors (2011) [11] to state that is preferable to have a DDTF with a BPR lower than the optimal, and consequently, a higher fuel consumption than having a DDTF with optimal BPR and higher LPT stages, because the maintenance and manufacturing costs due to high part count would outweigh the fuel costs.

Since the GTF congregates on itself a low fuel consumption, lightweight and higher component efficiencies when compared to a conventional turbofan, Larsson et al. (2011) [11] think the GTF is a strong candidate for future aeroengine applications.

Guynn et al. (2009) [12] carried a series of analytical studies that consisted in exploring the benefits, in terms of overall performance and noise, of incorporating on a single-aisle

transport aircraft airframe model (B737/A320) different configurations of advanced ultra-high bypass ratio (UHBR) turbofan engines.

In this study, the authors [2009) [12] considered the fan pressure ratio, which is inversely proportional to the bypass ratio, as the most important parameter.

The characteristics of the engines used in this analysis had to be consistent with the propulsion technology and materials available for 2015 and similar to the ones expected to be applied on advanced single-aisle transport aircrafts (B737/A320). Bearing this in mind, the authors (2009) [12] came up with a baseline engine architecture that consisted of a two-spool, separate flow turbofan.

Since 48 engine/airframe combinations were analysed for performance and noise, different variations were made, which included: the fan drive approach (geared or direct), the fan pressure ratio, the type of fan nozzle (fixed or variable geometry), the overall pressure ratio, the design Mach number, and the low spool – high spool compression work split. This last variation means that the "low work" engine has a lower pressure increase through the low-pressure compressor, when compared to the "high work" engine, but a higher pressure increase through the HPC.

All the 48 combinations were divided into three spirals (16 combinations for each). For a given spiral, the engines were all analysed for the same ADP (Mach number, altitude and thrust) and OPR. The ADP selected represented a top-of-climb (TOC) condition for the airframe. Moreover, for each specific engine, to achieve the thrust required at ADP, the inlet mass flow was calculated individually.

Guynn et al. (2009) [12] had in consideration that low FPR engines suffer from a greater thrust lapse (available thrust decreases more rapidly with increase in aircraft speed) than high FPR engines. This means that the former engines were operated at higher temperatures to achieve the thrust required at ADP. Despite the operating temperatures for low fan pressure engines did not reach the maximum allowed temperature for the materials considered, they, indeed, reduce the life expectation of the engine hot section and reduce the number of flight hours between maintenance cycles.

The authors (2009) [12] analysed the engines cycles by using the numerical tool called Numerical Propulsion System Simulation (NPSS). To estimate the engines weight, they used the code WATE and to estimate NO_X emissions they used a correlation created by NASA.

Returning to the spirals, on the first one, all the engines had the same overall pressure ratio (32), which coincides with the one found on the engine used on the Boeing 737 and Airbus

A320, the CFM56. On the second set of analyses, the OPR was increased to 42, which led to some changes on the pressure ratios of the LPC and HPC. The only difference between the third spiral and the second was the Mach number that was reduced from 0.8 to 0.72. This reduction occurred, because due to environmental and economic pressure, the airlines are willing to compromise productivity (speed) in exchange of reducing fuel consumption.

Guynn et al. (2009) [12] concluded that the optimum engine FPR depends on the metric of interest, baseline engine architecture and assumptions. To minimise the ramp weight, the FPR has to be higher, however, if the metric of interest is reducing fuel consumption the engine should have a FPR of approximately 1.6. To reduce noise and NO_X emissions per LTO cycle, a fan with a lower pressure ratio is more desirable.

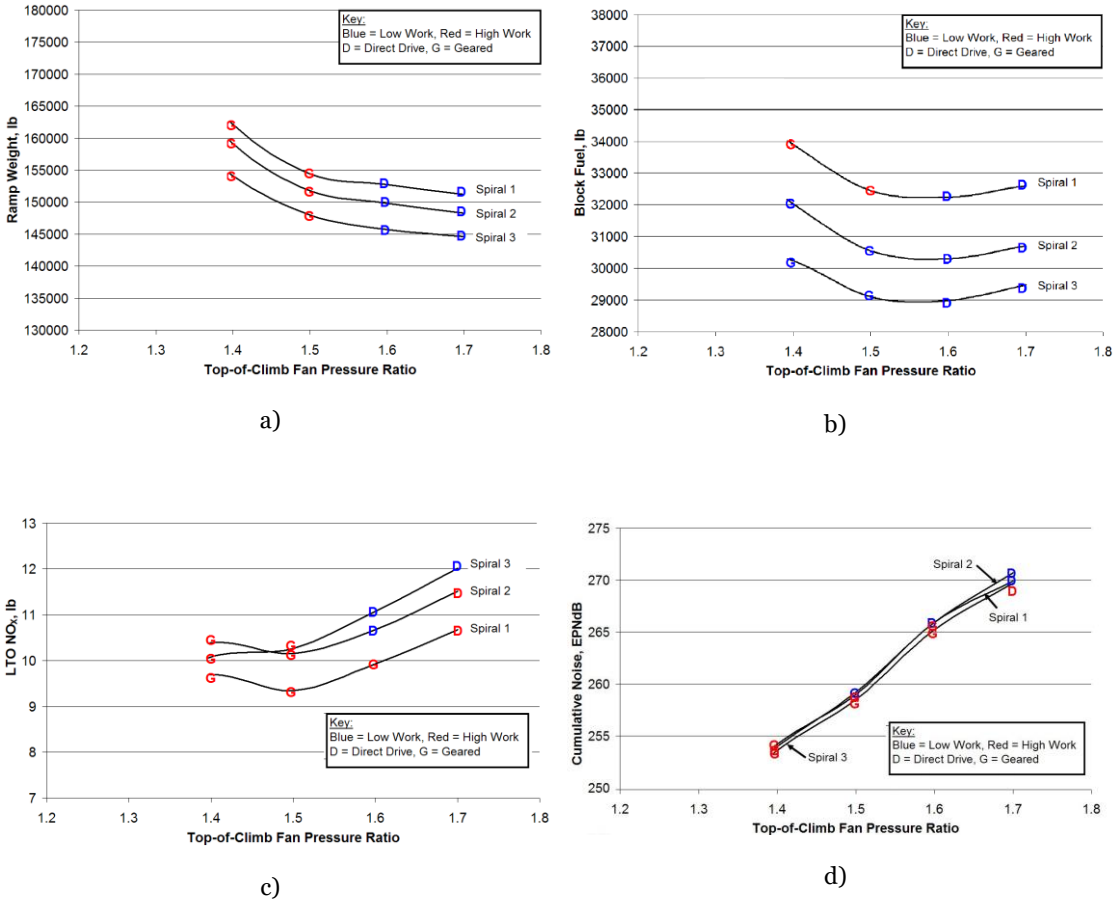

Figure 2.2: Variation of metrics of interest with fan pressure ratio: a) ramp weight; b) block fuel; c) NO_x per LTO cycle; d) noise [12].

Even though the OPR and the Mach number varied, the showed tendency of the ramp weight, fuel consumption, NO_X emissions and noise with FPR for each spiral was not affected (Figure 2.2). Therefore, the engine that revealed better results in terms of:

- Weight was the low work, direct drive engine with a FPR equal to 1.7;
- Fuel efficiency was the low work, direct drive engine with a FPR equal to 1.6;
- NO_X emissions per LTO cycle was the high work, geared engine with a FPR equal to 1.5;
- Noise was the high work, geared engine with a FPR equal to 1.4.

Considering all the metrics of interest in this study showed in Figure 2.2, the geared turbofan provided better results than a direct drive engine for FPR below 1.5 (roughly BPR>13). Above that, the direct drive engine was the preferable one. Moreover, the authors (2009) [12] reached the conclusion that if the design goal was to minimise airport area environmental impacts, then the geared engine would unquestionably be the best choice.

In order to understand the main differences in terms of design parameters between conventional and geared turbofans, Kurzke (2009) [13] developed a comparison study using the Gas Turb software.

All the engines were two-spool, analysed for the same take- off conditions (altitude, Mach number and temperature) and had to generate the same amount of thrust (103 kN).

For the same BPR (10), the fact of applying a reduction gear allowed to reduce the number of stages of both the LPC (from 7 to 2) and the LPT (from 9 to 3). This revealed the biggest advantage from the author's perspective of the geared turbofan when compared to the conventional. However, these parts are much more challenging to make than those of a conventional turbofan.

While the LPT pressure ratio was 5.9 for both the engines, the fan drive gear system reduced LPT stage loading and increased the isentropic efficiency from 92.8 (DDTF) to 93.4% (GTF). Moreover, the author (2009) [13] came across a reduction on the LPT spool torque from 77 (DDTF) to 27 kN·m (GTF).

Despite both engines had similar values of take-of thrust specific fuel consumption, the engine with the lowest TSCF was the GTF with a BPR of 14. Also, this geared engine had the same number of LPC and LPT stages as the one with a BPR of 10. So, it was possible to reduce fuel consumption and increase BPR, without adding more stages.

In another study, Larsson et al. (2011) [14] carried a multidisciplinary analysis, in which an ultra-high bypass ratio geared turbofan was compared to a geared open rotor (GOR) engine, with the level of technology expected in the year 2020.

For a given mission, both engines were analysed to find the specific thrust that minimises block fuel and the cleaner engine.

This study covered many types of analysis, such as engine performance, weight and dimensions, aircraft performance and design, emissions, and direct operating costs.

Regarding the engine configurations, the GTF was a two-spool turbofan with a conventional gearbox located between the fan and the LPC. The open rotor had a contra-rotating pusher configuration with the core of a two-spool turbojet. Moreover, the propulsor consisted of a free power turbine that drove two contra-rotating propellers with swept blades. The planetary gear box was placed between the free power turbine and the two propellers.

The authors (2011) [14] stated that to minimise block fuel there needed to be a compromise between propulsive and thermal efficiencies, engine weight and nacelle drag.

After the optimisation, the results regarding fuel consumption, weight, and costs for both engines were presented (Table 2.3). To achieve these results, a conceptual design tool called Weico was used with a code named EVA, which was developed in another work ([15]).

Table 2.3: Comparison of the optimisation results of the two geared engines at cruise conditions [14].

Parameter	GTF EIS 2020	GOR EIS 2020
Flight Level	350	350
Mach number	0.75	0.75
Net thrush [kN]	18	18
Specific fuel consumption [%]	Ref.	-14
Engine installed weight [%]	Ref.	11
Direct operating cost [%]	Ref.	-6

From the fuel saving perspective, the geared open rotor had a significant reduction (14%) in SFC, and a consequent decrease in CO_2 emissions, than the geared turbofan. Nevertheless, considering the weight of each component present in the engine, the geared open rotor appeared to be heavier (11%) than the geared turbofan. The main contributor for this, were the propellers and its associated structural components, and the gearbox. For the GTF the main weight contributor was the nacelle. Moreover, Larsson et al. (2011) [14] concluded that the GOR had 6% lower direct operating costs than the GTF at current fuel prices. In this

sense, if the fuel price continuous to rise, then the impact of fuel consumption on the DOC will be even higher, and this means that the open rotor configuration will be an even more attractive option. However, the technological risks involved in introducing new technology into the market need to be overcome.

Becker et al. (2013) [16] carried out a comparison study between three engine concepts. The first one consisted of a baseline turbofan that used the technology available in 2011. The other two concepts consisted of a geared turbofan and a counter rotating open rotor (CROR). To these two engines the same level of technology was applied (component efficiencies and cooling technology of the core), which consisted in the technology level expected in 2025.

Regarding the engine layouts, the baseline engine was a two-spool mixed flow turbofan similar to the IAE-V2500-A5. The open rotor was a counter rotating aft mounted three-spool pusher with a planetary gearbox that connected the free power turbine to the propellers. The GTF was a two-spool geared turbofan. Each engine was designed to be placed on a baseline civil aircraft for 150 passengers similar to the A320.

To assess the benefits of the novel engine configurations, the authors did a numerical optimisation of the concepts for a set of discrete operating points (cruise condition, top of climb and end of field condition). Since the most important flight condition in regard of fuel consumption is the cruise condition, then it was chosen as the master design point.

In order to capture the optimum solution in cruise fuel efficiency for the GTF and the CROR, some specific and independent variables were modified. For the GTF those parameters were LPC and HPC pressure ratios, TIT and BPR, whereas for the CROR the set of parameters was the same as on the GTF except the BPR.

After the optimisation study of both the engines at cruise conditions (flight Mach number of 0.78 and altitude of 10668 km), the following results were obtained.

Table 2.4: Optimisation results for GTF and CROR at cruise conditions [16].

Parameter	GTF EIS 2025	CROR EIS 2025
OPR	45.98	43.43
LPC pressure ratio	3.02	5.57

(continued on next page…)

Table 2.4: (continued)

Parameter	GTF EIS 2025	CROR EIS 2025
HPC pressure ratio	11.4	7.9
BPR	12.2	~90
TSFC [g/kN·s]	13.67	12.11
Nacelle wetted area [m^2]	31.10	19.30
Engine weight [kg]	3201	4097

By analysing the results, the GTF had a BPR of 12.2 while the CROR had a BPR of approximately 90. This translates on a 13% less consume of fuel from the CROR in relation to the GTF. When comparing the TSFC of the novel engines to the conventional one, the GTF showed a 20% reduction and the CROR a 36% reduction.

The GTF had a weight advantage of 28% in comparison with the CROR. To overcome this penalty in weight, the authors (2013) [16] suggested in applying composite materials to the propeller, because it is the main contributor for this discrepancy in weight.

While in this study the GTF fall short because it showed that weight and drag penalties cannot be diminished if there is not a change in conventional nacelle installations, the open rotor seemed to have the possibility to rival against the next generation engines (PW1000G and LEAP-X), because it has the potential to offer even more benefits.

Paul Adams (2013) [17], ex-president of Pratt & Whitney, stated that for the near future, it is not expected to have an open rotor engine available on the market. Paul Adams indicates that the main contributors for this situation are the noise and installation challenges, along with the need to provide a variable pitch mechanism for each contra rotating propeller. In terms of reliability, Adams (2013) [17] claims the gearbox mechanism on a GTF is ten times more reliable than a variable pitch propeller.

2.2 New Trends in Aeroengines

Nowadays, the main problem that the aeroengine designer faces is developing a high power and highly efficient engine, while maintaining low levels of fuel burn, emissions, and noise. To tick all the goals of future aeroengines that involve performance, economy and environment, several ideas were suggested and investigated. One of these ideas, that is under research, is the introduction of more complex thermodynamic cycles in turbofan engines. This involves the implementation of heat exchangers such as intercoolers and/or regenerators, that proved to be successful, in terms of fuel consumption and output power, in ground – based power plants and marine engines.

Bearing in mind the benefits of installing heat exchangers in ground power plants, the idea of using them in aeroengines seemed suitable and hence several studies, which appear beneath, were conducted.

2.2.1 Relevant Studies

Andriani and Ghezzi (2009) [18] performed a numerical thermodynamic cycle analysis on a turbofan with intercooling and regeneration.

To help understand how the regeneration process works, the authors (2009) [18] explained that part of the heat available in the exhaust stream is recovered, because otherwise it would be lost, to preheat the compressed air before it is introduced into the combustion chamber, saving fuel and if the output power reduction due to pressure loss in the recuperator is negligible, then the thermal efficiency rises.

Regarding the intercooler, Andriani and Ghezzi (2009) [18] explained that this type of heat exchanger is placed between the compressors (LPC and HPC), and so, the compressed air is cooled. As a consequence of this process, the intercooler reduces the compression work allowing more power available at the output shaft/exhaust nozzle. In comparison to the regenerator, the intercooler has a flow pattern less complicated, because the flow does not need to be turned from the rear to the leading direction. Moreover, the authors (2009) [18] referred that the main challenges of introducing heat exchangers in aeroengines lays on the fact that they add extra weight and size to the engine, which are always prohibited on an aircraft.

In order to assess the benefits, in terms of power increase and fuel consumption, of introducing a regenerator and an intercooler in a turbofan, the authors (2009) [18] developed a thermodynamic code, written in FORTRAN 77, to simulate its performance.

The engine in question was a two-spool unmixed flow turbofan with the intercooler located between the LPC and the HPC, and the regenerator located after the LPT, as can be seen in Figure 2.3.

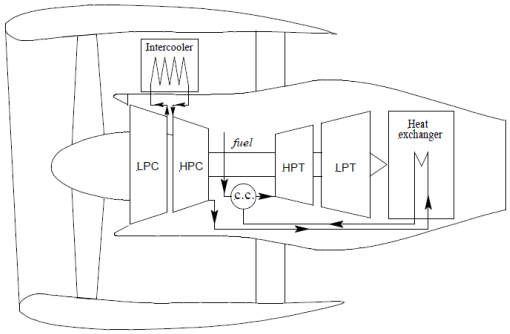

Figure 2.3: Scheme of a turbofan engine with intercooling and regeneration [18].

Since this numeric simulation was done to compare the differences, in terms of performance and efficiencies, between the baseline engine and another with an intercooler and a regenerator implemented, then some simplifications, although not realistic, were done in the engine operations: no air bleeding for auxiliary or cooling system, perfect gas and no auxiliary power extracted from the turbine.

Regarding the inputs, the engines were tested for the same cruise condition (altitude of 10000 meters and flight Mach number of 0.85), the maximum turbine inlet temperature assumed two values (1300 K and 1500K), the BPR was analysed for three values (3, 6 and 9), and the fan pressure ratio was kept constant (1.7). Moreover, the efficiency values of all the components used in this study, except the intercooler and regenerator, were kept constant. In this sense, the efficiency values for both the heat exchangers varied between 0 and 1.

All the main engine parameters analysed in this work (specific thrust, thermal efficiency, and specific fuel consumption) varied according to the overall pressure ratio.

The results showed that intercooling and regeneration had positive effects on the performance of the turbofan engine at cruise conditions, however, these positive effects were limited. The main reason for this to have happened laid on the fact that both the intercooler and regenerator had a double side effect. More precisely, the intercooler helped to improve the specific thrust of the engine, but it also contributed to the increase of fuel consumption. Additionally, although the regenerator pre heated the air before entering the combustion chamber, which lowered the specific fuel consumption, it also lowered the

enthalpy level present in the exhaust gases and, consequently, reduced the exhaust velocity and hence the specific thrust.

The authors (2009) [18] referred that if the values of TIT were higher, then the use of intercooling and regeneration would improve the TSFC, however problems related with the mechanic of the engine and with combustion emissions would emerge, due to very high values of TIT at high altitude.

Another fundamental aspect that the authors (2009) [18] took special attention in analysing was the efficiency of intercooling and regeneration. As efficiency increased, it uncovered great reductions in fuel consumption. However, the authors (2009) [18] also stated that at the present it was not possible to have such components on an aircraft engine with such high level of efficiency, mainly because, its integration entailed a significant increase in size and weight.

Lebre and Brójo (2011) [19] developed a parametric study, in which four engine configurations were analysed and compared in terms of thermal efficiency, specific thrust and specific fuel consumption.

The baseline engine was a turbofan with two-spools and the ability to produce 50000 lbs of thrust. All configurations had the same baseline engine, however three of them used an intercooler or a regenerator or even both. Regarding the location of the intercooler and regenerator, the former was located between the compressors, while the latter was placed at the exhaust nozzle.

To simplify the calculation work, the authors (2011) [19] decided to make several assumptions: steady and one-dimensional flow, perfect gas, isentropic bypass flow without external mechanical power, cooling air but not bleed, pressure drop for the components (except for the heat exchangers) and standard atmospheric conditions.

The engines were all tested for the same cruise conditions (altitude of 10668 meters and flight Mach number of 0.80) and the turbine inlet temperature was kept constant (1500K). Moreover, in these conditions and for a specific thrust of 200 (N·s)/kg, which was marked as the goal number, the main parameter values assumed for each engine are presented in Table 2.5.

Table 2.5: Main parameters for each engine [19].

Parameter	Baseline Engine	Engine with Intercooler	Engine with Regenerator	Intercooled Regenerative Engine
OPR	26	29	25	27
FPR	1.71	1.71	1.74	1.75
BPR	5	5	5	5

The performance parameters analysed in this study varied according with several independent variables, such as, pressure ratios and bypass ratio.

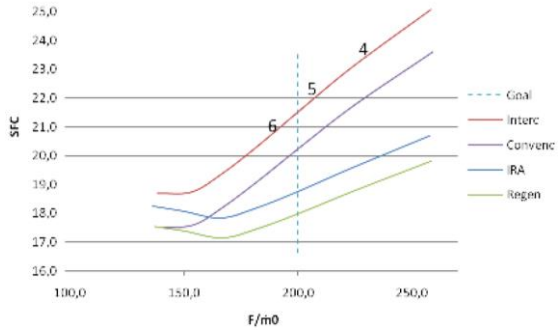

Figure 2.4: Specific fuel consumption in function of specific thrust [19].

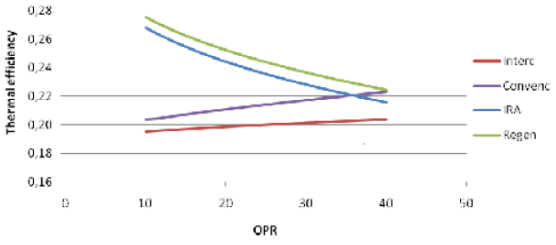

Figure 2.5: Thermal efficiency in function of overall pressure ratio [19].

When comparing the results for each engine configuration, the authors (2011) [19] concluded that the engine with intercooler was the one with higher values of specific fuel consumption and lower thermal efficiency, even when compared to the conventional engine. Lebre and Brójo (2011) [19] pointed that this was due to the low temperature output in the high-pressure compressor.

In contrast, the engine with regenerator was the one to reveal the lowest values of specific fuel consumption and the highest values for thermal efficiency. Regarding the engine with both heat exchangers, it showed better SFC and thermal efficiency than the conventional engine, which means that the use of a regenerator helps to improve the thermal efficiency.

Colmenares et al. (2007) [20] performed a preliminary parametric study for different turbofan engine configurations using the software Gas Turb 10. To start, the authors choose as baseline engine a three-spool turbofan with a bypass ratio of 5.3 with the level of technology expected in 2000. This engine was adapted to incorporate heat exchangers, which led to three engines configurations, i.e., one of the engines used only an intercooler, while the other a regenerator and the last one used both (IRA).

Regarding the location of these components in the engine, the intercooler was implemented between the intermediate pressure compressor and the high-pressure compressor and the regenerator was installed downstream the LPT.

Among all these turbofan engines configurations that were analysed for the same design point conditions (Take Off), the authors tried to identify which one had the most suitable cycle regarding less fuel consumption and emission reduction.

To meet the thrust required for the take-off condition at SLS, the working parameter varied was the OPR. According to the authors, this design point was chosen, because at take-off, it is when the engine is working at high power and so the levels of NOx are higher.

After the parametric study, Colmenares et al. (2007) [20] compared the results of the different engines (Table 2.6).

Table 2.6: Engine data at design point for selected engines [20].

Parameter	Baseline Engine	Engine with Intercooler	Engine with Regenerator	Intercooled Regenerative Engine
Thrust at Take Off [kN]	100.97	100.97	100.97	100.97
Bypass Ratio	5.3	5.3	5.3	5.3
TIT [K]	1605	1605	1605	1605
OPR	24.41	6.61	16.15	10.17
Thermal efficiency	0.43	0.31	0.47	0.49

(continued on next page…)

Table 2.6: (continued)

Parameter	Baseline Engine	Engine with Intercooler	Engine with Regenerator	Intercooled Regenerative Engine
ΔTSFC [%]	Ref.	36.65	-4.6	-5.55
ΔEI NO_x [%]	Ref.	-88.11	3.0	-11.88

The authors (2007) [20] observed that the engine with intercooler presented the lowest NO_x emissions, however this configuration is unattractive, because is the one that consumes the most fuel, and consequently, releases more CO_2. Additionally, the IRA configuration offered the higher thermal efficiency and lower fuel consumption. In this context, by combining the fuel consumption advantages and moderate NOx levels representative of the IRA, this makes this engine the most promising configuration at take-off.

Salpingidou et al. (2018) [21] presented a conceptual analysis to determine the improvements in thrust specific fuel consumption on a geared turbofan with the implementation of an intercooler and a regenerator. More specifically, a performance comparison was made between a non-intercooled recuperative geared turbofan and one with an intercooler and a regenerator. Additionally, to execute the performance calculations of the GTF the engine simulation software Gas Turb 11 was used.

The reference geared turbofan considered in this study was a three-spool with unmixed flow engine. Moreover, the IRA engine had the intercooler implemented between the intermediate pressure compressor and the high-pressure compressor, and the regenerator was installed downstream of the LPT to exploit the wasted heat energy at the exhaust nozzle.

In this work, just one performance parameter was analysed, thrust specific fuel consumption, and it varied according to the OPR, TIT, BPR and intercooler and regenerator efficiencies. This can be seen in Table 2.7.

Table 2.7: Main variables of the cycles [21].

Parameter	Range
OPR	20 - 50
TIT [K]	1580 - 1800
BPR	15 - 25
Intercooler efficiency	0.5 - 0.9
Regenerator efficiency	0.7 - 0.9

The results showed that the implementation of intercooler and regenerator with higher levels of efficiency led to an improvement in TSFC and NOx emission reduction. Moreover, the positive impact on the TSFC with the installation of the intercooler and the regenerator was only enhanced for a narrow range of OPR values. The authors suggested that the main explanation for this to have happened laid on the fact that for some values of OPR the temperature difference between the two flows (compressed air and hot gas) was not high enough and, therefore, the integration of a regenerator became unfavourable.

The TSFC also decreased with increasing the BPR and TIT values. However, Salpingidou et al. (2018) [21] pointed that to achieve extremely high values of TIT, special metal compositions for the turbine blades are needed which increase turbine costs.

2.3 Environment Friendly Programs

Associated to the civil aviation growth witnessed in the last decades, the public concern over its impact on the environment increases [15]. Emissions legislations are becoming even more stringent, which forces the emergence of new technological breakthroughs and novel aero-engine concepts.

Bearing in mind that in 2050 in Europe is expected that the number of commercial flights will reach 25 million, which results in a 166% increase when compared to the number of commercial flights in 2011. Then, new goals were drawn to make air travel environmentally sustainable [22]. With this, Europe outlined a set of goals to be reached by the next generation of engines entering in service in 2050. More specifically, these goals appear in

the Flightpath 2050 Europe's Vision for Aviation and target a 75% reduction in CO_2 emissions per passenger kilometer, a 90% reduction in NO_X emissions and a 65% reduction of noise. To reach the set out targets, a strategic plan that encompasses several measures, including technology development, as the ones mentioned below, and operational procedures are in progress [22].

In this context successive efforts from government authorities and international political organisations to reduce the environmental impact of air traffic were and still are being made. Towards this direction, the Advisory Council for Aviation Research and Innovation in Europe (ACARE), which comprises the European Commission, member states, research centres, airports, airlines, Air Navigation service providers, industry, and universities, is the responsible authority for most of the innovative technology programmes in Europe [21, 22].

2.3.1 VITAL

One of these programmes was the VITAL (EnVIronmenTALly aero engines) project that started in 2005 and ended in 2010. [23] The purpose of this program was to develop and validate engine technologies that allowed a noise reduction of 6dB and a 7% reduction in CO_2 emissions [23]. These objectives were accomplished by developing innovative low speed fan architectures, new low-pressure compressor concepts and technologies for weight and size reduction, new lightweight structures using new materials and manufacturing techniques, new low-pressure turbine technologies for weight and noise reduction, optimal installation of VHBR engines related to optimising weight, noise and fuel burn. All of these were evaluated through preliminary engine studies for three configurations, which were the DDTF supported by the Rolls Royce, the GTF by MTU Aero Engines and the CRTF by Snecma [23].

The existence of this programme enabled serious technological developments towards the next generation of commercial aeroengines (high performance, low noise and low emissions engines at an affordable cost) [23].

2.3.2 NEWAC

Another European project was the NEWAC (New Aero Engine Core concepts) that started in 2006 and ended in 2011 [24]. The purpose of this project was to improve core thermal efficiency and strongly reduce pollutant emissions (NO_x and CO_2) by developing and validating new engine core configurations and innovative types of combustion [6, 23].

Some of the new core concepts proposed for investigation were: intercooling, intercooling with regeneration, aspirated compression systems and active control of a cooled cooling air system [6].

For the intercooled core configuration (Figure 2.6), a compact and efficient intercooler with an aggressive ducting and an advanced compressor with improved transient behaviour were validated [23].

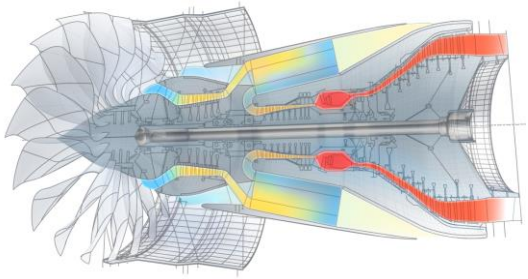

Figure 2.6: NEWAC intercooled aeroengine core configuration [14].

Regarding the intercooled recuperative aero engine configuration, the recuperator arrangement and a radial compressor were optimised, while the pressure losses in the ducts were reduced [24].

The NEWAC technologies enabled a 6% reduction in CO_2 emissions and a 16% reduction in NO_x relative to ICAO-LTO cycle [24].

2.3.3 Clean Sky

Launched in 2008 and still in progress is the Clean Sky programme, which is the largest European aviation research program, that focus on reducing the impact of air transport on the environment, while maintaining a firm commercially competitive position in international markets [25, 26].

To achieve its goal, a search for Sustainable and Green Engines (SAGE) was conducted, which resulted in the development of 6 engine projects to be tested in 5 full- scale demonstration vehicles, distinguished by application (regional, narrow body and wide body fixed wing aircraft and rotary wing aircraft) and by engine architecture (2-shaft, 3-shaft, geared and open-rotor) [25].

For the fixed wing aircraft, the research was conducted towards novel engine architectures (open-rotor and geared-fan engine) to power future aircrafts [27].

The research focused on geared fan engine technology, mainly because, its first generation successfully demonstrated significant reduction in fuel consumption and noise emission compared to a conventional turbofan engine in service in 2000 [25]. In this sense, convinced with the benefits of the first generation of GTF further improvements were made. Some of them consisted in a new highly efficient HPC, lightweight high speed LPT, advanced lightweight and efficiency turbine structures, lightweight and reliable fan drive gear system [24].

Additionally, the Advanced Geared Turbofan Demonstrator with all its new technological improvements was successfully tested in 2016 and key enablers to reduce CO2 emissions and noise, and engine weight were validated [25, 27]. After this, the technology has been maturated for future engine aircrafts that will take to the skies in the 2025 to 2050 timeframe, enabling a more affordable air travel and cleaner skies [27].

Chapter 3

Theoretical Framework

The first section of this chapter introduces the gas turbine concept, as well its thermodynamic cycle and other alternative cycles that encompass the usage of intercooling and regeneration.

The second section describes how a turbofan engine works and shows the different types there are according with its characteristics. Moreover, it is also introduced the bypass ratio concept and its importance in the aeronautical sector.

3.1 Gas Turbine

The 20th century was unquestionably marked with the introduction of the gas turbine, that would change our lives in various ways. Its development started before the Second World War with electric power applications in mind, however the early gas turbine built did not turn out to be a strong competitor against existing steam turbines and diesel engines [1, 28]. Nevertheless, towards the end of the Second World War, the gas turbine had its first major application in military jet engines. This contributed to a drastic change in speed when compared to the propeller engines used at the time. As a consequence of the phenomenal progress and growth of the gas turbine technology, in the early 1970s the high bypass ratio turbofan came to the light and the significant improvement in fuel consumption made possible the high-capacity wide body aviation [28].

Besides the aircraft propulsion application of gas turbines, there is a vast branch of markets that use this type of technology, for example: marine, industrial, oil, gas and electric power generation [29].

The simplest form of a gas turbine is illustrated in Figure 3.1 and it consists in three key components: compressor, combustion chamber and turbine.

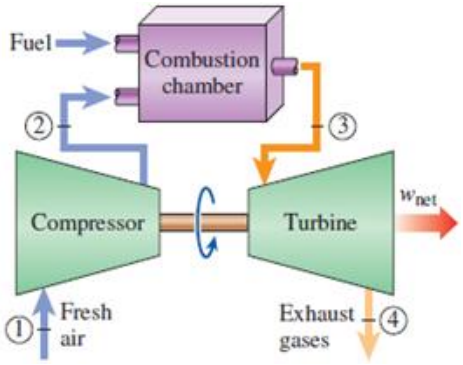

Figure 3.1: Simple gas turbine system (one-spool and open cycle) [30].

3.1.1 Ideal Gas Turbine Thermodynamic Cycle

A typical thermodynamic cycle consists of a series of consecutive thermodynamic processes that involve transferring heat and work into and out of the system, whereas state variables, like temperature or pressure, are varied within the system. At the end of a cycle, the system returns to its initial state [30].

Regarding the ideal gas turbine cycle, the incoming air is captured by the compressor and its temperature and pressure are raised. In this last component the air is compressed isentropically (reversible and adiabatic). As the compressed air reaches the combustion chamber, it is mixed with fuel and combustion occurs at constant pressure . Then, the hot gases, which are expelled at a high velocity, are expanded isentropically as they pass through the turbine, which in turn drives the compressor, and so a useful power is extracted [28, 31]. The hot exhaust gases after leaving the turbine are released directly to the atmosphere (not recirculated). Due to the exhaust gases being thrown out, this cycle is classified as an open cycle (Figure 3.1), which is the most used in gas turbines.

In order to turn this ideal open cycle into an ideal closed cycle, also known as the Brayton cycle (named after the person who invented it, George Brayton) some changes need to be done. While the compression and expansion processes remain the same (isentropic), the combustion and the exhaust phase are replaced by a constant pressure heat addition process from an external source and a constant pressure heat rejection process to the ambient air, respectively [30]. In Figures 3.2 and 3.3 are shown the closed cycle scheme and the respective T-s and P-v diagrams.

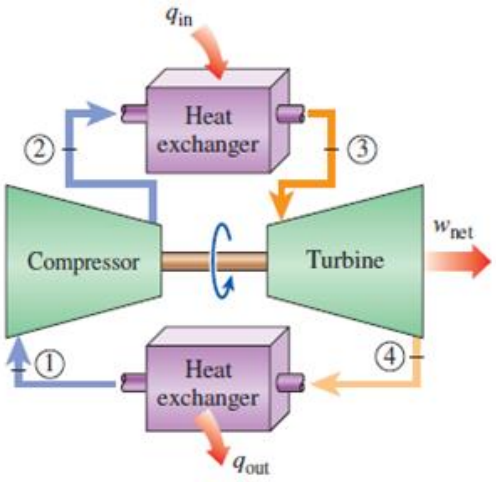

Figure 3.2: Brayton cycle gas turbine engine [30].

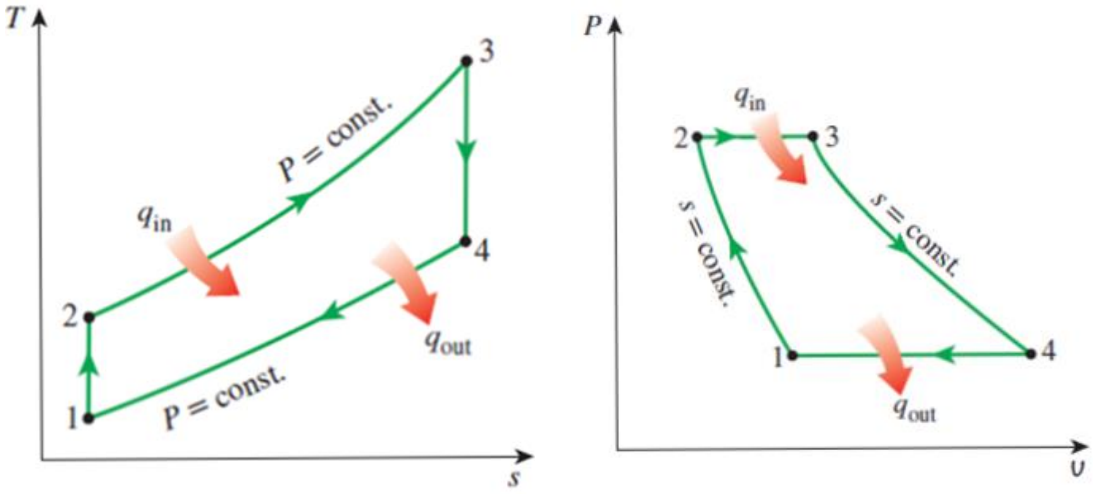

a) T-s diagram b) P-v diagram

Figure 3.3: T-s and P-v diagrams for ideal Brayton cycle [30].

3.1.2 Real Gas Turbine Thermodynamic Cycle

Previously was shown the ideal Brayton cycle, which is used as a model for the actual gas-turbine simple cycle, however in reality this is not verified. The justification for such is associated with the fact that pressure drop is inevitable, the component efficiencies does not reach its maximum value (100%) and in some of the stages the processes are not reversible (irreversibilities) [32]. More precisely, the pressure drops in the combustion chamber, the combustion process is incomplete (the combustion products contain any unburned fuel or components such as C, H_2, CO, NO, or OH) and during the compression process there is an

air bleed (this air can be utilized for cabin-air conditioning, as well as anti-icing activities) [1, 33].

In Figure 3.4 is illustrated the real Brayton cycle through a T-s diagram. In detail, the compression (1-2a) and expansion (3-4a) processes are no longer reversible, but still adiabatic. The combustion (2a-3) and the heat rejection (4a-1) are no more isobaric processes. Moreover, after the hot exhaust gases being expelled (at 4a), the pressure achieved is not the same as the ambient pressure, it is higher, and new air is ingested from the atmosphere (at 1), with this, a new cycle begins [1, 33]. The states 2s and 4s represent the exit states of the compressor and the turbine, respectively, for the isentropic case, whereas the states 2a and 4a are the actual states of a real gas turbine cycle.

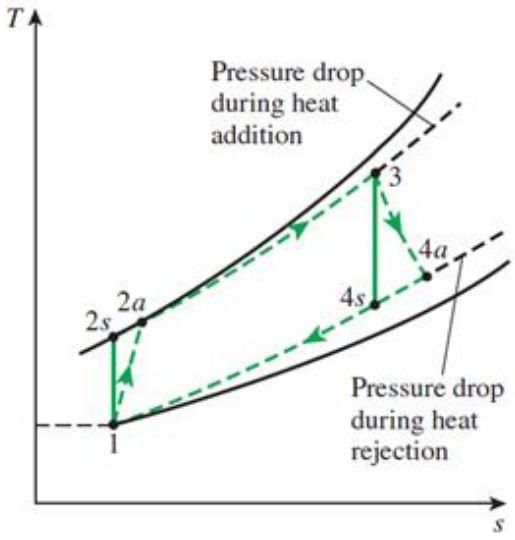

Figure 3.4: Real gas turbine cycle [30].

3.1.3 Alternative Thermodynamic Cycles

The first existing gas turbines had really low cycle efficiencies, of about 17%, because not only the turbine and compressor efficiencies were low, but also the turbine inlet temperature. Such happened, due to metallurgical limitations experienced back then.

To improve the cycle efficiency, multiple efforts were made. Besides trying to increase turbine inlet temperature and components efficiencies, some modifications to the simple cycle were attempted. Such modification implied the introduction of intercooling, regeneration and reheating to the basic cycle. This led the cycle efficiency to almost double. However, this came with a price, because unless the fuel costs offset the increase in

operation costs, it would not be of interest to invest in such technology [30]. Nevertheless, considering the outlook on today's concerns regarding the environment and fuel prices, this type of solution to improve cycle efficiency seems valid.

Bearing in mind what was discussed, next is given a more detailed insight about intercooling and regeneration.

3.1.3.1 Intercooling

By placing a heat exchanger between compression stages, usually between the low and high-pressure compressors, as illustrated in Figure 3.5, the incoming air is cooled between compressions and the compression work is reduced. This results in a higher power available at the output shaft for driving the load [18].

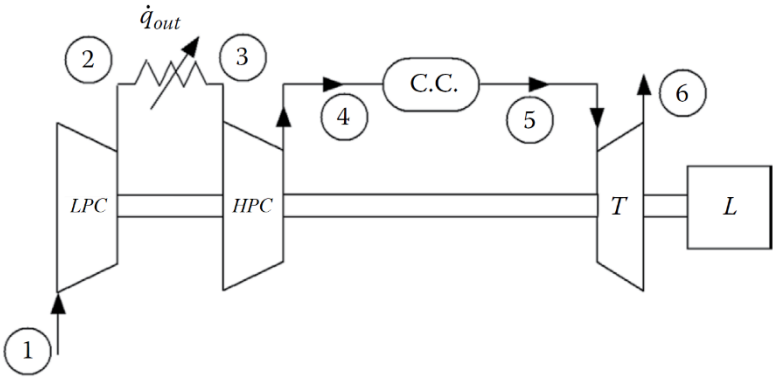

Figure 3.5: Gas turbine with two stage compression with intercooling [1].

As illustrated in Figure 3.6, the closed loop 1-2-3-4-5-6 represents the ideal cycle (T-s diagram) of a gas turbine with intercooler.

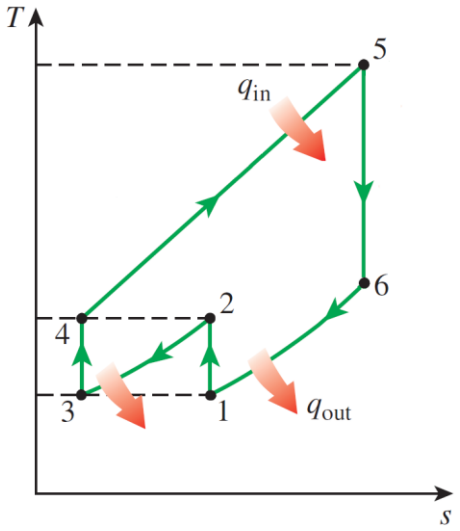

Figure 3.6: Ideal T-s diagram for a gas turbine with intercooler [30].

Paying close attention to the T-s diagram and to the Figure 3.5 (gas turbine station numbering system), this cycle is composed of six stages. In the first stage (1-2), the air enters the first compressor (LPC), and there, it is slowed down and compressed isentropically. After that, the compressed air enters the intercooler (2-3), where it is cooled at constant pressure and in state 3, the air reaches the same temperature as in state 1. In the next stage (3-4), the air is once again compressed isentropically by the HPC. Then, the heat addition process (4-5) occurs in the combustion chamber at constant pressure. The hot gases enter the turbine and are isentropically expanded (5-6). To complete this cycle, the gases exit the turbine and are cooled to the initial state (at 1) [30].

As a consequence of rejecting heat from the cycle (2-3), the temperature at the combustion chamber inlet (at 4) is lower than on a normal gas turbine and so more fuel will be required in order to achieve the desired temperature at the inlet of the turbine (at 5) [18].

The intercooler efficiency only reaches its maximum value theoretically, which means the temperatures of the air at the inlet of the HPC and the LPC are the same ($T_1 = T_3$). However, in reality the intercooler efficiency is less than unity, and so, the temperature at the HPC inlet is higher than at the LPC inlet ($T_3 > T_1$) [30].

The air responsible for cooling the compressed air can come from the ambient air (turboprop engine) or from the fan outlet duct if a turbofan is considered [1].

3.1.3.2 Regeneration

Since temperature of the exhaust gases leaving the turbine is appreciably higher than the temperature of the air leaving the compressor. Then, by placing a regenerator after the turbine, it is possible to recover heat from the exhaust gases to pre-heat the compressed air before introducing it to the combustion chamber. In this context, the use of a regenerator results in less fuel burned, higher thermal efficiency, less output power (due to pressure drop in the heat exchanger) and in a more complex flow pattern, because, as it can be seen in Figure 3.7, the flow needs to be turned from rear to leading direction [18].

The regenerator efficiency increases as the temperature of the pre-heated air increases, which results in less fuel needed to achieve the fixed turbine inlet temperature. Nevertheless, to achieve high values of efficiency (nowadays the higher value obtained is 0.85), a regenerator of considerable size is necessary, which reveals a major setback in aeronautical applications. However, the high efficiency and associated fuel cost reduction may compensate its integration in aeroengines [30].

In figures 3.7 and 3.8 are shown a sketch of the gas turbine using a regenerator and its T-s diagram cycle, respectively.

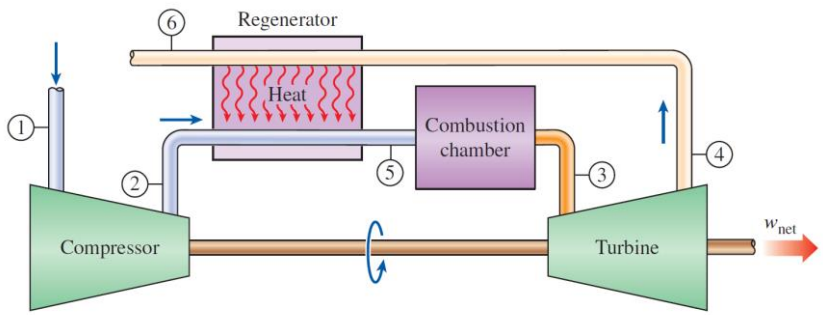

Figure 3.7: Gas turbine with regeneration [30].

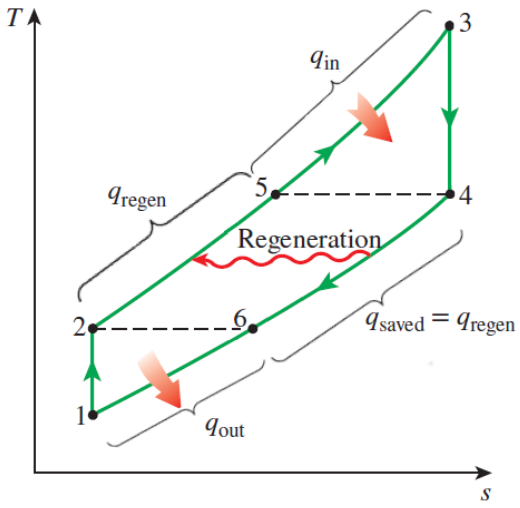

Figure 3.8: Ideal T-s diagram of a gas turbine with regeneration [30].

Regarding the ideal cycle with regeneration, after the air being isentropically compressed (1-2), it enters the regenerator (2-5), where it is heated to T_5 at constant pressure. Since this is an ideal cycle, then the air leaves the regenerator at the same temperature of the gases that leave the turbine ($T_4 = T_5$). After that, the heat addition process (5-3) happens at constant pressure. Following it, the hot gases enter the turbine at state 3, where they are isentropically expanded (3-4). The exhaust gases exit the turbine at state 4 and enter the regenerator. There, a heat exchange occurs between the exhaust gases and the compressed air at constant pressure. The exhaust gases are cooled, reaching the same temperature as the air before entering the regenerator ($T_2 = T_6$). To complete this cycle, the gases return to its initial state (at 1) [30].

Above was shown that the air exiting the regenerator had the same temperature of the exhaust gases entering it and the same happened with the air entering the regenerator and the gases exiting it. However, in the actual cycle this does not happen, instead the air leaves the regenerator at a lower temperature and the exhaust gases leave the regenerator at a higher temperature. Moreover, in the analysis of the real gas turbine with regenerator cycle, the pressure drops in the heat exchanger and combustion chamber, as well as the irreversibilities, present within the compressor and the turbine, should be taken into consideration [30].

3.1.3.3 Intercooling and regeneration

Combining the two heat exchangers mentioned above on a gas turbine, the intercooled and regenerated gas turbine emerges, which is shown in Figure 3.9 accompanied with the respective T-s diagram, Figure 3.10.

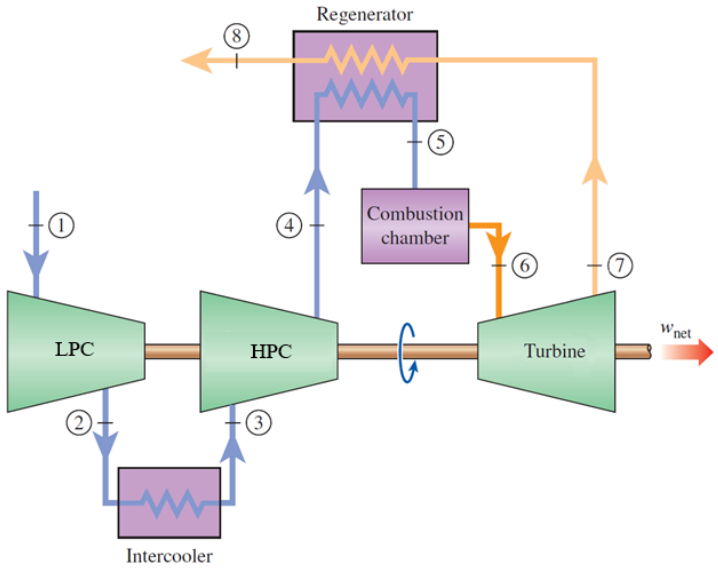

Figure 3.9: Gas turbine with two stage compression with intercooling and regeneration [30].

By using the intercooler in conjunction with the regenerator a significant increase in thermal efficiency is achieved. This happens because the intercooler is able to reduce the compression work by cooling the air between compressions, which in turns increases the net work (difference between the turbine work output and the compressor work input) of a gas turbine cycle. In this context, the combined utilisation of a regenerator with an intercooler seems feasible, because the latter increases the temperature difference between the high compressed air and the exhaust gases, which results in a more effective heat exchange process done by the regenerator [30].

Since the air temperature is raised before entering in the combustion chamber, then less fuel is used, and consequently, the thermal efficiency lost due to intercooling is compensated by the use of the regenerator [20].

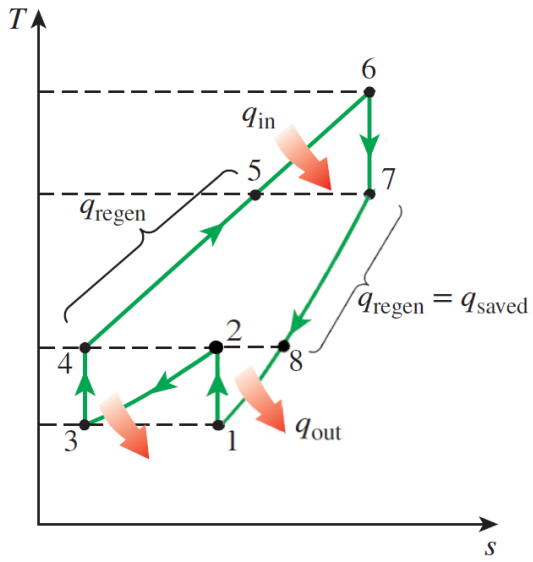

Figure 3.10: Ideal T-s diagram of a gas turbine with intercooling and regeneration [30].

Regarding the ideal cycle with intercooling and regeneration, the air enters the first compressor stage (LPC) and there it is slowed down and compressed isentropically (1-2). After that (2-3), the compressed air enters the intercooler. There it is cooled at constant pressure and in state 3, the air reaches the same temperature as in state 1. In the next stage (3-4), the air is once again compressed isentropically. Then, at state 4, the compressed air enters in the regenerator (4-5), where it is heated to T_5 at constant pressure. Since this is an ideal cycle, the air leaves the regenerator at the same temperature of the gases that leave the turbine ($T_5 = T_7$). After that, the heat addition process (5-6) happens at constant pressure. Following it, the hot gases enter the turbine at state 6, where they are isentropically expanded (6-7). The exhaust gases exit the turbine at state 7 and enter the regenerator. There a heat exchange occurs between the exhaust gases and the compressed air at constant pressure. The exhaust gases are cooled, reaching the same temperature as the air before entering the regenerator ($T_4 = T_8$). To complete this cycle, the gases return to its initial state (at 1) [30].

Above was analysed ideal alternative thermodynamic cycles for a gas turbine, however when analysing real cycles some things should be taken into consideration, such as, the pressure drops in the combustion chamber and heat exchangers, as well as the irreversibilities that are present within the compressors and the turbine [30].

3.2 The Turbofan Engine

In the 1950s the "bypass" principle was introduced on a jet engine, because at high subsonic speeds (around Mach 0.8) both the turboprop and the turbojet operated at low propulsive efficiency, since the flight speed was not the most adequate, i.e. too high or too low. Therefore, the turbofan filled the existing gap, which resulted in good efficiencies at that spectrum of flight velocities (Figure 3.11) [34].

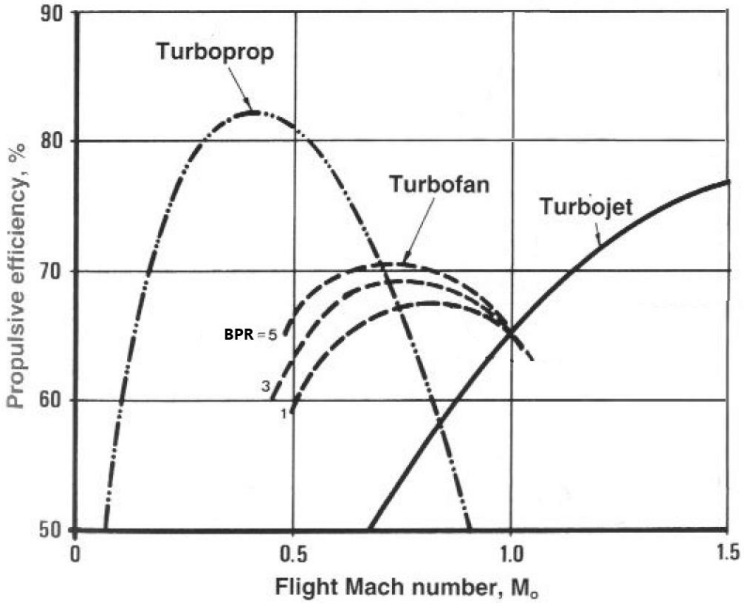

Figure 3.11: Propulsive efficiency for different types of engines [34].

In this context and due to the signs of tremendous reliability, fuel efficiency and quietness (low jet velocity results in less jet noise) that the turbofan has shown, this makes it the primary power source for today's civil aviation fleet and for military aircrafts, that travel long distances and still need to be fuel efficient below the sonic velocity [34, 35].

In this section, it will be explained how a turbofan engine works and the different variants there are of this engine. Moreover, it will also be discussed the importance of the bypass ratio in the aeronautical context.

3.2.1 Operation

The turbofan engine can be seen as the most modern variation of the basic gas turbine [31]. As such, both share some essentials components (compressor, combustion chamber and

turbine). However, to improve the performance of the turbofan engine more components were added, that made this engine unique in comparison with the turbojet.

For the turbofan to produce thrust, the ambient air has to pass an admission duct that decelerates the air, while increasing its pressure. After that, a large amount of air is drawn into a rotating fan, also known as the first compressor, and there it is compressed.

Next, the air is divided into two streams. As shown in Figure 3.12, the primary stream travels across all the components in the engine core (similar to a turbojet engine), while the second stream (cold stream) goes through a duct (bypass duct), that surrounds the engine, and then, it is either expelled through a separate nozzle (also identified as cold nozzle) or mixed with the hot gases and both are expelled from a single nozzle [1]. In this context, appears the bypass ratio concept which is nothing more than the ratio of the flow that passes through the bypass duct to the flow that goes through the core engine (hot stream).

As stated above, the primary stream passes through the core engine before being expelled through a nozzle. The core engine comprises a compressor, a combustion chamber and a turbine.

Once the hot stream enters in the compressor, there is a rise not only in pressure, but also in temperature.

Next, part of the pressurized air enters the combustion chamber, where fuel is injected and burned, while the other part is used to cool the combustion chamber walls and the combustion gases by diluting them. More specifically, in the combustion chamber a chemical reaction happens, in which a huge amount of energy is transferred to the airflow. In the combustion process, the temperature is greatly increased, whereas the pressure remains virtually the same.

After the combustion, the hot gases advance towards the turbine, which is linked by a hollow spool to the compressor and fan. The turbine function is to extract energy from the gases and convert it into mechanical work to drive the fan, the compressor and some accessories needed for engine operation. Moreover, since the turbine is located at the exit of the combustion chamber, the turbines blades are exposed to a hostile environment where temperatures can easily reach 1700°C. To withstand these conditions, it is necessary not only to develop new superalloys, but also the blades need to be coated (TBC's, CMC's) and internally cooled with air that is bleed from the compressor [33].

Once the exhaust gases leave the turbine, they reach the exhaust nozzle, that will conduct the gases out of the engine and back to the free stream. There, the heat and pressure energy still available in the gas is converted into kinetic energy (velocity) and so thrust to propel

the aircraft is generated. Moreover, since the turbofan has two nozzles, then the thrust comes from the bypass duct ("cold" thrust) and the core ("hot" thrust).

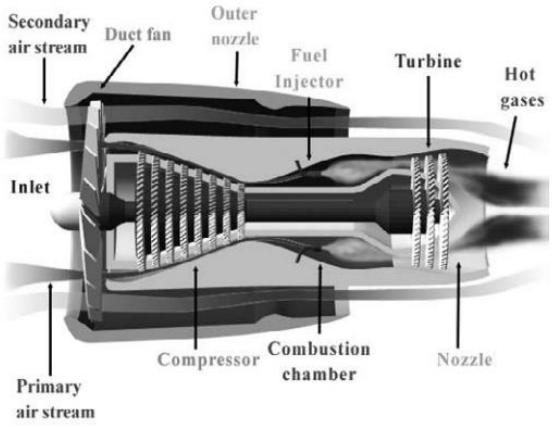

Figure 3.12: Cutaway view of a turbofan engine [35].

3.2.2 Different Types of Turbofan Engines

As illustrated in Figure 3.13, the turbofan engines can be classified according to the position of the fan (forward or aft), bypass ratio (low or high), mixed or unmixed flow, number of spools, duct size, existence or nonexistence of the afterburner and even the integration or not of a gearbox.

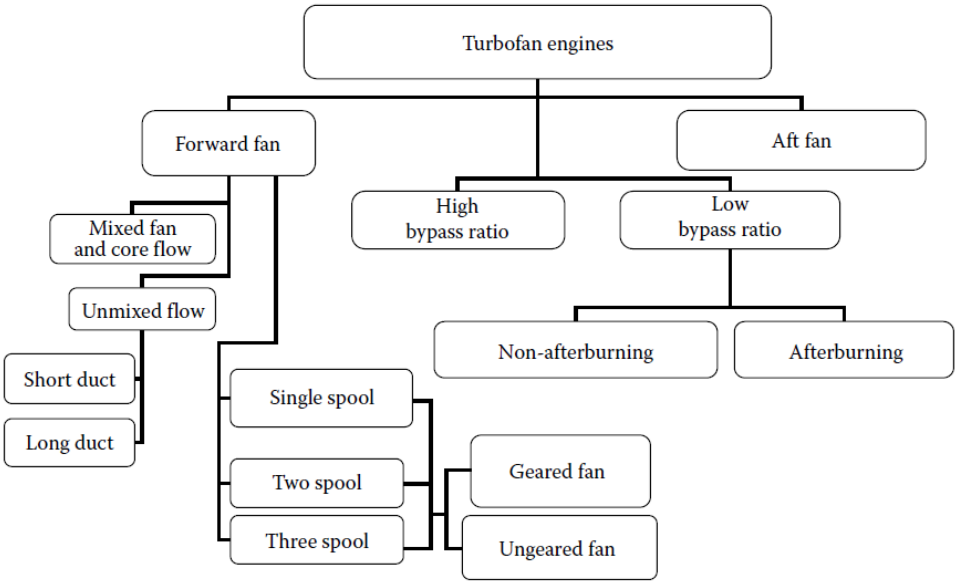

Figure 3.13: Classification of turbofan engines [1].

3.2.3 Bypass Ratio Importance

As seen in the previous sections, the bypass ratio plays a key role in the turbofan engines, which are classified according to the bypass ratio. For example, when the bypass ratio is high, a big fraction of the airflow that passed through the fan entered the bypass duct, and the engine is referred to as high bypass ratio engine.

The bypass ratio is defined as the fraction of the mass flow rate of the air that is bypassed around the engine (cold air) to that which does pass through the engine core (hot air):

$$\beta = \frac{\dot{m}_{cold}}{\dot{m}_{hot}} \tag{3.1}$$

Over the years, it has been shown a rising tendency for turbofans with higher bypass ratios. By increasing the bypass ratio, the benefits in terms of propulsive efficiency, fuel efficiency, noise (due to low exhaust velocities) and operation costs became clear. Nevertheless, increasing the bypass ratio, for a given core size, entails some negative consequences. Some of them are related to the integration of the engine in the aircraft, because the higher the bypass ratio, the heavier the engine (more stages in the LPT are necessary to drive the large fan) and the structure to support it. Moreover, the frontal area increases, which results in more drag, and the ground clearance (distance between the engine and the ground) becomes a problem.

Bearing in mind all the consequences of increasing the bypass ratio, one solution found by the researchers is to develop a more compact core, which results in a higher bypass ratio for the same fan size and frontal area.

Another way to reach high bypass ratio values is by reducing the fan pressure ratio. Since a turbofan with a higher fan pressure ratio produces more specific thrust, then there needs to be a trade-off between BPR and FPR, which privileges nowadays the BPR in detriment of the FPR, because of environmental concerns. In this context, in the future it is expected turbofans with even higher bypass ratios and lower fan pressure ratios.

Chapter 4

The Geared Turbofan

Since in this dissertation the turbofan engine chosen to be the baseline engine, that will be used as a way of comparison with the other configurations, is a geared turbofan, then below is shown some relevant information about this matter (history, evolution and advantages).

Dating back to the 1980s, the first geared turbofan engines appeared (Lycoming ALF502R and TFE731), promising less noise and fuel consumption in comparison with the engines used at the time. However, they did not convince most of the airline companies, because of the heavy weight of the gearboxes that made this concept impracticable for large aircraft aviation. Nevertheless, the GTF concept has been used in business aviation for many years, clocking up many millions of hours of flight time, and so, proving its reliability in service [17].

One of the biggest aeroengine manufacturers that showed tremendous interest since the beginning on the GTF concept was the Pratt & Whitney. The company goal was to make a lighter, more efficient and with less maintenance cost gearbox for large aircrafts. After 15 years of extensive technology development, the final product (PW8000) went to the skies in 1998. After that and due to the environmental problems associated with the growth of air traffic, Pratt & Whitney continued to invest in this concept and in 2016 the first GTF of the new family PW1000G entered in service (more details about the PW 1000G family are given below) [36].

Bearing in mind the environmental problems that humankind faces nowadays and that will face in the future, the geared turbofans are the recommended choice to drive the mid-range single aisle aircrafts, regional jets, and perhaps, wide body aircrafts [37].

The particularity of this engine (GTF) lays on the fact that, while the conventional engine has its fan and LPC revolving at same speed on the same spool (low spool), the geared turbofan features a fan drive gear system - driven by the low-pressure spool- that decouples the fan from the rest of the low-pressure spool, which allows for both of them to operate at their optimal speeds and higher efficiencies [37].

As a consequence of using a gearbox, the possibility of the formation of shock waves in the fan and the chances of blade damage from bird ingestion are also minimised. Moreover, the fuel efficiency is improved, the noise levels are reduced and the BPR is increased. The other

advantages include lower emissions (CO_2 and NO_x), fewer engine parts (compressors and turbine stages), which makes the engine lighter, smaller and easier to maintain (lower maintenance and direct costs) [38].

In Figure 4.1 is shown a comparison between a conventional turbofan and a geared one (the PW1000G). In terms of length, number of stages and airfoils, it is evident the benefits of what a gearbox can bring: less 6 stages and minus 45% airfoils.

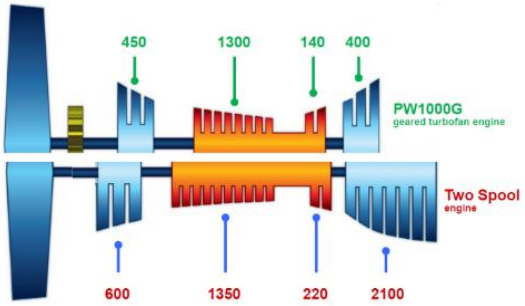

Figure 4.1: Comparison of a conventional two-spool turbofan with a geared one [39].

Bearing in mind that the geared turbofan is lighter than a conventional turbofan and with the introduction of two heat exchangers, weight is added to the engine, then this makes the geared turbofan the perfect candidate to receive an intercooler and/or a regenerator.

4.1 Pratt & Whitney PW 1000G Family

As a result of an international collaborative project between Pratt & Whitney, MTU Aero Engines, JAEC and GKN Aerospace, the Pratt & Whitney GTF™ Engine family emerged. Also known as, PurePower PW1000G, this is the newest generation of Pratt & Whitney's family of engines that powers the most recent narrow body aircrafts (Table 4.1). The reason why the PW1000G family was chosen, laid on the fact that these engines offered double digit improvements in fuel consumption, pollutant emissions, noise footprint and operating costs [40].

Table 4.1: Pure Power PW1000 Family specs [36,41].

Engine	Fan diameter [m]	Bypass Ratio	Truth [kN]	Fuel burn (vs. current engines) [%]	Noise Footprint(vs stage 4) [%]	NOx Emissions (margin to CAEP 6) [%]	Aircraft Models	Entry In Service
PW1124G-JM PW1127G-JM PW1133G-JM	2.057	12:1	106.8-146.8	-16	-75	-50	A319neo A320neo A321neo	2016-2017
PW1215G PW1217G	1.422	9:1	66.72-75.62	-16	-40	-40	MRJ70 MRJ90	2017
PW1428G-JM PW1431G-JM	2.057	12:1	124.6-137.9	-16	-75	-50	MC-21-200 MC-21-400;	2016
PW1519G PW1521G PW1525G	1.854	12:1	84.52-111.2	-16	-75	-50	CS100 CS300	2016
PW1700G	1.422	9:1	62.28-75.62	-12	-40	-50	E175-E2	2018
PW1900G	1.854	12:1	84.52-102.3	-16	-75	-50	E190-E2 E195-E2	2018-2019

Some of the technologies that contribute to obtain the improvements showed above are the engine's fan blade, which consists of an innovative hybrid metallic fan blade, and each stage of the high-pressure compressor is a single piece (blade integrated disks or "blisks"). At the same time, the PW1000G incorporates a high strength made of steel planetary gearbox with very low maintenance. This gearbox (Figure 4.2) consists of a sun gear attached to the low-pressure spool, that drives the five planetary gears enmeshed between the sun gear and a fixed ring gear. In its turn, the five planetary gears rotate the carrier cage, which is responsible for the fan rotation. Another key technology is the advanced combustion chamber, TALON-X, that uses a rich-quench-lean combustion cycle, which prevents nitrogen oxides of forming. Moreover, the PW1000 uses a new turbine cooling technology, which includes advanced thermal barrier coatings, powder metal blade alloys and new internal cooling airpath geometries.

Figure 4.2: Planetary gearbox found in the PW1000 engines [36].

4.1.1 The Baseline Engine

Having showed all the engines that compose the PW1000G family, the next step is to choose from the Table 4.1 one, to serve as the baseline engine in this dissertation. However, due to the lack of data relative to each engine model in specific, the author had to use the available data relative to the PW1000G in general, which was presented by Ahmed in [1].

Figure 4.3: PurePower PW1000G [42].

In this context, the assumed baseline engine is a high bypass ratio, unmixed flow, dual-spool, turbofan engine. Additionally, the low-pressure spool consists of a single stage fan attached to a gear speed reduction system, a three stage low-pressure compressor and a three stage low-pressure turbine that drives the remaining components of this spool. The high-pressure spool has an eight stage high-pressure compressor driven by a two stage cooled high-pressure turbine [43].

In Table 4.2 are shown the assumed values during cruise for the PW1000G, which were extracted from [1].

Table 4.2: Specifications of the PW1000G at cruise phase [1].

Property	Value
BPR, β	11.4
TIT [K]	1520
Overall Pressure Ratio, π_O	42
FPR, π_F	1.6
LPC pressure ratio, π_{LPC}	2.2
HPC pressure ratio, π_{HPC}	11.93
Intake polytropic efficiency, η_d	0.98

(continued on next page…)

Table 4.2: (continued)

Property	Value
Fan polytropic efficiency, η_F	0.91
Gearbox efficiency, η_{gb}	0.995
LPC polytropic efficiency, η_{LPC}	0.90
HPC polytropic efficiency, η_{HPC}	0.90
Combustion Chamber efficiency, η_{CC}	0.95
LPT polytropic efficiency, η_{LPT}	0.95
HPT polytropic efficiency, η_{HPT}	0.95
Nozzle efficiency, η_n	0.95
Mechanical efficiency, η_m	0.993
Combustion chamber pressure drop, ΔP_{CC}	0.02

Since the flight condition analysed is the cruise phase, then it is necessary to present the operation conditions (Table 4.3), in which this study was conducted. These are referent to the cruise phase of the A320neo, which is a single aisle aircraft that entered service in 2016. Additionality, to obtain some of the values present in Table 4.3, the author resorted to the ISA model.

Table 4.3: A320neo cruise flight characteristics [39].

Property	Value
Altitude [m]	11600
Ambient Temperature, T_0 [K]	216.65

(continued on next page…)

Table 4.3: (continued)

Property	Value
Ambient Pressure, P_0 [N/m²]	20589
Flight Velocity, C_0 [m/s]	233
Mach Number	0.79

Chapter 5

Parametric Study

To help understand the influence of certain parameters, such as flight conditions or project parameters, in the performance of an engine - for example, specific thrust or thrust specific fuel consumption - is necessary to carry a parametric study.

In this chapter not only is shown the assumptions made throughout this study, but also is described in detail the mathematical method utilized to analyse all the four configurations. Additionally, the results are displayed, accompanied with a brief discussion.

5.1 Assumptions

Before developing the numerical program, some constraints and assumptions are needed to be made, that directly affect the calculation process. Therefore, the assumptions are:

- Steady flow;
- One dimensional flow;
- The working fluid is a perfect gas, which specific gas constant is: $R = 287\ J/(kg \cdot K)$;
- Upstream of the combustion chamber the perfect gas properties remain constant and equal to: $\gamma_c = 1.4$ and $c_{pc} = 1005\ J/(kg \cdot K)$;
- Downstream of the combustion chamber the perfect gas properties remain constant and equal to: $\gamma_h = 1.333$ and $c_{ph} = 1148\ J/(kg \cdot K)$;
- The calorific value assumed for the fuel, which consists in the lower heating value of a hydrocarbon is equal to: $Q_{hv} = 42.80\ MJ/kg$;
- No air bleed;
- Polytropic compressions and expansions;
- The efficiencies of all the components are kept constants;
- There is no pressure drop inside the cold and hot nozzles;
- The pressure drops inside the combustion chamber and the heat exchangers;
- The intercooler is located between the LPC and the HPC and it uses the bypass air;
- The recuperator is located downstream of the LPT;

- For a viable incorporation of the intercooler, the air temperature after exiting the LPC has to be higher than the bypass air temperature;
- For a viable incorporation of the regenerator, the gases temperature after exiting the LPT have to be higher than the temperature of the air exiting the HPC.

The assumed values for the heat exchangers efficiencies and pressure drop, which were based on previous studies ([21, 44]), are:

- Heat Exchanger Efficiency, η_{HE}: 0.75;
- Heat Exchanger Pressure Drop, ΔP_{HE}: 0.05.

5.2 Mathematic Model

After defining the constraints and assumptions, the mathematical model used for the conventional cycle was based in one present in [1] for a geared turbofan, and then, it was adapted for the other three alternative cycles. Moreover, the software utilized to help create the code was MATLAB.

By creating for each cycle/ configuration and for each independent variable a calculation routine with successive increments on the independent variable and a filter, that guarantees that only the logical combinations are used, a matrix with all the accepted values of the output variables and its corresponding independent variables is extracted, and then, plotted.

To initialize the parametric study, it is necessary to first select the independent variables, which in this study were: the BPR, the TIT, the FPR and the CPR. Considering the actual values, future prospects and the expected technological development for a two-spool geared turbofan engine ([20], [40], [45], [46]), the variables assumed the following values:

- BPR: from 10 to 15;
- TIT: 1520 K or 1850 K;
- FPR: from 1.4 to 1.7;
- CPR: from 20 to 28.75.

In this parametric study, for each value of TIT (1520 K or 1850 K), the remaining independent variables varied at a time, and while they were not varying, they assumed the following fixed values, which coincide with the values of the baseline engine:

- BPR: 11.4;
- FPR: 1.6;
- CPR: 26.25.

Bearing in mind some of the worries present on the aeronautical industry, the author understood that would be purposeful to study the influence of these independent variables and of these different configurations on the following engine performance parameters: specific thrust and thrust specific fuel consumption. On one hand, the former parameter is nothing more than the thrust per unit of air mass flow rate and in terms of comparison with other engines it works as an indicator of engine efficiency. In other words, if an engine as a higher value of specific thrust, this means that for the same amount of airflow it produces more thrust and so it is more efficient. On the other hand, the latter parameter is defined as the ratio between the fuel mass flow rate and the produced thrust. In contrary to the specific thrust, the engine with lower value of thrust specific fuel consumption is the most fuel-efficient engine, because to generate the same amount of thrust, it burns less fuel [47].

After defining the baseline engine and all the other three configurations, the assumptions, the independent variables and its range, and the output variables, the next step is the creation of the mathematical models in MATLAB. These were based on the methodology presented by Ahmed [1] for a forward fan, two-spool unmixed geared turbofan.

5.2.1 Conventional Geared Turbofan

To help organize the mathematical model is necessary to firstly present the schematic engine layout (Figure 5.1) and its station numbering, followed by the description of each station (Table 5.1).

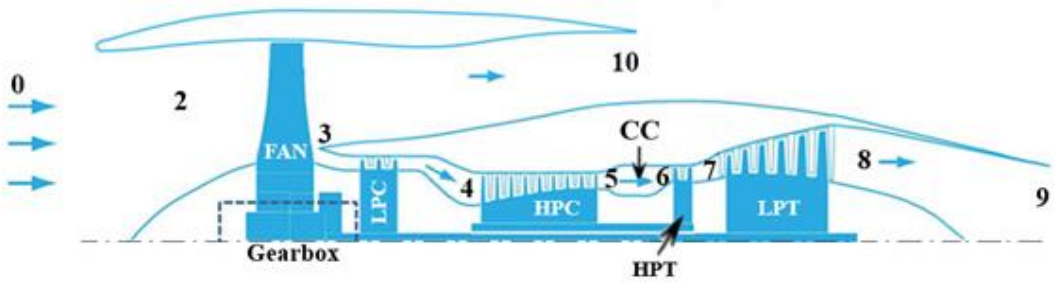

Figure 5.1: Station numbering adopted for the conventional geared turbofan [48].

Table 5.1: Description of the stations for the conventional geared turbofan.

Station number	Description
0	Free stream
2	Admission
3	Fan outlet
4	LPC outlet
5	HPC outlet
6	Combustion chamber outlet
7	HPT outlet
8	Hot nozzle duct
9	Hot nozzle outlet
10	Cold nozzle outlet

Taking into account the station numbering, the mathematical model adopted, and its equations are presented below.

- Admission: station 2

As the air enters the engine, it passes through the admission diffusor, where is verified a slightly temperature and pressure increase:

$$T_2 = T_0 + \frac{C_0^2}{2c_{p_c}} \tag{5.1}$$

$$P_2 = P_0\left(1 + \eta_d \frac{C_0^2}{2c_{p_c}T_0}\right)^{\frac{\gamma_c}{\gamma_c - 1}} \tag{5.2}$$

The values for the freestream conditions (T_0, P_0, C_0) are in Table 4.3.

- Fan outlet: station 3

To determine the air conditions after it passed the fan, the pressure ratio of the component itself is used, and a thermodynamic relation representative of a polytropic compression is applied:

$$P_3 = P_2 \pi_F \tag{5.3}$$

$$T_3 = T_2 \left(\frac{P_3}{P_2}\right)^{\frac{\gamma_c - 1}{\gamma_c \eta_F}} \tag{5.4}$$

- LPC outlet: station 4

After the passage through the fan, the air is divided. According with the bypass ratio, an amount of air is directed to the bypass duct, while the rest enters the low-pressure compressor. In analogy with station 3, the pressure ratio of the component is used, and the same thermodynamic relationship is applied:

$$P_4 = P_3 \pi_{LPC} \tag{5.5}$$

$$T_4 = T_3 \left(\frac{P_4}{P_3}\right)^{\frac{\gamma_c - 1}{\gamma_c \eta_{LPC}}} \tag{5.6}$$

- HPC outlet: station 5

Likewise for the high-pressure compressor, the same relations are used:

$$P_5 = P_4 \pi_{HPC} \tag{5.7}$$

$$T_5 = T_4 \left(\frac{P_5}{P_4}\right)^{\frac{\gamma_c - 1}{\gamma_c \eta_{HPC}}} \tag{5.8}$$

- Combustion chamber outlet: station 6

As the compressed air passes through the combustion chamber, it suffers a slightly pressure drop and the temperature of the hot gases before entering the high-pressure turbine is a considered value:

$$P_6 = P_5(1 - \Delta P_{CC}) \tag{5.9}$$

$$T_6 = TIT \tag{5.10}$$

Knowing the air conditions before and after its combustion, it is possible to determine the fuel-air ratio by applying the energy balance equation to the combustion chamber:

$$(\dot{m}_h + \dot{m}_f)c_{p_h}T_6 = \dot{m}_h c_{p_c}T_5 + \dot{m}_f \eta_{CC} Q_{hv} \tag{5.11}$$

With,

$$f = \frac{\dot{m}_f}{\dot{m}_h} \tag{5.12}$$

Then, the fuel to air ratio is determined from the relation:

$$f = \frac{c_{p_h}T_6 - c_{p_c}T_5}{\eta_{CC}Q_{hv} - c_{p_h}T_6} \tag{5.13}$$

- HPT outlet: station 7

Through the energy balance of the high-pressure spool is possible to obtain the temperature of the gases at the exit of the HPT. This energy balance is based on the fact that the HPT is directly connected, through a spool, to the HPC. Therefore, the power consumed by the HPC must be supplied by the HPT, considering the spool mechanic efficiency:

$$\dot{W}_{HPT} = \frac{\dot{W}_{HPC}}{\eta_m} \tag{5.14}$$

$$(1 + f)c_{p_h}(T_6 - T_7) = \frac{c_{p_c}(T_5 - T_4)}{\eta_m} \tag{5.15}$$

$$T_7 = T_6 - \left(\frac{c_{p_c}(T_5 - T_4)}{(1 + f)c_{p_h}\eta_m}\right) \tag{5.16}$$

To calculate the pressure at this station, it is necessary to use the thermodynamic relation representative of a polytropic expansion:

$$P_7 = \frac{P_6}{\left(\frac{T_6}{T_7}\right)^{\frac{\gamma_h}{(\gamma_h-1)\eta_{HPT}}}} \tag{5.17}$$

- LPT outlet: station 8

At the exit of the LPT the hot gases temperature is calculated by using the energy balance of the low-pressure spool. For this case, the LPT is connected, through the spool, with the LPC and the gearbox that drives the fan. Therefore, the worked consumed by the LPC and the fan must be supplied by the LPT, considering the spool mechanic efficiency and the gearbox efficiency:

$$\dot{W}_{LPT} = \frac{\dot{W}_{LPC}}{\eta_m} + \frac{\dot{W}_F}{\eta_m \eta_{gb}} \tag{5.18}$$

$$(1+f)c_{p_h}(T_7 - T_8) = \frac{c_{p_c}(T_4 - T_3)}{\eta_m} + \frac{(1+\beta)c_{p_c}(T_3 - T_2)}{\eta_m \eta_{gb}} \tag{5.19}$$

$$T_8 = T_7 - \left(\frac{c_{p_c}(T_4 - T_3)}{\eta_m(1+f)c_{p_h}} + \frac{(1+\beta)c_{p_c}(T_3 - T_2)}{\eta_m \eta_{gb}(1+f)c_{p_h}}\right) \tag{5.20}$$

To calculate the pressure at this station, it is necessary to use the thermodynamic relation representative of a polytropic expansion:

$$P_8 = \frac{P_7}{\left(\frac{T_7}{T_8}\right)^{\frac{\gamma_h}{(\gamma_h-1)\eta_{LPT}}}} \tag{5.21}$$

- Hot nozzle outlet: station 9

To calculate the hot gases conditions at the exit of the hot nozzle is necessary, to firstly, check for nozzle choking. Therefore, the critical conditions need to be determined:

$$P_{c_h} = P_8\left(1 - \frac{1}{\eta_n}\left(\frac{\gamma_h - 1}{\gamma_h + 1}\right)\right)^{\frac{\gamma_h}{\gamma_h - 1}} \tag{5.22}$$

$$T_{c_h} = \frac{T_8}{\left(\frac{\gamma_h + 1}{2}\right)} \tag{5.23}$$

$$C_{c_h} = \sqrt[2]{\gamma_h R T_{c_h}} \tag{5.24}$$

Having calculated the critical conditions, the next step is to verify if the hot nozzle is chocked:

$$P_{c_h} > P_0 \tag{5.25}$$

If this last condition is verified, then:

$$P_9 = P_{c_h} \tag{5.26}$$

$$T_9 = T_{c_h} \tag{5.27}$$

$$C_9 = C_{c_h} \tag{5.28}$$

Otherwise, the hot nozzle is unchoked and:

$$P_9 = P_0 \tag{5.29}$$

$$T_9 = T_8 - T_8 \eta_n \left(1 - \left(\frac{P_9}{P_8}\right)^{\frac{\gamma_h - 1}{\gamma_h}}\right) \tag{5.30}$$

$$C_9 = \sqrt[2]{2 c_{p_h} (T_8 - T_9)} \tag{5.31}$$

- Cold nozzle outlet: station 10

Similar to what was presented for the hot nozzle, the same is done for the cold nozzle. Therefore, this nozzle also needs to be verified if it is choked or not:

$$P_{c_c} = P_3\left(1 - \frac{1}{\eta_n}\left(\frac{\gamma_c - 1}{\gamma_c + 1}\right)\right)^{\frac{\gamma_c}{\gamma_c - 1}} \tag{5.32}$$

$$T_{c_c} = \frac{T_3}{\left(\frac{\gamma_c + 1}{2}\right)} \tag{5.33}$$

$$C_{c_c} = \sqrt[2]{\gamma_c R T_{c_c}} \tag{5.34}$$

Having calculated the critical conditions, the next is to verify if the cold nozzle is chocked:

$$P_{c_c} > P_0 \tag{5.35}$$

If this last condition is verified, then:

$$P_{10} = P_{c_c} \tag{5.36}$$

$$T_{10} = T_{c_c} \tag{5.37}$$

$$C_{10} = C_{c_c} \tag{5.38}$$

Otherwise, the cold nozzle is unchoked:

$$P_{10} = P_0 \tag{5.39}$$

$$T_{10} = T_3 - T_3\eta_n\left(1 - \left(\frac{P_{10}}{P_3}\right)^{\frac{\gamma_c - 1}{\gamma_c}}\right) \tag{5.40}$$

$$C_{10} = \sqrt[2]{2c_{p_c}(T_3 - T_{10})} \tag{5.41}$$

After all this being done, the next step is to calculate the output variables:

- Specific thrust

$$F_s = \frac{F}{\dot{m}_a} = \left(\frac{\beta}{1+\beta}\right)C_{10} + \left(\frac{\beta}{1+\beta}\right)\left(\frac{RT_{10}}{P_{10}C_{10}}\right)(P_{10} - P_0) + \left(\frac{1}{1+\beta}\right)(1+f)C_9 + \left(\frac{1+f}{1+\beta}\right)\left(\frac{RT_9}{P_9C_9}\right)(P_9 - P_0) - C_0 \quad (5.42)$$

- Thrust Specific Fuel Consumption

$$TSFC = \frac{\dot{m}_f}{F} = \frac{\dot{m}_h f}{F_s \dot{m}_a} = \frac{\frac{\dot{m}_a}{(1+\beta)} f}{F_s \dot{m}_a} = \frac{f}{F_s(1+\beta)} \quad (5.43)$$

5.2.2 Geared Turbofan with Intercooler

The second configuration presented is the geared turbofan with the intercooler positioned between the compressors.

The compressed air after leaving the LPC is diverted to pass through the intercooler, where it will be cooled down by the air in the bypass duct. After its temperature being decreased, the compressed air returns to its normal path and enters the HPC.

To help organize the mathematical model is necessary, to firstly, present the schematic engine layout (Figure 5.2) and its station numbering (Table 5.2), followed by the description of each station.

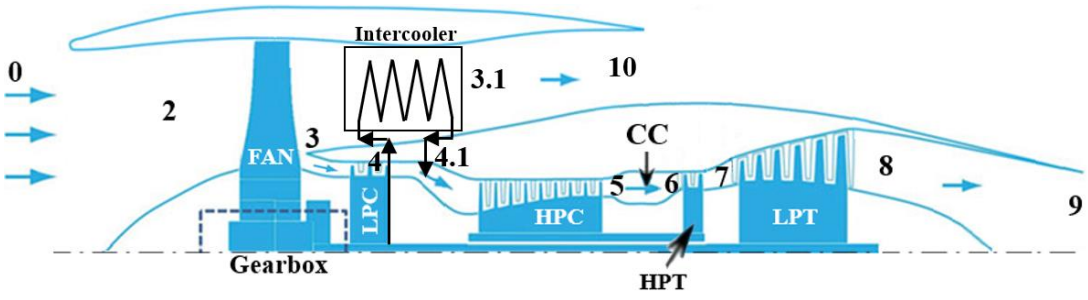

Figure 5.2: Station numbering adopted for the geared turbofan with intercooler [48].

Table 5.2: Description of the stations for the geared turbofan with intercooler.

Station number	Description
0	Free stream
2	Admission
3	Fan outlet
3.1	Intercooler exit
4	LPC outlet
4.1	HPC inlet
5	HPC outlet
6	Combustion chamber outlet
7	HPT outlet
8	Hot nozzle duct
9	Hot nozzle outlet
10	Cold nozzle outlet

With the introduction of the intercooler, the mathematical model for the conventional engine needs to be adapted to this new engine configuration. More precisely, the stations 3.1 and 4.1 are added and to calculate the air conditions in the other stations it is necessary to considerer them.

From station 0 to station 4, the path of the compressed air destined to enter the engine core is not changed, however after this last station it enters the intercooler, and so, its conditions (pressure and temperature) are changed, according with the following equations:

$$P_{4.1} = P_4(1 - \Delta P_{HE}) \tag{5.44}$$

$$T_{4.1} = T_4 - (T_4 - T_3)\eta_{HE} \tag{5.45}$$

It is of extreme importance to verify if the $T_4 > T_3$, because otherwise, the implementation of the intercooler becomes unviable.

Regarding the bypass duct, to calculate the air temperature at station 3.1, it is required to make the energy balance and to calculate the pressure is considered the pressure drop inside this specific heat exchanger:

$$T_4 + \beta T_3 = T_{4.1} + \beta T_{3.1} \tag{5.46}$$

$$T_{3.1} = T_3 + \left(\frac{T_4 - T_{4.1}}{\beta}\right) \tag{5.47}$$

$$P_{3.1} = P_3(1 - \Delta P_{HE}) \tag{5.48}$$

5.2.3 Geared Turbofan with Regenerator

The third configuration presented is the geared turbofan with the other heat exchanger analysed in this study, the regenerator. Being located after the LPT, it recovers heat from the exhaust gases to preheat the compressed air before introducing it into the combustion chamber.

To help organize the mathematical model is necessary, to firstly, present the schematic engine layout (Figure 5.3) and its station numbering, followed by the description of each station (Table 5.3).

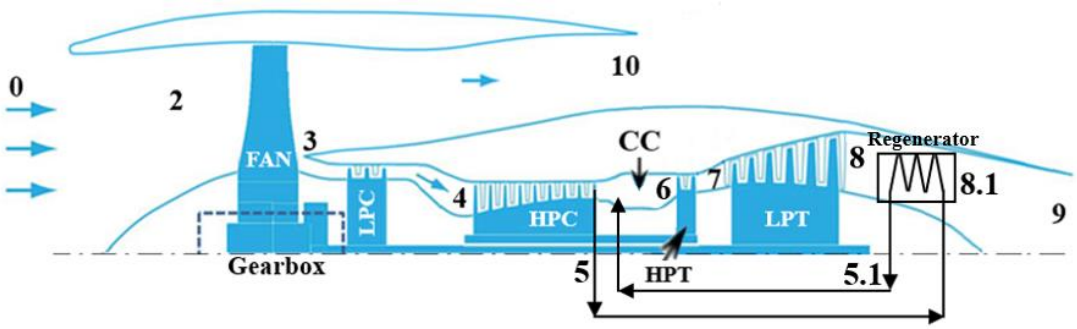

Figure 5.3: Station numbering adopted for the geared turbofan with regenerator [48].

Table 5.3: Description of the stations for the geared turbofan with regenerator.

Station number	Description
0	Free stream
2	Admission
3	Fan outlet
4	LPC outlet
5	HPC outlet
5.1	Combustion chamber inlet
6	Combustion chamber outlet
7	HPT outlet
8	Hot nozzle duct
8.1	Regenerator exit
9	Hot nozzle outlet
10	Cold nozzle outlet

With the introduction of the regenerator, the mathematical model for the conventional engine needs to be adapted to this new engine configuration. More precisely, the stations 5.1 and 8.1 are added and to calculate the conditions of the air and the exhaust gases in the other stations, it is necessary to considerer them.

From station 0 to station 5, the path of the compressed air was not changed, however after this last station it enters the regenerator, and so, its conditions (pressure and temperature) are changed. To determine the pressure at the station 5.1, the following equation is used:

$$P_{5.1} = P_5(1 - \Delta P_{HE}) \tag{5.49}$$

After that, the same reasoning presented above for the station 6 is followed. However, to determine the temperature of the air before entering the combustion chamber, it was assumed, to simplify, that the fuel to air ratio was zero, and so, by taking the equations used for the conventional geared turbofan and equalling the fuel to air ratio to zero, it is possible to calculate the conditions for the stations 7 and 8. By using the efficiency equation for the regenerator, the temperature at station 5.1 is obtained:

$$T_{5.1} = T_5 + \eta_{HE}(T_8 - T_5) \tag{5.50}$$

Having calculated the temperature of the compressed air after passing the regenerator, then it is possible to determine the new value of fuel to air ratio.

It is of extreme importance to verify if the $T_8 > T_5$, because otherwise, the implementation of the regenerator becomes unviable.

As the exhaust gases pass by the recuperator, they suffer a pressure drop and a temperature decrease, which is calculated with the aid of the energy balance equation of the regenerator:

$$P_{8.1} = P_8(1 - \Delta P_{HE}) \tag{5.51}$$

$$(1 + f)c_{p_h}(T_8 - T_{8.1}) = c_{p_c}(T_{5.1} - T_5) \tag{5.52}$$

Therefore,

$$T_{8.1} = T_8 - \left(\frac{(T_{5.1} - T_5)c_{p_c}}{(1 + f)c_{p_h}}\right) \tag{5.53}$$

5.2.4 Geared Turbofan with Intercooler and Regenerator

The fourth and last configuration presented is the geared turbofan with the intercooler and the regenerator. The position for both the heat exchangers remains the same, and so, to analyse this configuration, the last two mathematical models described need to be arranged and incorporated on the first one.

To help organize the mathematical model is necessary to firstly present the schematic engine layout (Figure 5.4) and its station numbering, followed by the description of each station (Table 5.4).

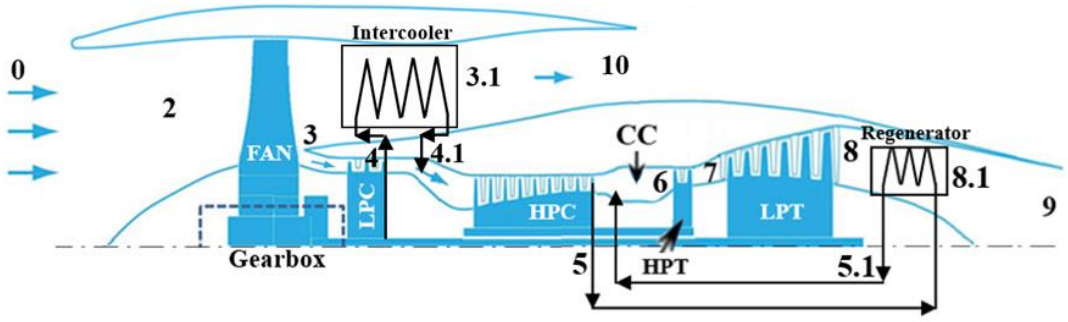

Figure 5.4: Station numbering adopted for the geared turbofan with intercooler and regenerator [48].

Table 5.4: Description of the stations for the geared turbofan with intercooler and regenerator.

0	Free stream
2	Admission
3	Fan outlet
3.1	Intercooler exit
4	LPC outlet
4.1	HPC inlet
5	HPC outlet
5.1	Combustion chamber inlet
6	Combustion chamber outlet
7	HPT outlet
8	Hot nozzle duct
8.1	Regenerator exit
9	Hot nozzle outlet
10	Cold nozzle outlet

Bearing in mind the mathematical model used for this last configuration, which is the most embracing, because it uses both heat exchangers, the next flowchart (Figure 5.5) demonstrates in a simplified and summarized scheme, the logical sequence of ideas applied:

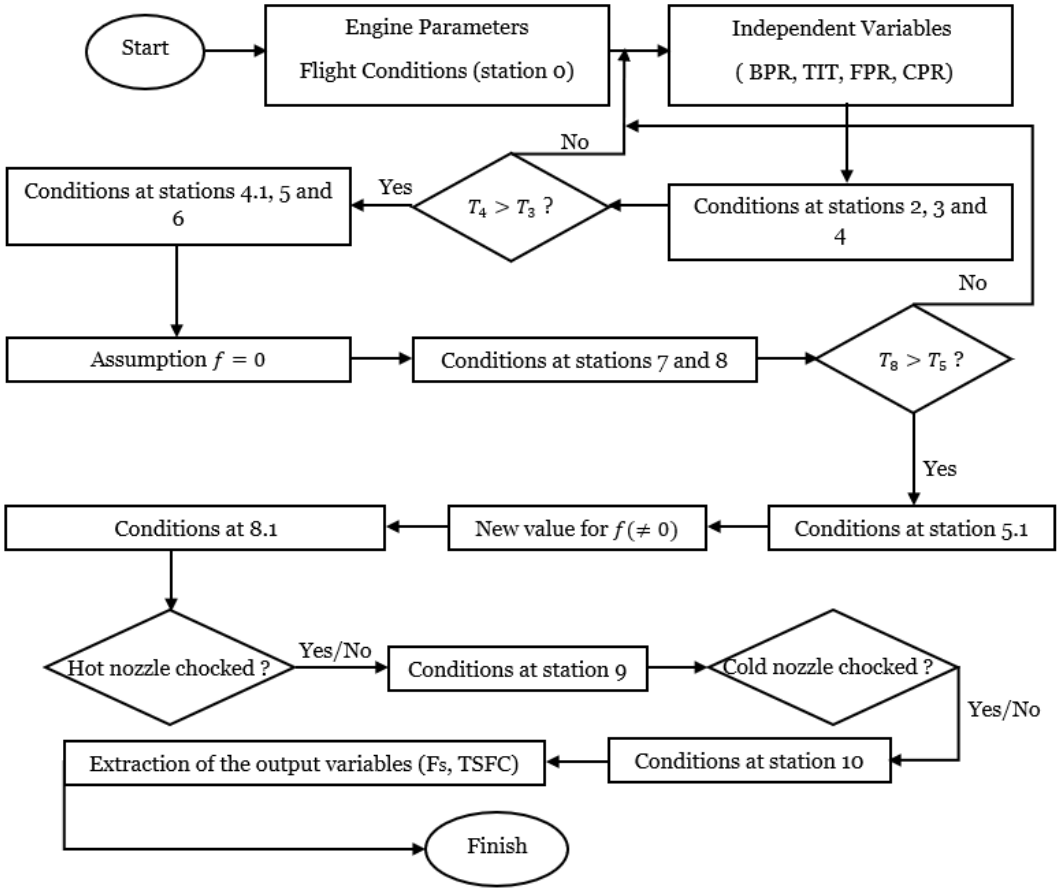

Figure 5.5: Calculation flowchart used for the geared turbofan with intercooler and regenerator.

5.3 Results

In this section are displayed the obtained results from the parametric study.

For an easier comparison between configurations, the results followed a thoughtful and logical presentation. Therefore, for each independent variable that varied for two values of turbine inlet temperature, its effects on the output variables are shown for all the engine configurations.

5.3.1 Bypass Ratio Influence

By varying the bypass ratio (from 10 to 15) for two values of turbine inlet temperature (1520 K and 1850 K), it is possible to obtain for all the configurations, two sets of two graphics each that represent the influence of the bypass ratio on the specific thrust and on the thrust specific fuel consumption.

Firstly, the Figures 5.6 and 5.7 illustrate for all the configurations the influence that the bypass ratio has on the specific thrust for two values of turbine inlet temperature, 1520 K and 1850 K, respectively.

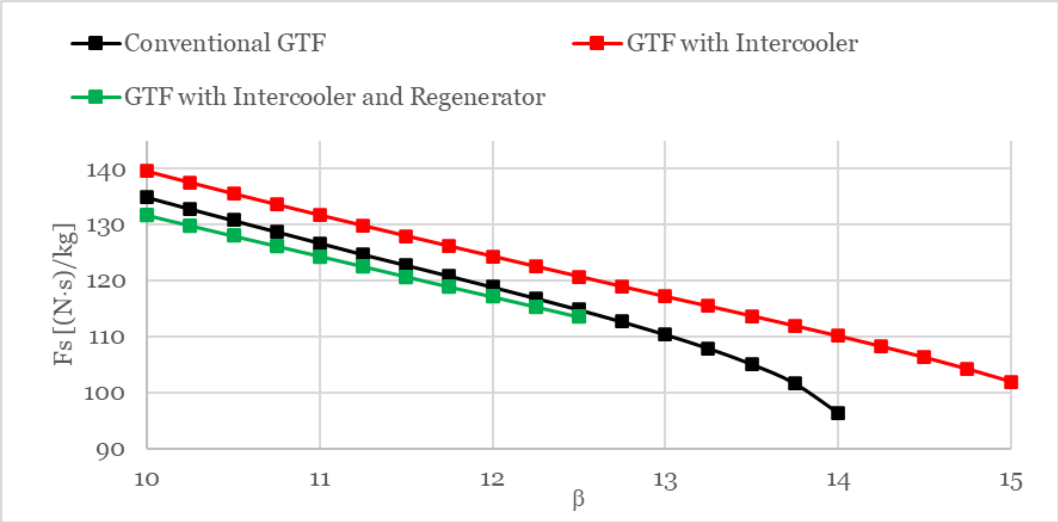

Figure 5.6: Variation of specific thrust with bypass ratio for TIT = 1520 K.

All the configurations showed in this graphic exhibit the same behaviour, i. e., as the bypass ratio rises, the specific thrust decreases. Which means that each configuration has its maximum value of specific thrust at minimum bypass ratio (10).

With a higher value of bypass ratio, more air enters in the bypass duct, and so, the amount of specific thrust produced by the bypassed air increases. Nevertheless, this increment does not prevail against the specific thrust reduction made by the hot stream, and that is why the (total) specific thrust decreases with BPR.

Even though the use of an intercooler leads to a pressure and temperature drop inside the bypass duct, which results in less specific thrust produced by the bypass air, the compression work is reduced, and so, more output power is available in the hot stream. In a nutshell, this makes the intercooler configuration, the one with higher values of specific thrust. Additionally, this configuration is the only one that can operate at high values of

BPR, while the TIT is low. This happens because, since the intercooler reduces the compression work, the LPT is able to extract enough energy from the hot gases to drive the low spool.

As stated above the intercooler improves the amount of specific thrust produced by the hot stream, however the introduction of a regenerator weakens it. Therefore, this makes the configuration with both heat exchangers the one that produces less thrust per unit of air mass flow rate. Whereas the conventional configuration is positioned between the two other configurations.

Although the upper limit considered for the bypass ratio is 15, not all the configurations reach it, nor the configuration with the regenerator is showed. These happens because the turbine inlet temperature is not high enough to allow the low-pressure turbine to drive the low spool. For the configurations with the regenerator having such a low value of turbine inlet temperature is impracticable the use of a regenerator ($T_5 > T_8$) . Bearing these justifications in mind, the following graphic (Figure 5.7) reveals for all the configurations the influence that the bypass ratio has on the specific thrust for a higher value of turbine inlet temperature, 1850 K.

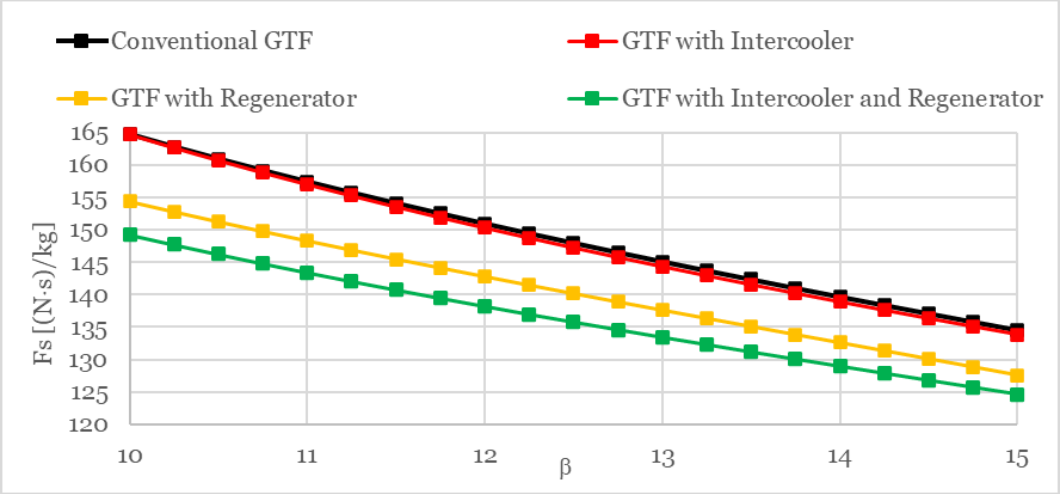

Figure 5.7: Variation of specific thrust with bypass ratio for TIT = 1850 K.

The increase of the turbine inlet temperate does not change the tendency shown in Figure 5.6, therefore, each configuration has its maximum value of specific thrust at minimum bypass ratio (10).

The configuration with intercooler produces slightly less specific thrust than the conventional configuration, which has the highest specific thrust. The reason for this to

happen lays on the fact that, even though the configuration with intercooler has higher values of specific thrust produced by the hot flow, it is not high enough to bridge the difference of specific thrust produced by the bypass air. The same applies for the configuration with the regenerator in comparison with the IR configuration.

The advantage of incorporating an intercooler, in terms of specific thrust produced by the hot flow, almost disappears with the regenerator. Additionally, to aggravate this situation the intercooler decreases the specific thrust produced by the bypass air. All this combined makes the configuration with both the heat exchangers the one that produces less specific thrust, followed by the configuration with regeneration.

With the increase of the turbine inlet temperature, the specific thrust produced by the hot stream increases, which leads to higher values of specific thrust for all configurations. Furthermore, neither there are problems associated with the lack of power to drive both the fan and the LPC, nor the use of a regenerator reveals impracticable.

Secondly, the Figures 5.8 and 5.9 illustrate for all the configurations the influence that the bypass ratio has on the thrust specific fuel consumption for two values of turbine inlet temperature, 1520 K and 1850 K, respectively.

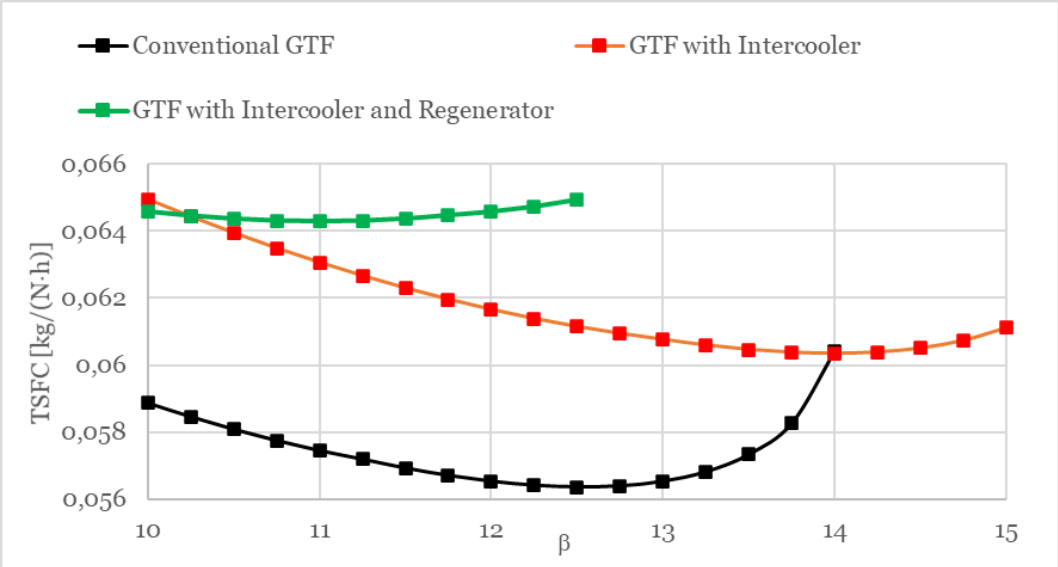

Figure 5.8: Variation of thrust specific fuel consumption with bypass ratio for TIT = 1520 K.

From the graphic shown above, it is possible to verify, even though for the IR configuration the tendency is less pronounced, that all the configurations have the same tendency, i.e., up to a certain value of bypass ratio the TSFC decreases, and after, it increases. The reason why

there is an increase is because the specific thrust suffers a stepper decrease that is not annulled by the bypass ratio increase.

At this low TIT, the regenerator effect is almost neglected, which translates into an amount of fuel consumption of the IR configuration slightly lower than the one verified for the configuration with the intercooler. Moreover, since the former configuration has lower values of specific thrust than the latter, then this makes the IR configuration the one that has the highest values of TSFC for most of the bypass ratio interval.

With the utilisation of the intercooler the temperature at the combustion chamber inlet is lower than for a conventional turbofan, then more fuel needs to be injected in order to achieve the temperature of 1520 K at the inlet of the high-pressure turbine. In this sense, the configuration with intercooler has values of TSFC between the two other configurations.

The non-use of the intercooler allows that the amount of fuel burned is lower, and so the GTF conventional benefits from it. In other words, this configuration has the lowest values of TSFC.

For the same reasons mentioned above (low value of TIT) it is not possible to extend this study to values of bypass ratio near 15 nor to show the configuration with only the regenerator. Therefore, the following graphic (Figure 5.9) reveals for all the configurations the influence that the bypass ratio has on the thrust specific fuel consumption for a higher value of turbine inlet temperature, 1850 K.

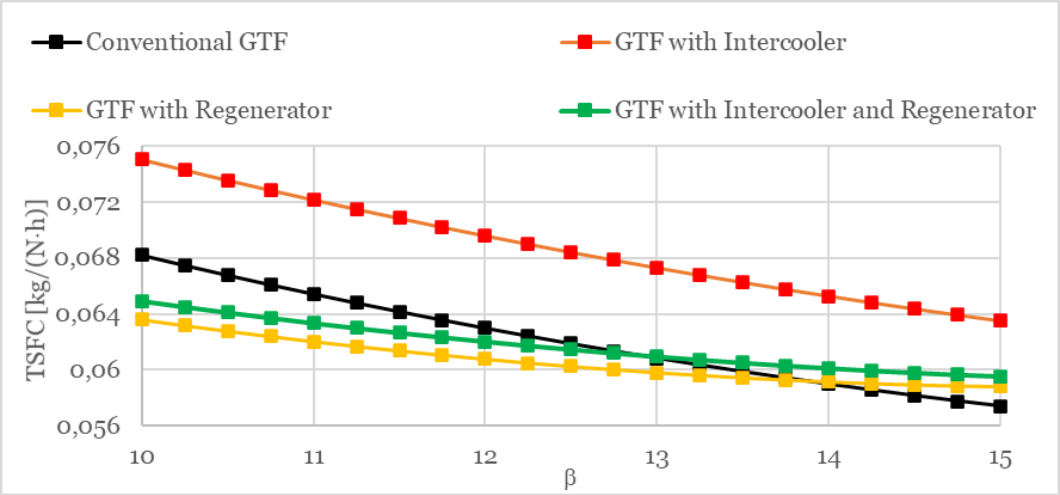

Figure 5.9: Variation of thrust specific fuel consumption with bypass ratio for TIT = 1850 K.

Unlike the previous figure, in this one, the TSFC presents as the bypass ratio rises a steady downward trend that is evident for all the configurations.

By increasing the TIT more fuel needs to be added to reach the temperature of 1850 K at the entrance of the high-pressure turbine, in all the configurations. Since the temperature difference is more significant in the configuration with intercooler, then it has the highest TSFC.

For both the configurations with the regenerator, as the bypass ratio increases, more power is extracted from the LPT, and so, the temperature of the hot gases before entering the regenerator is less. Consequently, this translates into a lower temperature at the entry of the combustion chamber and more fuel is burned. Even though, the amount of fuel burned by the configurations with regenerator is less than the one burned by the conventional configuration, beyond certain values of bypass ratio the configurations with regeneration have higher values of TSFC than the conventional configuration, because the specific thrust is lower.

Additionally, for most of the bypass ratio interval the configuration with regenerator has the lowest values of TSFC, but not the lowest values of fuel consumption, which belongs to the IR configuration. This happens because the intercooler decreases the compression work, and so, the temperature of the gases at the exit of the LPT is higher, and consequently, the temperature of the air after exiting the regenerator is higher, which leads to less fuel burned.

Moreover, by increasing the turbine inlet temperature from 1520 K to 1850 K, there are no longer problems associated with the lack of power to drive both the fan and the LPC, nor the use of a regenerator reveals impracticable.

5.3.2 Fan Pressure Ratio Influence

By varying the fan pressure ratio (from 1.4 to 1.7) for two values of turbine inlet temperature (1520 K and 1850 K), it is possible to obtain for all the configurations, two sets of two graphics each that represent the effect of the fan pressure ratio on the specific thrust and on the thrust specific fuel consumption.

Firstly, the Figures 5.10 and 5.11 illustrate for all the configurations the influence that the fan pressure ratio has on the specific thrust for two values of turbine inlet temperature, 1520 K and 1850 K, respectively.

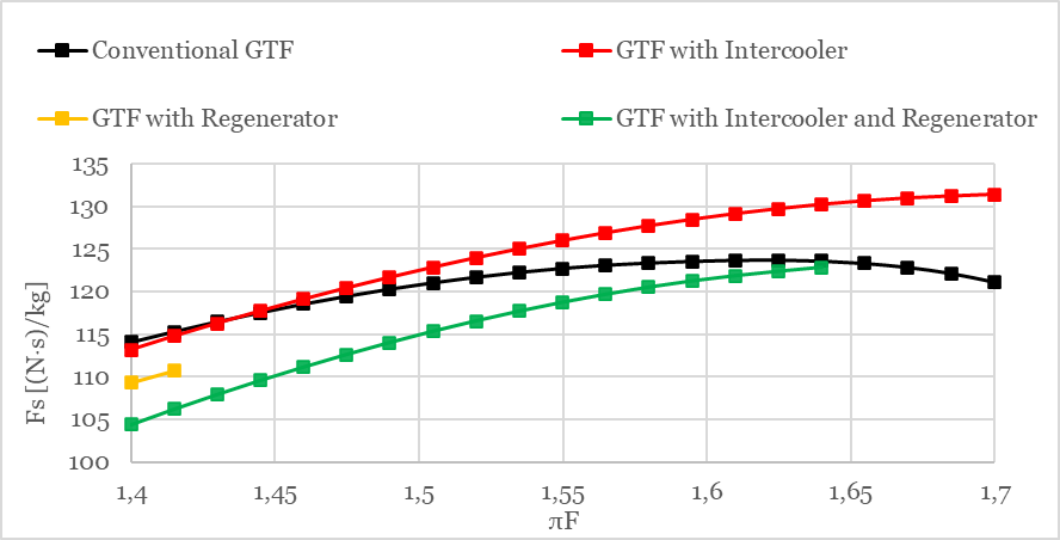

Figure 5.10: Variation of specific thrust with fan pressure ratio for TIT = 1520 K.

For most of the configurations, as the fan pressure ratio increases so does the specific thrust, because the increment of specific thrust produced by the bypassed air prevails against the reduction of specific thrust made by the hot stream. Nevertheless, for high values of FPR, the specific thrust of the conventional configuration diminishes, because the decrease of the specific thrust produced by the hot stream is intensified.

The configuration with intercooler presents for most part of the interval considered the highest values of specific thrust, whereas the configuration with both the heat exchangers reveals the lowest values of specific thrust.

Due to the low impose value of TIT, the use of the regenerator reveals impractical for such high values of FPR (above 1.41), however by combining an intercooler with the regenerator, the conditions of application of this last one are extended.

Since in Figure 5.10, not all the configurations have their specific thrust computed until a fan pressure ratio near 1.7, because the power absorbed by the fan is too high and the TIT is too low to supply it. Therefore, the following graphic (Figure 5.11) reveals for all the configurations the influence that the fan pressure ratio has on the specific thrust for a higher value of turbine inlet temperature, 1850 K.

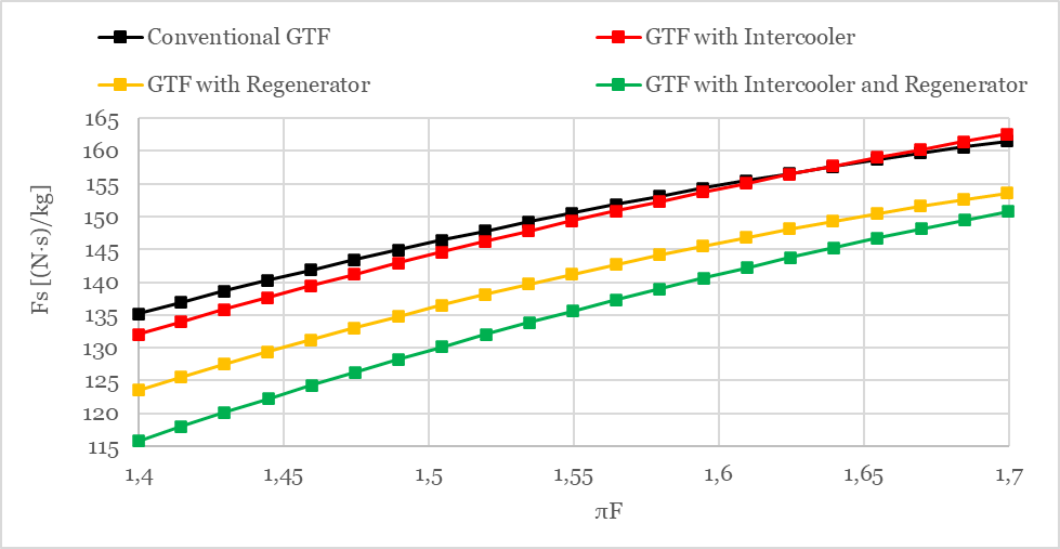

Figure 5.11: Variation of specific thrust with fan pressure ratio for TIT = 1850 K.

For Figure 5.11, all the configurations show the same behaviour, i. e., the specific thrust increases with the fan pressure ratio. Therefore, all configurations reach their maximum of specific thrust at maximum fan pressure ratio (1.7).

Regarding of which configuration produces more thrust per unit of air mass flow rate, the order is more or less similar to the one presented in Figure 5.7. Except, the specific thrust produced by the conventional configuration, which is lower than the one produced by the configuration with intercooler beyond a certain value of fan pressure ratio. This happens because the decrease of the specific thrust produced by the hot stream is intensified with the fan pressure ratio and with the intercooler that decrease is attenuated.

By increasing the TIT, the amount of specific thrust rises, and all configurations are able to operate at higher fan pressure ratios.

Secondly, the Figures 5.12 and 5.13 illustrate for all the configurations the influence that the fan pressure ratio has on the thrust specific fuel consumption for two values of turbine inlet temperature, 1520 K and 1850 K, respectively.

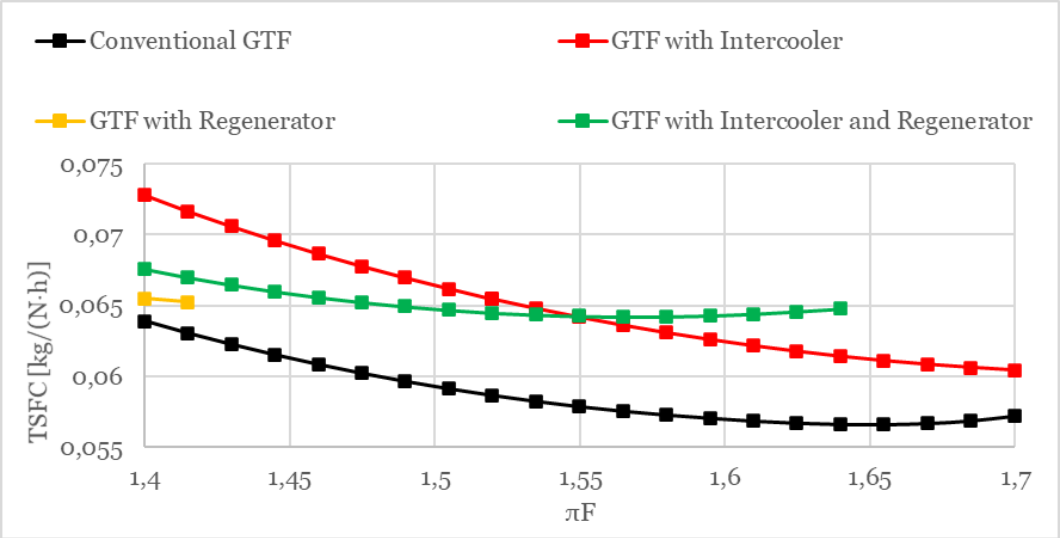

Figure 5.12: Variation of thrust specific fuel consumption with fan pressure ratio for TIT = 1520 K.

The effect of the fan pressure ratio on the thrust specific fuel consumption is similar to the one showed in Figure 5.8. However, the increase of TSFC is more subtle and in the configuration with intercooler the TSFC continues to decrease with fan pressure ratio.

The conventional GTF has the lowest values of TSFC, because even though it has one of the highest values of fuel consumption, it makes the most of it by producing more specific thrust.

Despite the configuration with the regenerator is one of the engines that consumes less fuel, the regenerator is not very efficient at low TIT, which translates into low values of specific thrust, and so, it has higher values of TSFC than the conventional GTF and a narrower interval of operation (from 1.4 to 1.41).

Regarding the two configurations with higher TSFC, while the TSFC of the IR configuration decreases it presents lower values of TSFC than the ones of the configuration with the intercooler. However, beyond a certain FPR it rises, and it is higher. This happens because the specific thrust increase cannot compensate the amount of fuel burned that increases with the fan pressure ratio. The fuel to air ratio only increases for the IR configuration, because more power is needed to drive the fan, and so, the temperature at the entrance of the combustion chamber is lower. With this, below FPR of 1.55, the IR configuration has better values of TSFC, while above 1.55 the opposite is verified.

Since it was not possible to extend this study to values of fan pressure ratio near 1.7, then the following graphic reveals for all the configurations the influence that the fan pressure

ratio has on the thrust specific fuel consumption for a higher value of turbine inlet temperature, 1850 K.

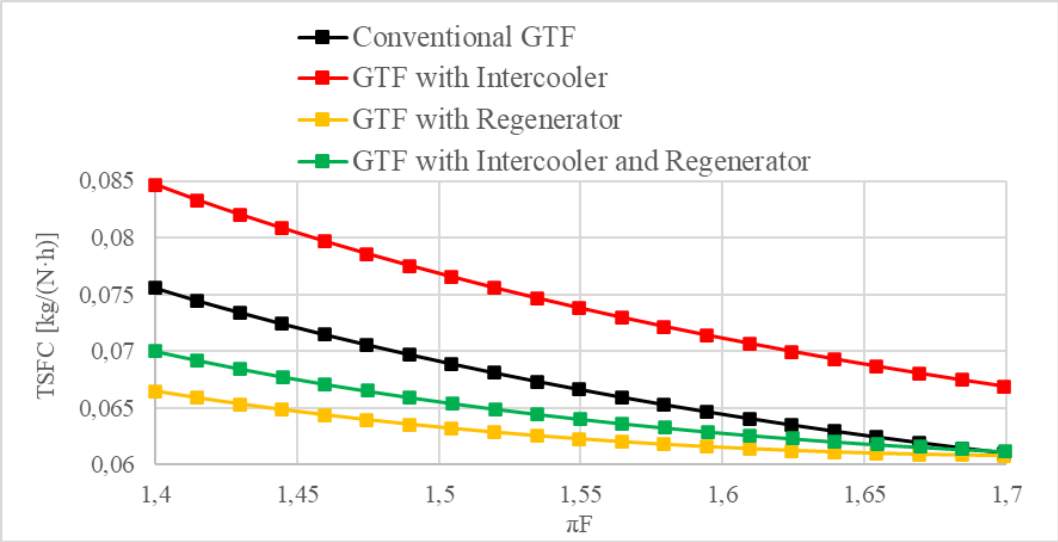

Figure 5.13: Variation of thrust specific fuel consumption with fan pressure ratio for TIT = 1850 K.

The TSFC presents as the fan pressure ratio increases a steady downward trend that is evident for all the configurations. This means that they all reach their optimum value of TSFC at maximum fan pressure ratio (1.7).

By increasing the TIT, the TSFC in all configurations increases, however this increase is more evident on the configurations that do not have the regenerator, because without the help of it, more fuel is burned to reach such high value of TIT. With this, the configuration with intercooler has the highest values of TSFC, followed by the conventional configuration. Whereas the configuration with only the regenerator has the lowest values of TSFC, followed by the IR configuration.

Moreover, by increasing the turbine inlet temperature from 1520 K to 1850 K, neither there are problems associated with the lack of power to drive both the fan and the LPC, nor the use of a regenerator reveals impracticable.

5.3.3 Compressor Pressure Ratio Influence

By varying the compressor pressure ratio (from 20.00 to 28.75) for two values of turbine inlet temperature (1520 K and 1850 K), it is possible to obtain for all the configurations two

sets of two graphics each that represent the effect of the compressor pressure ratio on the specific thrust and on the thrust specific fuel consumption.

Firstly, the Figures 5.14 and 5.15 illustrate for all the configurations the influence that the compressor pressure ratio has on the specific thrust for two values of turbine inlet temperature, 1520 K and 1850 K, respectively.

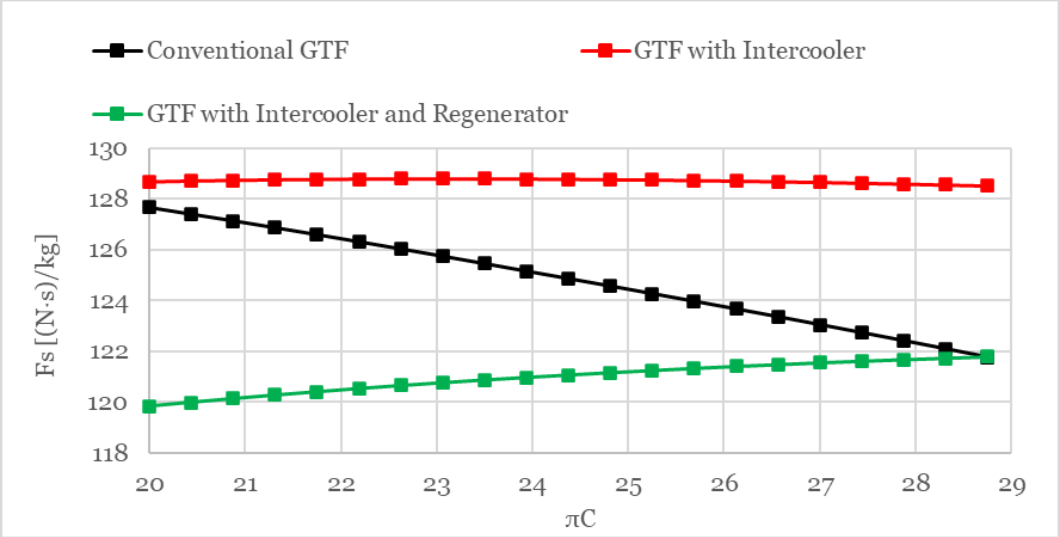

Figure 5.14: Variation of specific thrust with compressor pressure ratio for TIT = 1520 K.

Looking at the graphic (Figure 5.14) for the first time, it is evident that the configurations do not have a common tendency.

As the CPR increases the specific thrust of the conventional GTF decreases. Therefore, this configuration has its maximum value of specific thrust (127 N·s/kg) at minimum pressure ratio (20). Moreover, since this configuration does not have a heat exchanger incorporated, then by varying the compressor pressure ratio the specific thrust produced by the bypass air is not affected and the one produced by the hot stream decreases, because more power is necessary to drive the two compressors.

Regarding the configuration with lower specific thrust (IR configuration), it shows the opposite behaviour, the specific thrust is small at low pressure ratio and then rises with it.

Furthermore, the specific thrust produced by the bypass air also increased with CPR, because the air conditions (temperature and pressure) improve.

As expected for low values of TIT, the configuration with intercooler has the highest value of specific thrust.

In order to obtain results for all the dimension of the compressor pressure ratio interval, the temperature of the LPT inlet was increased to 1850 K. The Figure 5.15 represents that situation.

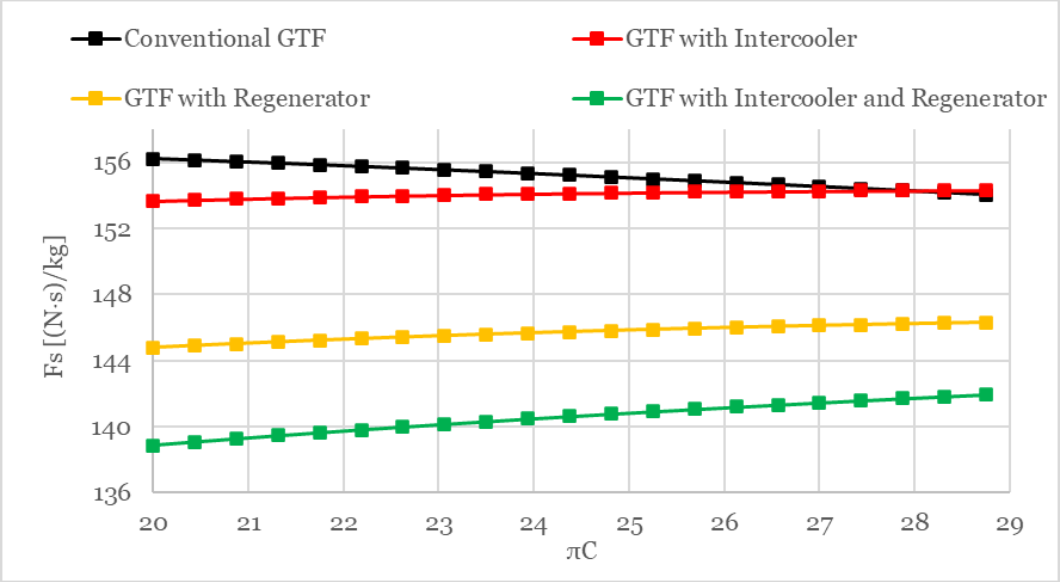

Figure 5.15: Variation of specific thrust with compressor pressure ratio for TIT = 1850 K.

Considering all the other figures relatives to the specific thrust for the same TIT, the configurations appeared with the same order of specific thrust production.

Looking at Figure 5.15, as the CPR rises, the specific thrust for the IR configuration, GTF with Regenerator have a growth much more pronounced than the one showed for the GTF with Intercooler. Moreover, this means that these configurations reach their specific thrust maximum at the higher value of CPR.

For the conventional GTF the contrary occurs, i. e., the specific thrust decreases with CPR. Additionally, this configuration has the highest value of specific thrust of all configurations, which is reached at minimum CPR (162 N·s/kg at 20).

Similarly to what was verified with temperature increase, the values of specific thrust increase in general, and the use of a regenerator become feasible.

Secondly, the Figures 5.16 and 5.17 illustrate for all the configurations the influence that the compressor pressure ratio has on the thrust specific fuel consumption for two values of turbine inlet temperature, 1520 K and 1850 K, respectively.

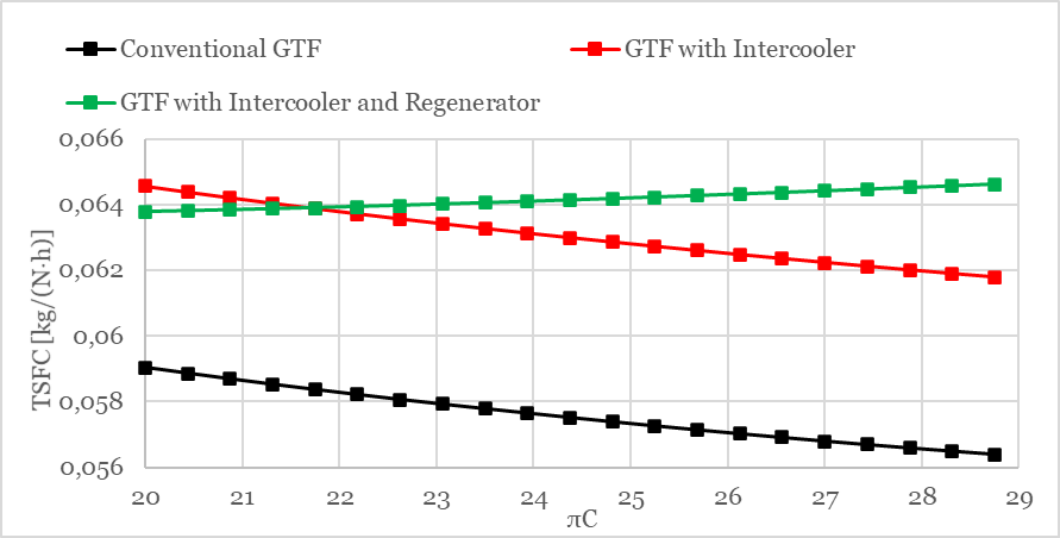

Figure 5.16: Variation of thrust specific fuel consumption with compressor pressure ratio for TIT = 1520 K.

Looking at Figure 5.16, the configurations without a regenerator have the same tendency, which is, the TSFC decreases with CPR, and so, the minimum value of TSFC is reached at high CPR (28.75). This happens because the temperature of the compressed air before entering the combustion chamber increases with CPR, and so less fuel is burned.

The IR configuration has the opposite tendency, reaching its TSFC minimum at low CPR (20), because as the CPR increases, the temperature of the air after exiting the regenerator decreases, and so, more fuel is needed.

As it has been recurrent for the TIT of 1520 K, the conventional configuration has the lowest values of TSFC, whereas the IR configuration has the highest values of TSFC beyond a certain CPR (21.7), overtaking the configuration with the intercooler.

In order to obtain results for all the values of the compressor pressure ratio interval, the temperature of the LPT inlet was increased to 1850 K. The Figure 5.17 represents that situation.

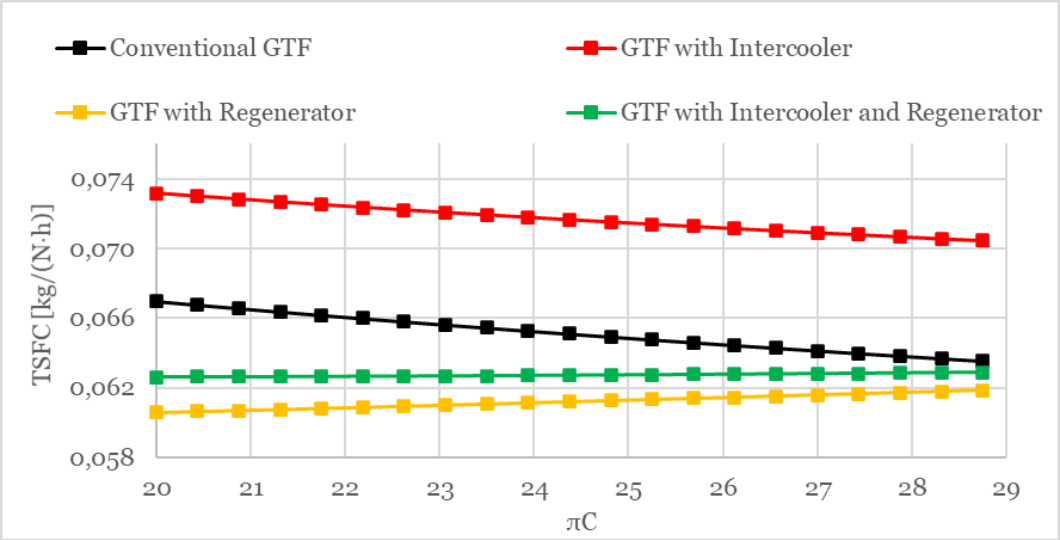

Figure 5.17: Variation of thrust specific fuel consumption with compressor pressure ratio for TIT = 1850 K.

Once again, not only the GTF with Regenerator presents the best behaviour in comparison with all the other configurations, but also the GTF with Intercooler revels to be the configuration with higher values of TSFC.

Similarly to Figure 5.16, the IR configuration, the GTF with Intercooler and the Conventional GTF keep the same tendency as the CPR rises.

For the GTF with Regenerator, as the CPR rises the TSFC increases. This happens because the compressors need more energy to operate, and therefore, the turbines need to extract more energy from the hot gases, which translates into a lower temperature at the entry of the regenerator, and consequently, less heat is transferred to the air, and more fuel is consumed to achieve the defined TIT value (1850 K).

Additionally, with the increase of the TIT, the regenerator effect becomes much more significant, and this translates into the IR configuration, which passes from being one of the configurations with highest values of TSFC to one with the lowest.

Chapter 6

Evolutionary Computation

Although the parametric study was a good indicator of the influence of each parameter on the specific thrust and thrust specific fuel consumption, it is necessary to go further and optimise all the configurations. For this, the author resorts to the concept of evolutionary computation, as a way to use an algorithm that can vary all parameters at the same time, in order to achieve the optimum engine performance.

Before proceeding to the optimisation study, it is necessary to define and explain the concepts - evolutionary computation and genetic algorithms - that serve as a starting point for this study and give an overview of other related aspects. The book "Computational Intelligence" by Engelbrecht [49] is used as a guide for this chapter.

6.1 Evolution

Since the whole world is constantly changing, then for an organism to survive in a dynamically changing and competitive environment, it must improve its ability to adapt to its surroundings. Therefore, the evolution concept consists in an adaptation process with the purpose of optimising the survival skills of a certain organism (or system) through processes, such as, natural selection, survival of the fittest, reproduction, mutation, competition and symbiosis [49].

The concept of evolution can be applied to countless areas (cosmic, chemical and others) and for each one, it may have different interpretations. Nevertheless, since a genetic algorithm is used in the optimisation, then it is best for the purpose of this study to establish an analogy with the biological evolution.

When the subject is biological evolution, it is unavoidable not to mention the names of two great contributors, Jean-Baptiste Lamarck (1744 – 1829) and Charles Darwin (1809 – 1882), and their theories.

On one hand, Lamarck was probably the first to theorize about biological evolution and his theory focused on the inheritance of acquired characteristics. In other words, individuals during their lifetimes have to adapt to the environment they are inserted and transmit their

characteristics to their offspring. In turn, the offspring continues the adaptation process. Additionally, the Lamarckism emphasises that the adaptation method derives from the concept of use and disuse, which succinctly means that with time the individuals lose traits not needed and develop others that are useful for survival [49].

On the other hand, Darwin is considered not only the founder of the theory of evolution, but also of the principle of common descent. The former theory, also known as theory of natural selection, became the foundation of biological evolution. It means that in a world with limited resources and stable population, each individual competes with others to survive, and evidently, those with best characteristics have more chances to survive and to reproduce. This implies that these desirable characteristics will be passed on to their offspring, and so, by the following generations inheriting these characteristics, with time they become dominant amongst the population. Darwin's theory also refers that, during the conception of a child organism, random events may occur, leading to random changes to the child organism's traits. If these new traits turn out to be benefic to the organism, then it has more chances of surviving [49].

Bearing in mind all this, the evolutionary computation (EC) implies solving computer-based problem systems by using computational models based on evolutionary processes (natural selection, survival of the fittest and reproduction) [49].

6.2 Generic Evolutionary Algorithm

The concept of evolution through natural selection of a randomly chosen population of individuals can be defined as a search through the space of possible chromosome values, where each individual is encoded by a chromosome. In this context, an evolutionary algorithm (EA) can be described as a stochastic search for an optimal solution to a given problem [49]. The key elements of an EA that influence the evolutionary search process are [49]:

- Encoding the solutions as a chromosome;
- Creation of a function to evaluate the fitness (objective function), or the survival strength of each individual;
- Initialization of the first population;
- Selection operators;
- Reproduction operators.

To understand how these key elements are combined to form a generic EA, it is easier to consider the instant t=0, in which the initial population is created. Then, while the stopping criteria is not met, the iteration process begins and for each individual the fitness is evaluated, reproduction is performed to create offspring and a new population is created for the next generation. Each iteration corresponds to a new generation.

Additionally, the EA incorporates both parts of Darwin's theory:

- Natural selection, which choses the "best" individuals to produce offspring and to be selected for the new generation;
- Random changes may occur due to the mutation operator.

6.3 Representation of the Chromosome

In nature, organisms possess a set of characteristics that affect their ability to survive and to reproduce. From a biology perspective, these characteristics are represented by long strings of information contained in the chromosomes of the organism [49]. A chromosome, also known as a genome, is a structure found inside the nucleus of a cell that carries genetic information in the form of genes. Genes are the basic unit of heredity, and they contain the information related to the individual's anatomical and physiological characteristics. In that sense, each individual has a unique sequence of genes.

From the EC standpoint, each individual is a candidate solution to an optimisation problem. Moreover, its characteristics are represented by a chromosome and each characteristic, also referred to as gene, corresponds to a certain variable that needs to be optimised.

When designing an EA, one of the most important things to do, is to choose the appropriate way of representing the candidate solutions (chromosomes), because otherwise, the efficiency and complexity of the algorithm will be negatively affected. Although different paradigms use different representation schemes, the most common is to encode the solutions/individuals as vectors [49].

6.4 Initial Population

When using EA to solve an optimisation problem the first step is to create an initial population and the standard way to do it is by assigning random values from the allowed domain to each of the genes of each chromosome. Although it seems simple, if the initial

population is not a uniform representation of the entire search space, then some regions will be neglected, and the EA will be critically affected [49].

One other aspect that needs to be chosen for the initial population, because eventually, it will affect the computational complexity and exploration abilities, is its size. On one hand, a bigger number of individuals translates into a more diverse population, which improves the exploration abilities, but increases the computational complexity per generation. Additionally, it also increases the time per generation, but fewer generations are required to find an acceptable solution. On the other hand, a small population will represent a small region of the search space, and so, not only the complexity per generation is low, but also the execution time (per generation). However, the EA might need more generations to locate the optimum solution. [49]

For a small population, one of the problems is low diversity of individuals and a way to overcome this is by forcing the EA to explore more of the search space by increasing the mutation rate (which will be discussed later).

6.5 Fitness Function

In accordance with the Darwinian model of evolution, individuals with the "best" traits are more likely to survive and to reproduce. Therefore, to evaluate the ability of an individual to survive, a mathematical function, known as fitness function, is used. This function indicates how good the solution encoded by a chromosome is and it helps to represent the chromosome into a scalar value [49]:

$$f : \Gamma^{n_x} \rightarrow \mathbb{R} \tag{6.1}$$

Where Γ is the data type of the elements of an n_x dimensional chromosome.

The fitness function acts like a representation of the objective function, Ψ, which describes the optimisation problem. However, in such cases, the chromosome representation does not correspond to the expected representation of the objective function. In that sense, a more detailed description of the fitness function is used [49]:

$$f: S_C \mathbb{R} \xrightarrow{\Phi} S_X \xrightarrow{\Psi} \mathbb{R} \xrightarrow{\Upsilon} \mathbb{R}_+ \tag{6.2}$$

Where S_C is the search space of the objective function, and Φ, Ψ and Υ respectively represent the chromosome decoding function, the objective function and the scaling function.

Normally, the fitness function gives an absolute fitness measure, and so, it is possible to evaluate the solution by directly applying the objective function. However, for some applications it is not possible to determine an absolute measure of fitness, and hence, a relative fitness measure is used to quantify the performance of an individual in comparison to others in the population [49].

Since exist different types of optimisation problems, then it also exists different types of fitness functions, they are [49]:

- Unconstrained problems: the fitness function is the objective function;
- Constrained problems: some EAs suffer some changes to have a fitness function with two objectives. One is the original objective function, while the other is just a constraint in the shape of a penalty function;
- Multi-Objective problems: multiple objectives need to be simultaneously optimised and one of the approaches is to use weight aggregation methods, where the fitness function is a weighted sum of all the sub-objectives, or the Pareto-based optimisation algorithm;
- Dynamic and noisy problems: function values of solutions are time dependent.

6.6 Selection Operators

According to the Darwinian theory, the natural selection choses the fittest individuals to survive, thereby, the selection operators are used to help finding the best solutions. This can be achieved by two ways [49]:

- Selection of the new population: at the end of each generation, a new population of candidate solutions is selected, in order to serve as the population of the next generation. The individuals for this new population can be selected from the offspring, or from both the parents and the offspring. Moreover, the selection operator needs to guarantee that good individuals do survive to next generations;
- Reproduction: offspring are created through crossover and/or mutation operators. When selecting parents for crossover, they should be the most fit ones, in order to ensure that the offspring contains genetic material of the best individuals. In terms of mutation, the least fit individuals are selected with hope that the mutation will result in introducing better traits, and so, increasing their chances of survival.

6.7 Reproduction Operators

Reproduction is one of the main operators in EAs and is the process of generating offspring from selected parents by applying crossover and/or mutation operators [49].

The idea behind crossover is to create one or more individuals by randomly combining genetic material from two or more parents - hopefully the best characteristics of each parent [49].

Mutation is the process of randomly selecting genes in a chromosome and changing its values. With this, new genetic material is introduced into the population, and so, the genetic diversity is increased. Nevertheless, the mutation operator needs to be use with care, because otherwise, it might negatively affect the good genetic material in highly fit individuals. In this sense, mutation is normally applied at a low probability, but for least fit individuals the mutation probability can be changed to higher values, i.e., less fit the individual is, more it is mutated [49].

One last important information about reproduction is that newly generated individuals (offspring) only replace their parents if their fitness is better than of the corresponding parents.

6.8 Stopping Conditions

The EA generates at each iteration a new generation that gets closer to the optimum solution. Therefore, it is necessary to define conditions that after being satisfied stops the EA from producing more generations. The simplest way of doing this is by limiting the number of generations, however this number should not be too small, because otherwise, not all the search space is explored. As a complement to this stopping condition, normally is used a convergence criterion to detect if the population has become stagnant. The following convergence criteria can be applied [49]:

- Stop when no significant improvement is observed over a number of consecutive generations;
- Stop when there is no change in the population;
- Stop when an acceptable solution has been found;
- Stop when the objective function slope is approximately zero.

6.9 Genetic Algorithms

Genetic algorithms (GAs) consist in optimisation techniques based on the principle of biological evolution through natural selection.

The genetic algorithms are used to solve constrained and unconstrained optimisation problems. Furthermore, when the objective function is discontinuous, nondifferentiable, stochastic, or highly nonlinear, the GA is more suited to solve this kind of problems than the standard optimisation algorithms [50].

The genetic algorithm, which models genetic evolution, works as follows [50]:

1. A random initial population of candidate solutions is created through the allowed domain of the selected variables;
2. A sequence of new populations is created, using the individuals in the previous generation, according to the following steps:

a. Within the current population, the survival strength (fitness value) of each individual is measured using the fitness function;
b. The best individuals (elite) of the current population survive to the next population without being mutated;
c. Basing on the fitness values, the parents are selected;
d. The offspring is produced either by making random changes to a single parent (mutation) or by combining the characteristics of a pair of parents (crossover);
e. The offspring accompanied with the elite forms the new population for the next generation;

3. When the stopping criteria is satisfied the algorithm stops.

Chapter 7

Multi-Objective Optimisation

In most real-world problems, several objective functions subject to a set of constraints must be optimised simultaneously. Usually, these objectives are in conflict with one another, and so, to find solutions, it is important to have a trade-off between the objectives.

Since in this chapter the optimisation problem consists in optimising a parameter that is in conflict with other, then it is important to first provide to the reader a theoretical overview of multi-objective problems and its formulation. Moreover, in this chapter is given an overview about the method used to solve the MOP and are presented the conditions in which the MOP took place, followed by its results for all the configurations.

7.1 Multi-Objective Problem

Before proceeding to the MOO configuration used in this dissertation, it is necessary to define some concepts that were essential for its creation. These concepts can be found in the book "Computational Intelligence" by Engelbrecht [49].

To achieve the goal of an optimisation problem, the optimisation algorithm needs to search for a solution in the search space, also referred to as decision space.

Considering $\mathcal{S} \subseteq \mathbb{R}^{n_x}$ the n_x dimensional search space and the $\mathcal{F} \subseteq \mathcal{S}$ the feasible space. Assuming the vector $x = (x_1, x_2, \dots, x_n) \in \mathcal{S}$, the decision vector, which satisfies the constraints and optimises the objective vector whose elements represent the objective functions. A single objective function, $f_k(x)$, is defined as $f_k : \mathbb{R}^{n_x} \rightarrow \mathbb{R}$. Therefore, an objective vector containing n_k objective functions is represented by: $f(x) = \left(f_1(x), f_2(x), \dots, f_{n_k}(x)\right) \in \mathcal{O} \subseteq \mathbb{R}^{n_k}$, where $\mathcal{O}$ is the objective space [49].

Taking into consideration the notation above, the multi-objective optimisation problem is defined as [49]:

$$\text{Minimise} \quad f(x) \tag{7.1}$$

Subject to $$g_m(x) \leq 0,\ m = 1, \dots, n_g$$

$$h_m(x) = 0,\ m = n_g + 1, \dots, n_g + n_h$$

$$x \in [x_{min}, x_{max}]^{n_x}$$

Where g_m and h_m represent, respectively, the inequality and equality constraints, while $x \in [x_{min}, x_{max}]$ is the boundary constraint.

In uni-objective optimisation the term "optimum" is easy to be defined, because only one objective is optimised. However, for a MOO, it is not that simple. As referred above, the problem lays on the fact that there are conflicting objectives, i.e., to improve one objective another might be deteriorated. Therefore, to find solutions a balanced trade-off needs to occur. By balance comprehend a solution that cannot improve any objective without degrading one or more of the other objectives. For example, in this chapter the optimisation goal is to maximise specific thrust and to minimise thrust specific fuel consumption. However, these two parameters enter in conflict, because to maximise the specific thrust, the thrust specific fuel consumption needs to increase. So, this latter is degraded by the improvement of the former. To solve this, instead of a single solution, a set of good compromises is produced. This set is known as the non-dominated set, or the Pareto-optimal set.

In that sense, there are two ways of solving the MOP with the genetic algorithm:

- Weighted Aggregation Method: the objective function is a weighted sum of the sub-objectives;
- Pareto Optimisation Method: a dominance relation is used to obtain the Pareto front.

Since the last method was the one chosen, then this chapter will focus on it and in its associated concepts.

7.2 Pareto Optimisation Method

In this section, several concepts related to the Pareto Optimisation Method that served as base for this study are reviewed.

A decision vector, x_1, dominates a decision vector, x_2, if and only if:

- x_1 is not worse than x_2 in all objectives, i.e. $f_k(x_1) \leq f_k(x_2), \forall\, k = 1, \dots, n_k$;
- x_1 is strictly better than x_2 in at least one objective, i.e. $\exists k = 1, \dots, n_k$: $f_k(x_1) < f_k(x_2)$.

Following a similar line of though, an objective vector, f_1, dominates another objective vector, f_2, if f_1 is not worse than f_2 in all objective functions and f_1 is better than f_2 in at least one of the objective values.

For a function with two objectives, $f(x) = (f_1(x), f_2(x))$, the concept of dominance is well expressed in Figure 7.1, where the striped represents the area of objective vectors dominated by f.

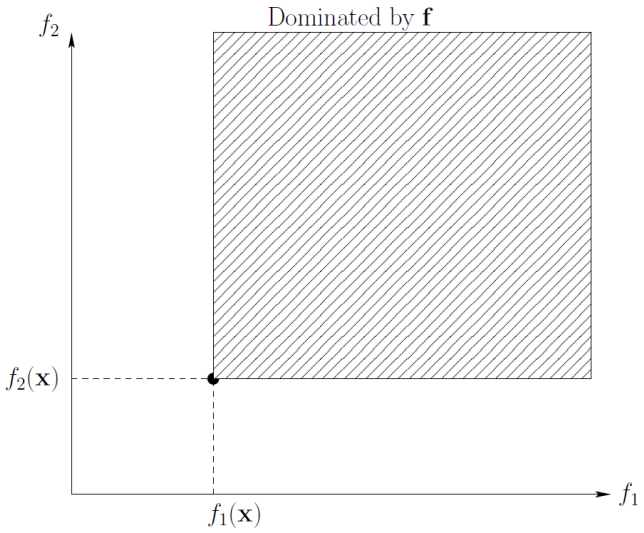

Figure 7.1: Illustration of the dominance concept [49].

The Pareto-optimal can be defined as follows: a decision vector, $x^* \in \mathcal{F}$ is Pareto-optimal, i.e. vector optimised by the Pareto method, if there does not exist a decision vector, $x \neq x^* \in \mathcal{F}$ that dominates it. In this sense, $\nexists$: $f_k(x) < f_k(x^*)$. An objective vector, $f^*(x)$, is Pareto-optimal if x is also Pareto-optimal.

Therefore, for a multi-objective problem, it is necessary to define a set that contains all the Pareto-optimal decision vectors, also referred to as Pareto-optimal set:

$$\mathcal{P}^* = \{x^* \in \mathcal{F} | \nexists x \in \mathcal{F} : x \prec x^*\} \tag{7.2}$$

Where, $x \prec x^*$, means that x dominates x^*.

The corresponding objective vectors of the Pareto-optimal set are named the Pareto-optimal front, $\mathcal{P}^*\mathcal{F} \subseteq \mathcal{O}$, which is defined as:

$$\mathcal{P}^*\mathcal{F} = \{f = (f_1(x^*), f_2(x^*), \dots, f_k(x^*)) | x^* \in \mathcal{P}\} \quad (7.3)$$

As illustrated in Figure 7.2, the Pareto front contains all the not dominated objective vectors.

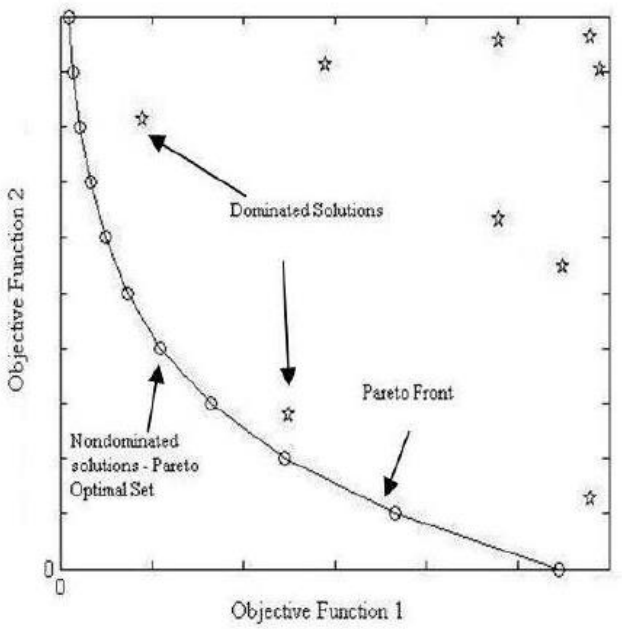

Figure 7.2: Pareto front example [51].

7.3 Multi-Objective Optimisation Configuration

In this section, it is shown the conditions in which the MOO was performed.

To solve this MOO, the author re-used the scripts utilized in the parametric study and the algorithm was created using the MATLAB.

Following the parametric study, a multi-objective optimisation was performed to find a set of parameter values that optimise all the different engine configurations in terms of specific thrust and thrust specific fuel consumption. These parameters, also referred to as independent variables, assumed non fixed values, which means that they all varied simultaneously inside the allowed domain. In this sense, the independent variables are the same ones considered for the parametric study and the range for each considered variable is:

- BPR: from 10 to 15;
- TIT: from 1520 K to 1850 K;

- FPR from 1.4 to 1.7;
- CPR from 20 to 27.06.

To meet the needs and the requirements of today and future's turbofan engines, this optimisation aims to maximise the specific thrust and minimise the thrust specific fuel consumption. Therefore, the decision vector has a dimension of four (equal to the number of variables) and the objective vector is composed of two objective functions, as shown below:

Minimise
$$f(x) = \begin{bmatrix} f_1(x) \\ f_2(x) \end{bmatrix} = \begin{bmatrix} -F_s(x) \\ TSFC(x) \end{bmatrix} \tag{7.4}$$

Where,

$$x = \begin{bmatrix} x_1 \\ x_2 \\ x_3 \\ x_4 \end{bmatrix} = \begin{bmatrix} BPR \\ TIT \\ FPR \\ CPR \end{bmatrix} \tag{7.5}$$

Subject to
$$\begin{bmatrix} x_1 \\ x_2 \\ x_3 \\ x_4 \end{bmatrix} \in \begin{bmatrix} 10, 15 \\ 1520, 1850 \\ 1.4, 1.7 \\ 20, 27.06 \end{bmatrix} \tag{7.6}$$

To execute the optimisation, several decisions had to be made due to the variety of options available. In Table 7.1 are summarized the MOO settings.

Table 7.1: MATLAB solver settings.

Parameter/ Option	Configuration/ Value
Constraints Domain	[10, 1520, 1.4, 20] to [15, 1850, 1.7, 27.06]
Population dimension	150
Creation Function	Linear Feasible
Crossover Function	Heuristic

(continued on next page…)

Table 7.1: (continued)

Parameter/ Option	Configuration/ Value
Crossover Fraction	0.6
Distance Measure Fraction	@distancecrowding, 'phenotype'
Function Tolerance	1×10^{-4}
Generations	1000
Stall Generation Limit	10
Migration Direction	'both'
Migration Fraction	0.10
Mutation Function	Adaptive Feasible
Pareto Fraction	0.5
Selection Function	'Tournament'

Regarding Table 7.1, several new concepts are presented, and so, there descriptions are summarized below [52]:

- Creation Function: creates a random well dispersed initial population within the defined domain;
- Crossover Function: combines two parents to produce a child for the next generation. This particular function, heuristic, produces a child that has more similarities with the fittest parent than with the less fit. It is possible to specify how far the child is from the fittest parent (parameter ratio);
- Crossover Fraction: fraction of individuals in each population made up of crossover;
- Distance Measure Function: calculates the distance between individuals by using the fitness functions space ('phenotype'). This function helps ensuring diversity on the Pareto front and favours the individuals closer to it;

- Function Tolerance: the algorithm stops when the average relative change in the fitness function value is less than the Function Tolerance for a defined number of generations (Stall Generation Limit);
- Generations: maximum number of populations that the genetic algorithm generates;
- Stall Generations Limit: the algorithm stops when for a defined number of generations, the average relative change in the fitness function value is less than the Function Tolerance;
- Migration Direction: individuals move between subpopulations, i.e., the best individuals from one subpopulation migrate to another and there replace the worst individuals. The term 'both' means that the individuals move from the n^{th} subpopulation to the subpopulations: $(n-1)$ and $(n+1)$;
- Migration Fraction: fraction of individuals in each subpopulation that migrate;
- Mutation Function: responsible for generating mutated children by randomly changing the individuals' characteristics. The option 'adaptivefeasible' randomly chooses a direction that varies according with the success of unsuccess of the previous generation. Moreover, a step length is defined in order that for each iteration the defined boundaries are not exceeded;
- Pareto Fraction: fraction of individuals from the population present in the Pareto front;
- Selection Function: selects individuals for the next generation based on their fitness value. The option 'tournament' works by selecting two random individuals to be potential parents, and then, the best individual is chosen to be a parent.

7.4 Results

This section introduces the results of all configurations stemming from the MOO.

The following tables and graphics exhibit the solutions that compose the Pareto front of each configuration.

7.4.1 Conventional GTF

Table 7.2 shows the values of the independent variables that optimise the chosen performance parameters for the conventional configuration.

Table 7.2: Pareto front results for the conventional GTF.

BPR	TIT [K]	FPR	CPR	Fs [(N·s)/kg]	TSFC [kg/(N·h)]
10.00	1847	1.700	20.01	173.8	0.06699
10.05	1847	1.700	20.18	173.4	0.06678
10.15	1844	1.699	20.32	172.2	0.06636
10.18	1844	1.700	20.35	172.0	0.06623
10.27	1841	1.700	20.54	171.1	0.06584
10.28	1844	1.700	20.57	171.3	0.06592
10.40	1839	1.699	20.75	169.7	0.06530
10.47	1838	1.698	20.90	168.9	0.06507
10.60	1841	1.699	21.14	168.2	0.06467
10.61	1835	1.699	21.06	167.8	0.06452
10.66	1835	1.700	21.22	167.3	0.06428
10.71	1835	1.699	21.27	166.9	0.06417
10.76	1835	1.697	21.35	166.4	0.06408
10.92	1832	1.699	21.63	165.0	0.06341
11.01	1828	1.699	21.76	163.9	0.06303
11.03	1834	1.699	21.90	164.2	0.06309
11.32	1825	1.699	22.36	161.3	0.06197
11.41	1818	1.697	22.45	159.9	0.06162

(continued on next page…)

Table 7.2: (continued)

BPR	TIT [K]	FPR	CPR	Fs [(N·s)/kg]	TSFC [kg/(N·h)]
11.51	1822	1.698	22.65	159.6	0.06139
11.58	1820	1.697	22.77	158.9	0.06118
11.66	1816	1.699	22.96	158.0	0.06077
11.69	1812	1.699	22.88	157.5	0.06066
11.85	1819	1.700	23.27	156.9	0.06031
11.86	1806	1.697	23.16	155.6	0.06011
11.91	1812	1.698	23.34	155.7	0.06006
11.99	1815	1.698	23.52	155.4	0.05991
12.05	1812	1.697	23.59	154.6	0.05970
12.11	1811	1.699	23.69	154.2	0.05949
12.29	1806	1.697	24.13	152.4	0.05895
12.39	1832	1.700	24.69	153.8	0.05903
12.43	1794	1.693	23.98	150.1	0.05859
12.44	1782	1.698	23.88	149.2	0.05825
12.45	1801	1.696	24.19	150.7	0.05856
12.51	1804	1.697	24.50	150.6	0.05840
12.62	1797	1.696	24.56	149.2	0.05808
12.71	1789	1.698	24.49	147.9	0.05777

(continued on next page…)

Table 7.2: (continued)

BPR	TIT [K]	FPR	CPR	Fs [(N·s)/kg]	TSFC [kg/(N·h)]
12.77	1807	1.697	25.03	148.8	0.05782
12.83	1802	1.696	25.05	148.0	0.05765
12.85	1802	1.696	25.05	147.9	0.05762
13.01	1801	1.697	25.41	146.6	0.05723
13.03	1780	1.695	24.94	144.5	0.05706
13.04	1784	1.696	25.20	144.8	0.05700
13.08	1796	1.699	25.44	145.7	0.05701
13.18	1782	1.693	25.30	143.6	0.05681
13.27	1778	1.695	25.58	142.4	0.05650
13.40	1776	1.692	25.68	141.2	0.05634
13.51	1776	1.690	25.80	140.4	0.05622
13.51	1776	1.695	26.17	140.4	0.05603
13.65	1769	1.692	26.07	138.6	0.05588
13.71	1765	1.698	26.34	137.8	0.05563
13.81	1773	1.696	26.56	137.8	0.05558
13.87	1775	1.695	27.06	137.3	0.05541
13.94	1722	1.678	25.95	131.2	0.05539
13.98	1756	1.694	26.58	134.7	0.05527

(continued on next page…)

Table 7.2: (continued)

BPR	TIT [K]	FPR	CPR	Fs [(N·s)/kg]	TSFC [kg/(N·h)]
14.06	1761	1.689	26.77	134.5	0.05526
14.23	1728	1.696	26.81	129.3	0.05497
14.24	1733	1.685	26.45	130.2	0.05508
14.30	1725	1.700	26.67	128.2	0.05501
14.39	1743	1.689	26.94	130.0	0.05490
14.52	1735	1.682	26.94	128.1	0.05486
14.61	1730	1.679	26.94	126.8	0.05484

The Pareto front corresponding to these results is showed in Figure 7.3, accompanied with the tendency line.

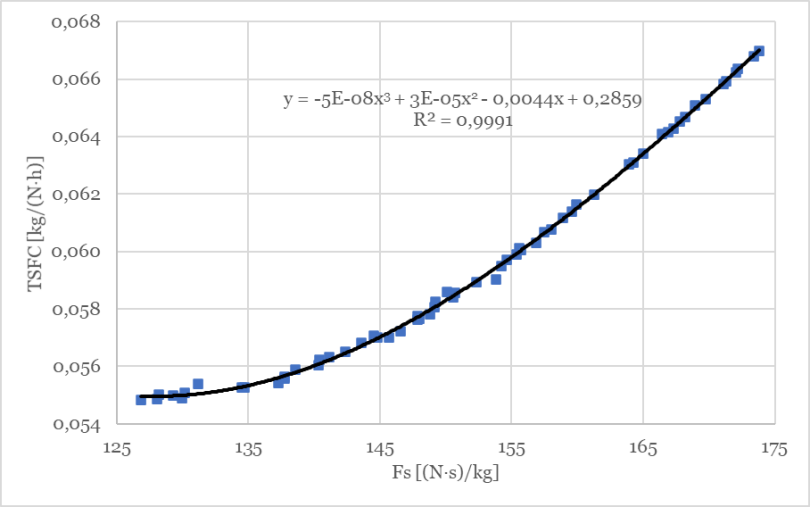

Figure 7.3: Variation of TSFC with Fs for the conventional GTF (Pareto front results).

This choice of values by the algorithm met the tendency shown in the parametric study, i.e., to maximise the specific thrust, the algorithm chose high values of TIT and FPR, and low

values of BPR and CPR. Whereas to minimise the TSFC, the BPR, the FPR and the CPR achieved high values and the TIT lower values.

7.4.2 GTF with Intercooler

Table 7.3 shows the values of the independent variables that optimise the chosen performance parameters for the configuration with intercooling.

Table 7.3: Pareto front results for the GTF with Intercooler.

BPR	TIT [K]	FPR	CPR	Fs [(N·s)/kg]	TSFC [kg/(N·h)]
10.00	1753	1.700	26.02	166.5	0.06779
10.04	1753	1.700	26.03	166.2	0.06767
10.07	1752	1.699	26.05	165.8	0.06762
10.09	1752	1.700	26.04	165.7	0.06750
10.17	1751	1.699	26.06	164.9	0.06729
10.23	1751	1.700	26.09	164.4	0.06709
10.28	1750	1.700	26.08	164.0	0.06696
10.33	1750	1.700	26.11	163.5	0.06678
10.34	1750	1.700	26.10	163.4	0.06677
10.39	1749	1.700	26.11	163.0	0.06662
10.43	1749	1.699	26.12	162.7	0.06654
10.47	1748	1.700	26.13	162.3	0.06639
10.52	1748	1.700	26.14	161.9	0.06627
10.58	1747	1.700	26.15	161.3	0.06609

(continued on next page…)

Table 7.3: (continued)

BPR	TIT [K]	FPR	CPR	Fs [(N·s)/kg]	TSFC [kg/(N·h)]
10.63	1747	1.700	26.17	161.0	0.06598
10.68	1747	1.700	26.17	160.5	0.06582
10.73	1746	1.700	26.19	160.0	0.06569
10.79	1746	1.700	26.19	159.5	0.06553
10.91	1744	1.700	26.23	158.5	0.06521
10.98	1744	1.699	26.24	157.9	0.06506
11.05	1743	1.700	26.25	157.4	0.06484
11.06	1743	1.700	26.24	157.3	0.06483
11.14	1742	1.700	26.28	156.6	0.06462
11.23	1741	1.700	26.29	155.9	0.06440
11.33	1740	1.700	26.31	155.0	0.06415
11.39	1740	1.698	26.32	154.5	0.06405
11.51	1739	1.700	26.34	153.6	0.06372
11.61	1738	1.700	26.36	152.8	0.06351
11.67	1737	1.695	26.39	152.0	0.06350
11.74	1737	1.700	26.40	151.8	0.06321
11.79	1736	1.698	26.40	151.3	0.06315
11.84	1736	1.700	26.41	151.0	0.06299
12.17	1733	1.700	26.49	148.4	0.06228

(continued on next page…)

Table 7.3: (continued)

BPR	TIT [K]	FPR	CPR	Fs [(N·s)/kg]	TSFC [kg/(N·h)]
12.21	1732	1.700	26.50	148.0	0.06220
12.26	1732	1.699	26.51	147.7	0.06212
12.40	1731	1.700	26.53	146.6	0.06183
12.50	1730	1.699	26.55	145.8	0.06165
12.55	1729	1.699	26.56	145.4	0.06155
12.69	1728	1.700	26.62	144.4	0.06129
12.85	1727	1.700	26.64	143.1	0.06100
12.89	1726	1.700	26.63	142.8	0.06095
12.96	1725	1.699	26.65	142.2	0.06085
12.98	1725	1.700	26.65	142.1	0.06079
13.06	1725	1.700	26.68	141.5	0.06067
13.16	1724	1.700	26.71	140.7	0.06051
13.22	1723	1.700	26.72	140.2	0.06042
13.27	1723	1.700	26.73	139.8	0.06035
13.34	1722	1.700	26.75	139.3	0.06025
13.45	1721	1.700	26.75	138.5	0.06011
13.54	1720	1.700	26.81	137.8	0.05998
13.64	1719	1.699	26.80	137.0	0.05987
13.70	1719	1.700	26.83	136.5	0.05977

(continued on next page…)

Table 7.3: (continued)

BPR	TIT [K]	FPR	CPR	Fs [(N·s)/kg]	TSFC [kg/(N·h)]
13.78	1718	1.700	26.83	135.9	0.05969
13.85	1717	1.700	26.83	135.4	0.05961
13.88	1717	1.700	26.84	135.1	0.05957
13.95	1716	1.700	26.86	134.6	0.05950
14.03	1716	1.700	26.87	133.9	0.05941
14.09	1715	1.700	26.89	133.4	0.05936
14.26	1713	1.700	26.96	132.1	0.05919
14.30	1713	1.700	26.93	131.8	0.05918
14.39	1712	1.700	26.92	131.1	0.05909
14.44	1712	1.698	26.98	130.7	0.05907
14.49	1711	1.700	26.96	130.3	0.05900
14.53	1711	1.700	26.99	130.0	0.05896
14.56	1711	1.700	27.00	129.8	0.05894
14.67	1710	1.700	27.02	128.9	0.05886
14.75	1709	1.700	27.04	128.2	0.05880
14.82	1708	1.700	27.03	127.7	0.05877
14.88	1708	1.700	27.04	127.3	0.05874
14.95	1707	1.700	27.04	126.6	0.05871
15.00	1706	1.700	27.06	126.2	0.05868

The Pareto front corresponding to these results is showed in Figure 7.4, accompanied with the tendency line.

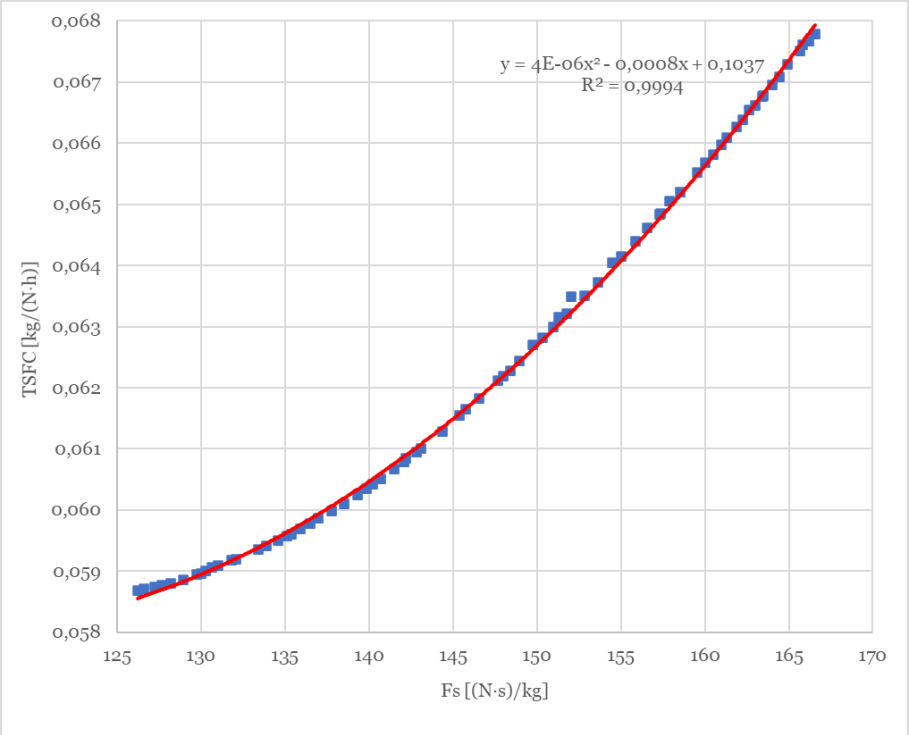

Figure 7.4: Variation of TSFC with Fs for the GTF with Intercooler (Pareto front results).

This choice of values by the algorithm met the tendency shown in the parametric study, i.e., to maximise the specific thrust, the algorithm chose high values of TIT and FPR and CPR, and low values of BPR. Whereas to minimise the TSFC, the BPR, the FPR and the CPR achieved high values and the TIT lower values.

7.4.3 GTF with Regenerator

Table 7.4 shows the values of the independent variables that optimise the chosen performance parameters for the configuration with regeneration.

Table 7.4: Pareto front results for the GTF with Regenerator.

BPR	TIT [K]	FPR	CPR	Fs [(N·s)/kg]	TSFC [kg/(N·h)]
10.00	1830	1.700	22.72	161.4	0.06181
10.00	1830	1.700	22.59	161.4	0.06179
10.07	1831	1.696	22.39	160.6	0.06169
10.08	1831	1.699	22.51	160.8	0.06167
10.15	1833	1.699	21.66	160.2	0.06144
10.21	1833	1.699	21.66	159.8	0.06136
10.27	1833	1.699	21.79	159.4	0.06130
10.46	1832	1.699	21.81	158.0	0.06106
10.55	1833	1.699	21.61	157.5	0.06092
10.62	1832	1.698	21.87	157.0	0.06089
10.70	1833	1.698	21.39	156.4	0.06072
10.74	1832	1.698	20.43	155.9	0.06052
10.82	1835	1.696	20.12	155.3	0.06039
10.89	1835	1.696	20.12	154.9	0.06032
10.95	1835	1.696	20.12	154.5	0.06025
11.06	1834	1.695	20.26	153.7	0.06015
11.06	1834	1.696	20.46	153.9	0.06017
11.15	1835	1.694	20.07	153.1	0.06004
11.18	1835	1.697	21.00	153.3	0.06014

(continued on next page…)

Table 7.4: (continued)

BPR	TIT [K]	FPR	CPR	Fs [(N·s)/kg]	TSFC [kg/(N·h)]
11.32	1835	1.696	20.37	152.2	0.05991
11.47	1835	1.691	20.00	150.9	0.05973
11.79	1835	1.691	20.19	149.0	0.05948
12.01	1830	1.675	20.35	146.4	0.05940
12.07	1831	1.690	20.41	147.0	0.05934
12.15	1837	1.683	20.56	146.5	0.05928
12.31	1840	1.663	20.46	144.5	0.05918
12.44	1827	1.666	20.82	143.2	0.05920
12.68	1828	1.665	20.73	141.9	0.05903
12.88	1814	1.651	20.99	139.0	0.05906
13.08	1830	1.657	20.90	139.2	0.05884
13.09	1842	1.637	21.05	138.7	0.05878
13.17	1821	1.642	21.17	137.3	0.05888
13.20	1843	1.614	21.52	136.7	0.05886
13.45	1828	1.618	21.31	134.8	0.05872
13.57	1847	1.621	21.15	135.5	0.05852
13.86	1820	1.620	22.26	132.4	0.05876
14.18	1821	1.623	21.64	130.8	0.05856
14.54	1819	1.618	21.40	128.6	0.05845

(continued on next page…)

Table 7.4: (continued)

BPR	TIT [K]	FPR	CPR	Fs [(N·s)/kg]	TSFC [kg/(N·h)]
14.58	1816	1.607	22.17	127.7	0.05855
14.89	1829	1.626	21.84	127.8	0.05843

The Pareto front corresponding to these results is showed in Figure 7.5, accompanied with the tendency line.

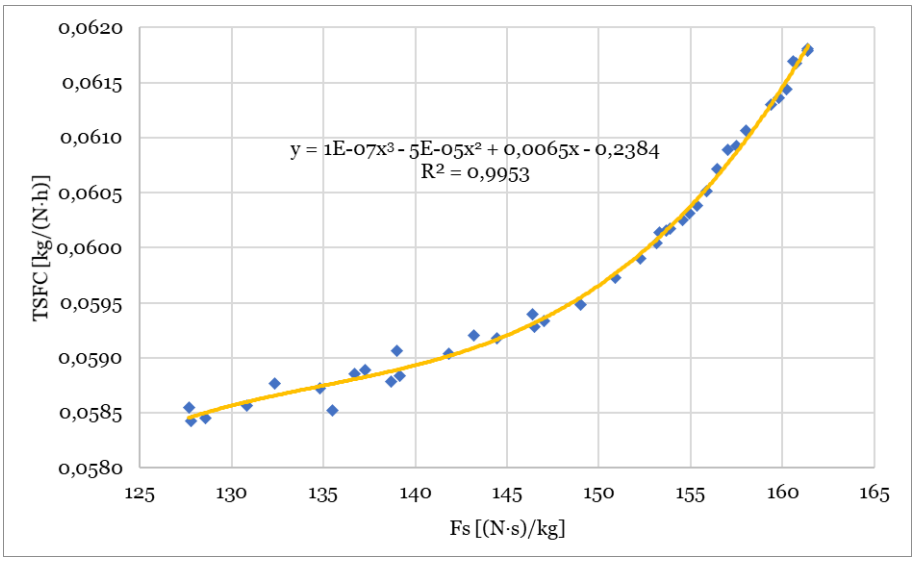

Figure 7.5: Variation of TSFC with Fs for the GTF with Regenerator (Pareto front results).

This choice of values by the algorithm met the tendency shown in the parametric study, i.e., to maximise the specific thrust, the algorithm chose high values of TIT and FPR, and low values of BPR and CPR. Whereas to minimise the TSFC, the BPR, the TIT and the FPR achieved high values and the CPR low values.

Moreover, this type of study proves that the regenerator operates better, i.e., exchanges more heat, at higher TIT values.

7.4.4 GTF with Intercooler and Regenerator

Table 7.5 shows the values of the independent variables that optimise the chosen performance parameters for the configuration with intercooling and regeneration.

Table 7.5: Pareto front results for the GTF with Intercooler and Regenerator.

BPR	TIT [K]	FPR	CPR	Fs [(N·s)/kg]	TSFC [kg/(N·h)]
10.00	1806	1.697	26.10	157.7	0.06238
10.15	1836	1.699	24.12	157.6	0.06221
10.15	1817	1.698	25.38	157.0	0.06217
10.22	1807	1.698	26.22	156.4	0.06207
10.34	1818	1.698	24.82	155.7	0.06188
10.40	1814	1.699	25.76	155.5	0.06182
10.43	1808	1.698	26.39	155.1	0.06179
10.48	1829	1.699	24.50	155.3	0.06171
10.55	1820	1.699	25.16	154.6	0.06161
10.65	1802	1.698	26.36	153.5	0.06149
10.70	1819	1.698	25.14	153.6	0.06144
10.81	1819	1.699	24.79	152.8	0.06127
10.87	1831	1.699	24.20	152.8	0.06122
10.98	1829	1.699	25.00	152.4	0.06110
11.04	1831	1.698	24.55	151.9	0.06104
11.11	1826	1.699	24.65	151.4	0.06094

(continued on next page…)

Table 7.5: (continued)

BPR	TIT [K]	FPR	CPR	Fs [(N·s)/kg]	TSFC [kg/(N·h)]
11.12	1839	1.699	23.20	151.4	0.06091
11.21	1835	1.699	23.98	151.0	0.06082
11.27	1839	1.699	23.88	150.7	0.06076
11.34	1834	1.700	23.59	150.0	0.06066
11.42	1838	1.698	23.53	149.6	0.06060
11.45	1832	1.699	24.00	149.4	0.06055
11.46	1823	1.698	24.38	149.0	0.06055
11.63	1838	1.699	22.99	148.3	0.06035
11.79	1836	1.699	23.34	147.4	0.06020
11.83	1839	1.698	23.14	147.2	0.06019
11.95	1834	1.697	23.49	146.3	0.06008
12.01	1841	1.699	23.06	146.3	0.06001
12.05	1834	1.699	23.83	146.0	0.05998
12.11	1836	1.698	23.30	145.6	0.05993
12.18	1850	1.696	21.75	145.0	0.05987
12.28	1831	1.698	23.95	144.5	0.05981
12.32	1826	1.700	23.65	144.1	0.05976
12.32	1839	1.700	22.75	144.4	0.05973
12.44	1840	1.697	22.57	143.6	0.05966

(continued on next page...)

Table 7.5: (continued)

BPR	TIT [K]	FPR	CPR	Fs [(N·s)/kg]	TSFC [kg/(N·h)]
12.47	1840	1.699	22.60	143.6	0.05962
12.60	1839	1.696	23.04	142.8	0.05956
12.69	1840	1.698	22.49	142.2	0.05947
12.79	1838	1.697	23.15	141.8	0.05943
12.97	1850	1.698	22.14	141.1	0.05927
13.01	1849	1.698	22.43	141.0	0.05925
13.07	1847	1.699	22.88	140.8	0.05922
13.07	1849	1.697	21.70	140.3	0.05921
13.23	1848	1.695	21.05	139.0	0.05913
13.28	1849	1.693	21.55	138.9	0.05911
13.30	1849	1.696	21.95	139.1	0.05909
13.53	1848	1.695	22.31	137.9	0.05900
13.60	1848	1.694	21.10	137.0	0.05896
13.73	1849	1.699	21.32	136.8	0.05889
13.82	1847	1.691	20.72	135.4	0.05889
13.91	1848	1.692	20.94	135.2	0.05886
14.16	1848	1.692	21.19	134.0	0.05878
14.18	1846	1.690	21.62	133.8	0.05880
14.31	1848	1.688	20.37	132.7	0.05876

(continued on next page…)

Table 7.5: (continued)

BPR	TIT [K]	FPR	CPR	Fs [(N·s)/kg]	TSFC [kg/(N·h)]
14.38	1848	1.685	20.45	132.1	0.05874
14.46	1847	1.683	20.22	131.4	0.05874
14.53	1846	1.673	20.06	130.3	0.05875
14.60	1846	1.676	20.82	130.4	0.05872
14.69	1846	1.679	20.67	130.1	0.05871

The Pareto front corresponding to these results is showed in Figure 7.6, accompanied with the tendency line.

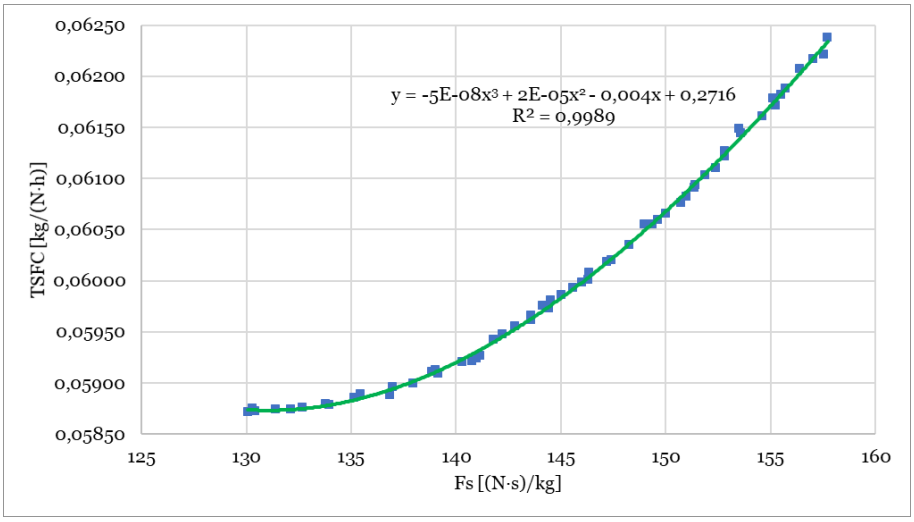

Figure 7.6: Variation of TSFC with Fs for the GTF with Intercooler and Regenerator (Pareto front results).

This choice of values by the algorithm met the tendency shown in the parametric study, i.e., to maximise the specific thrust, the algorithm chose high values of TIT, FPR and CPR, and low values of BPR. Whereas to minimise the TSFC, the BPR, the TIT and the FPR achieved high values and the CPR low values.

7.4.5 All configurations: TSFC vs Fs

Figure 7.7 shows the tendency lines of all the configurations.

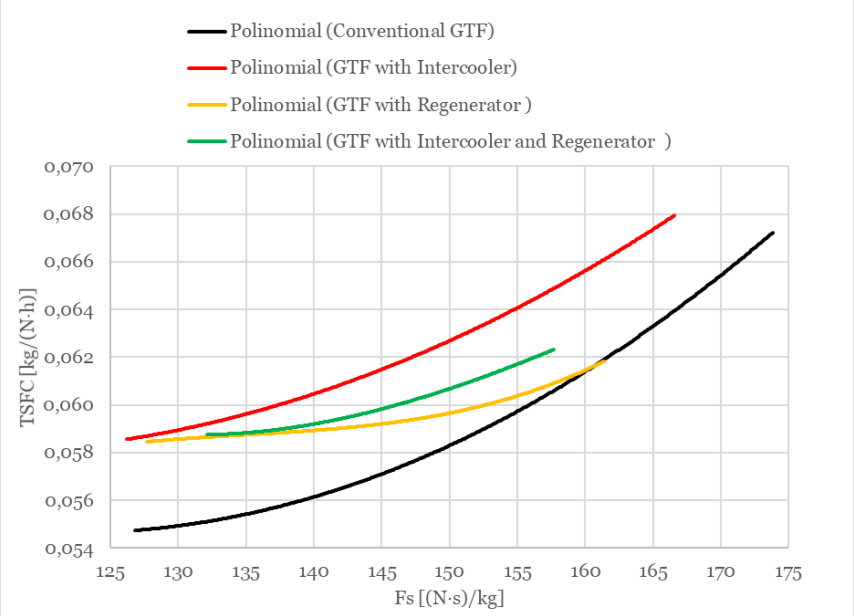

Figure 7.7: Variation of TSFC with Fs for all the configurations.

By plotting the tendency lines of all the configurations into the same graphic, it is possible to state that all of them show the same tendency: as the specific thrust rises so does the TSFC.

The conventional configuration and the one with the intercooler reveal a broader range of results, from 126.8 (N·s)/kg to 173.8 (N·s)/kg and from 126.2 (N·s)/kg to 166.5 (N·s)/kg, respectively. While the other two configurations have narrow intervals, which are inserted in the other intervals. Additionally, the configuration with both the heat exchangers has the smaller interval, which varies from 130.1 (N·s)/kg to 157.7 (N·s)/kg.

For the same amount of specific thrust the conventional configuration has the lowest TSFC values, except for a small interval (160– 161.4 (N·s)/kg), in which the results of this configuration coincide with the one that has a regenerator. Moreover, the configuration with the intercooler shows the highest values of TSFC for the entire interval, whereas the configuration with both the heat exchangers has the second highest TSFC values.

Chapter 8

Closure

In this final chapter, two different sections are presented. The first addresses the relevant conclusions from both the studies (parametrization and optimisation) and the viability, in terms of performance, of introducing heat exchangers into aero engines. The second section is dedicated to future work, where several suggestions are proposed.

8.1 Conclusions

This dissertation, firstly, carried out a parametric study using a modern geared turbofan engine, the PW1000G, which was adapted by incorporating two innovative components: intercooler and regenerator. In this sense, this study was composed of four configurations: conventional engine, engine with intercooler, engine with regenerator and engine with intercooler and regenerator. Furthermore, a comparison between all the configurations, in the cruise point, was conducted to understand how the performance parameters are affected by some project variables. More precisely, this parametric study compared the performance of the configurations in terms of specific thrust and thrust specific fuel consumption by varying some project parameters, which were: bypass ratio, fan pressure ratio, compressor pressure ratio and turbine inlet temperature.

In this study several parameters were considered constant or even unconsidered, such as bleed air, which means that the obtained results may not match the real ones, nevertheless they still provide viable conclusions.

Returning to the parametric study, the following conclusions, regarding the independent variables and its effect on the performance parameters, were extracted from the results:

- The turbine inlet temperature affects significantly the performance parameters of all the configurations, i.e. a rise in the turbine inlet temperature translates into an increase of both specific thrust and thrust specific fuel consumption;
- Lower bypass ratios favour higher specific thrust, whereas higher bypass ratios benefit lower thrust specific fuel consumption;

- As the fan pressure ratio increased, all configurations showed considerable improvements in the performance parameters. Nevertheless, the current tendency is for engines with lower fan pressure ratios, which produce less fan noise and allow higher bypass ratios;
- In comparison with the other independent variables, the compressor pressure ratio reveals a small influence on both the performance parameters of the configurations.

Now, looking at each configuration and the combination of independent variables that provide better performance results:

- The conventional engine operates better at higher turbine inlet temperatures, which translates into the configuration that produces more specific thrust and consumes less fuel than the intercooler configuration;
- At low turbine inlet temperature (1520 K), the intercooler configuration produces, in general terms, more specific thrust than all the other configurations, but with the sacrifice of having one of the highest values of thrust specific fuel consumption. Moreover, at higher turbine inlet temperatures (1850 K), this high TSFC is even more intensified, being undoubtedly the highest.
- The regenerator configuration can only operate at high turbine inlet temperatures or at low, but with low values of fan pressure ratio. Its advantages come to the surface at high turbine inlet temperature, and this configuration reveals better performance values, i.e., higher specific thrust and lower thrust specific fuel consumption than the configuration with both the heat exchangers.
- Although the intercooler and regenerator configuration can operate in both turbine inlet temperatures, this configuration does not bring any advantages in terms of performance parameters when compared with the other configurations.

This parametric study served to elucidate the author regarding which combinations of independent variables privileged certain performance parameters of each configuration. Moreover, it served as base for the next phase of this dissertation, the multi-objective optimisation, which used a genetic algorithm and the Pareto front to obtain the results.

The optimisation had the purpose of minimising the thrust specific fuel consumption and maximising the specific thrust, while varying the same independent variables used in the first study. The algorithm generated a series of successive generations, and at each generation the configurations were closer to the optimum results. Eventually, the algorithm met the stopping criteria, and the final Pareto front results were obtained. These results

gave several optimised combinations. Some of them privileged the specific thrust, while others the thrust specific fuel consumption or even both. In general terms, the results were well distributed and there was, within the boundaries, a wide variety of combinations.

From the optimisation study, the following conclusions can be drawn:

- The introduction of an intercooler on a geared turbofan does not seem viable, because not only the conventional engine can produce the same amount of specific thrust, but also at the expense of less fuel consumed;
- The conventional configuration presents as the best choice, because not only it can operate at a wider range, but also it consumes less fuel than the other configurations for a given specific thrust.

The intercooler configuration was able to produce more specific thrust than the other configurations at lower turbine inlet temperatures and at this condition the components are under less thermal stress, which allows extended periods of use without maintenance. In this sense, the intercooler is more of a viable option in industrial gas turbines than in aero engines, because they are more concerned in power production and maintenance costs than in fuel costs.

Bearing in mind the operating conditions and the defined boundaries for the independent variables, in which this study was conducted, the conventional configuration is the one with lowest thrust specific fuel consumption values for a given specific thrust. Therefore, there is no need of adding a regenerator. However, if the turbine inlet temperature were to increase, the regenerator effect would be more pronounced and perhaps it would present better values of TSFC than the conventional configuration. Nevertheless, the use of extremely high turbine inlet temperatures results in costlier turbines (production and maintenance costs) and in NO_X emissions increase.

8.2 Future Work

The first suggestion is to complement this work with the introduction of an inter turbine burner and study its viability in commercial aircrafts.

With access to more engine data, such as bleed air and maximum rotational speeds of each spool, a different method or software (for example Gas Turb) could be used that would be more accurate and would show the true benefits of using a geared turbofan. However, unfortunately, these kinds of information are not disclosed to the public.

In future works, the integration aspects (weight and drag), emissions and costs of using heat exchangers should be included to provide a more realistic and detailed quantification of the effect of these two on the aircraft.

Finally, since this study was limited to only a flight condition, cruise point, it would be interesting to extend this study to a broader range of operating conditions, for example, take-off point, or even an aircraft mission, which encompasses several flight phases.

Bibliography

[1] A. F. El-Sayed, "Aircraft Propulsion and Gas Turbine Engines," *CRC Pres Taylor & Francis Group*, 2nd edition, 2017.

[2] National Aeronautics and Space Administration (NASA), "Quest for Performance: The Evolution of Modern Aircraft," [Online]. Available: https://history.nasa.gov/SP-468/ch10-3.htm [Accessed: 24-Mar.-2021].

[3] ICAO Secretariat, "Aircraft Technology Improvements," *ICAO Environmental Report*, vol. 53, no. 9, pp. 1689–1699, 2010.

[4] P. Gloeckner, and C. Rodway, "The Evolution of Reliability and Efficiency of Aerospace Bearing Systems," *Engineering*, vol. 09, no. 11, pp. 962–991, 2017, doi: 10.4236/eng.2017.911058.

[5] I. Takagi, T. Ando, and S. Suzuki, "Development of Trent Series Large Turbo Fan Engines," *Kawasaki Technical Review,* no.179, 2018.

[6] D. Dewanji, A. G. Rao, and J. P. Van Buijtenen, "Conceptual study of future aero-engine concepts," *Int. J. Turbo Jet Engines*, vol. 26, no. 4, pp. 263–276, 2009, doi: 10.1515/TJJ.2009.26.4.263.

[7] K. G. Kyprianidis, T. Grönstedt, S. O. T. Ogaji, P. Pilidis, and R. Singh, "Assessment of future aero-engine designs with intercooled and intercooled recuperated cores," *J. Eng. Gas Turbines Power*, vol. 133, no. 1, 2011, doi: 10.1115/1.4001982.

[8] W. Lu, G. Huang, X. Xiang, J. Wang, and Y. Yang, "Thermodynamic and aerodynamic analysis of an air-driven fan system in low-cost high-bypass-ratio turbofan engine," *Energies*, vol. 12, no. 10, 2019, doi: 10.3390/en12101917.

[9] D. Giesecke, M. Lehmler, J. Friedrichs, J. Blinstrub, L. Bertsch, and W. Heinze, "Evaluation of ultra-high bypass ratio engines for an over-wing aircraft configuration," *J. Glob. Power Propuls. Soc.*, vol. 2, pp. 493–515, 2018, doi: 10.22261/jgpps.8shp7k.

[10] W. Humhauser, W. Waschka, M. Metscher, and A. Michel, "ATFI-HDV : Design of a new 7 stage innovative compressor for 10 – 18 klbf thrust," *ISABE-2005-1266*, pp. 1–9, 2005.

[11] L. Larsson, R. Avellán, and T. Grönstedt, "Mission optimisation of the geared turbofan engine," *ISABE-2011-1314*, 2011.

[12] M. D. Guynn, J. J. Berton, K. L. Fisher, W. J. Haller, M. T. Tong, and D. R. Thurman, "Analysis of turbofan design options for an advanced single-aisle transport aircraft," *9th AIAA Aviat. Technol. Integr. Oper. Conf. Aircr. Noise Emiss. Reduct. Symp.*, no. September, 2009, doi: 10.2514/6.2009-6942.

[13] J. Kurzke, "Fundamental differences between conventional and geared turbofans," *Proc. ASME Turbo Expo*, vol. 1, pp. 145–153, 2009, doi: 10.1115/GT2009-59745.

[14] L. Larsson, T. Grönstedt, and K. G. Kyprianidis, "Conceptual design and mission analysis for a geared turbofan and an open rotor configuration," *Proc. ASME Turbo Expo*, vol. 1, no. January, pp. 359–370, 2011, doi: 10.1115/GT2011-46451.

[15] K. G. Kyprianidis, R. F. C. Quintero, D. S. Pascovici, S. O. T. Ogaji, P. Pilidis, and A. I. Kalfas, "Eva - A tool for environmental assessment of novel propulsion cycles," *Proc. ASME Turbo Expo*, vol. 2, pp. 547–556, 2008, doi: 10.1115/GT2008-50602.

[16] R. Becker, M. Schaefer, S. Reitenbach, and L. Hoehe, "Assessment of the efficiency gains introduced by novel aero engine concepts," *Am. Inst. Aeronaut. Astronaut.*, pp. 1–10, 2013.

[17] C. Kjelgaard, " Gearing up for the GTF," *Aircraft Technology: Regional Persperctive*, Issue 105, 2010, [Online]. Available: https://www.yumpu.com/en/document/read/7313134/quality-purepowerr-pw1000g-engine/04%20%C3%80s%2010:58 [Accessed: 30-Apr.-2021].

[18] R. Andriani and U. Ghezzi, "Performances analysis of high by pass jet engine with intercooling and regeneration," *45th AIAA/ASME/SAE/ASEE Jt. Propuls. Conf. Exhib.*, no. August, pp. 1–8, 2009, doi: 10.2514/6.2009-4800.

[19] J. Lebre and F. Brójo, "Performance of a turbofan engine with intercooling and regeneration," *World Acad. Sci. Eng. Technol.*, vol. 78, no. March, pp. 359–363, 2011, doi: 10.5281/zenodo.1332144.

[20] F. Colmenares, D. Pascovici, S. Ogaji, and P. Pilidis, "A preliminary parametric study for geared, intercooled and/or recuperated turbofan for short range civil aircrafts," *Proc. ASME Turbo Expo*, vol. 3, pp. 95–102, 2007, doi: 10.1115/GT2007-27234.

[21] C. Salpingidou, D. Misirlis, Z. Vlahostergios, M. Flouros, F. Donus, and K. Yakinthos, "Conceptual design study of a geared turbofan and an open rotor aero engine with intercooled recuperated core," *Proc. Inst. Mech. Eng. Part G J. Aerosp. Eng.*, vol. 232, no. 14, pp. 2713–2720, 2018, doi: 10.1177/0954410018770883.

[22] European Commission, "Flightpath 2050, Europe's Vision for Aviation," Report of the High Level Group on Aviation Research, Publications Office of the European Union, 2011, [Online]. Available: https://ec.europa.eu/transport/sites/transport/files/modes/air/doc/flightpath2050.pdf [Accessed: 19-May- 2021].

[23] European Commission, "Environmentally Friendly Aero-Engine," *VITAL Project*, 2005, [Online]. Available: https://trimis.ec.europa.eu/project/environmentally-friendly-aero-engine#tab-outline [Accessed: 13-May-2021].

[24] European Commission, "NEW Aero Engine Core concepts," *CORDIS EU research results*, 2012, [Online]. Available: https://cordis.europa.eu/project/id/30876 [Accessed: 13-May-2021].

[25] European Commission, "Sustainable and Green Engine (SAGE), "*Clean Sky,* [Online]. Available: https://www.cleansky.eu/sustainable-and-green-engine-sage [Accessed: 19-May-2021].

[26] MTU Aero Engines, "Research and development," *Technologies*, 2011, [Online]. Available: https://www.mtu.de/technologies/research-and-development/technology-funding-programs [Accessed: 26-May-2021].

[27] European Commission, "Engines," *Clean Sky*, [Online]. Available: https://www.cleansky.eu/engines [Accessed: 19-May-2021].

[28] H. Saravanamuttoo, G. Rogers, H. Cohen, P. Straznicky, and A. Nix, "Gas Turbine Theory," *Pearson Education Limited*, 7th edition, 2017.

[29] Siemens energy, "Reliable gas turbines, "*Power generation*, 2020, [Online]. Available: https://www.siemens-energy.com/global/en/offerings/power-generation/gas-turbines.html [Accessed: 27-May-2021].

[30] Y. Çengel, M. Boles, and M. KanoĞlu, "Thermodynamics: an engineering approach," *McGraw Hill Education*, 9th edition, 2019.

[31] National Aeronautics and Space Administration (NASA) – Edited by Nancy Hall, "Turbofan Engine," [Online]. Available: https://www.grc.nasa.gov/www/k-12/airplane/aturbf.html [Accessed: 27-May-2021].

[32] F. Romão, "Estudo paramétrico do motor Eurojet EJ200 para velocidades supersónicas e altas altitudes," *Master's Thesis, Aerospace Science Department, University of Beira Interioir,* 2018.

[33] U. Honegger, "Gas Turbine Combustion Modeling for a Parametric Emissions Monitoring System," *Master's Thesis, Mechanical and Nuclear Engineering Department, Kansas State University*, 2007.

[34] K. Hünecke, "Jet Engines: fundamentals of theory, design and operation," *Motorbooks International Publishers & Wholesalers*, 6th edition, 2003.

[35] A. Faghri, and Y. Zhang, "Transport Phenomena in Multiphase Systems," *Transp. Phenom. Multiph. Syst.*, pp. 1–1030, 2006, doi: 10.1007/978-3-319-91062-8.

[36] A. Epstein, " The Pratt & Whitney PurePower Geared Turbofan Engine," *Academie de l'Air et de l'Espace*, 2015, [Online]. Available: https://academieairespace.com/wp-content/uploads/2018/05/prattw.pdf [Accessed: 22-July-2021].

[37] F. Oliveira, and F. Brójo, "Multi - Objective Optimisation of a Conventional and Regenerated UHB Turbofan," *American Institute of Aeronautics and Astronautics*, 2014.

[38] Pratt & Whitney, "PurePower Family of Engines," 2015, [Online]. Available: https://www.yumpu.com/en/document/read/7312901/purepowerr-family-of-engines-purepowerr-pw1000g-engine [Accessed: 23-July-2021].

[39] S. Atsushi, I. Mitsuo, and F. Tetsuji, "Development of PW1100G-JM Turbofan Engine," *IHI Eng. Rev.*, vol. 47, no. 1, pp. 23–28, 2014, [Online]. Available: https://www.ihi.co.jp/var/ezwebin_site/storage/original/application/b2153d6b4a59e36870a3c642bd26d313.pdf. [Accessed: 23-July-2021].

[40] MTU Aero Engines, "PurePower PW1000G Engine," *Product Leaflet PW1000G*, 2014, [Online]. Available: https://www.mtu.de/fileadmin/EN/2_Engines/1_Civil_Aircraft_Engines/2_Narro

wbody_and_Regional_Jets/PW1000G/Product_Leaflet_PW1000G.pdf [Accessed: 26-July-2021].

[41] Pratt & Whitney, "PRATT & WHITNEY GTF ENGINE FAST FACTS," 2021, [Online]. Available: https://pwgtf.com/-/media/project/pw/pw-internet/commercial-aircraft/gtf-engine/gtf-site/pdf/gtf_fastfacts_2021_06-june.pdf?rev=02af07944b854df5aedf455e76c10dde&hash=9385C48E1EE76F3250F16DDE6B541DB1 [Accessed: 27-July-2021].

[42] Pratt & Whitney, "PRATT & WHITNEY GTF ENGINE," 2020, [Online]. Available: https://prattwhitney.com/products-and-services/products/commercial-engines/pratt-and-whitney-gtf [Accessed: 27-July-2021].

[43] European Union Aviation Safety Agency, "TYPE-CERTIFICATE DATA SHEET No. IM.E.093 for PW1100G-JM Series Engines," no. December, pp. 1–12, 2019.

[44] F. Oliveira and F. Brójo, "Parameterization of a Conventional and Regenerated UHB Turbofan," *Open Eng.*, vol. 5, no. 1, pp. 349–359, 2015, doi: 10.1515/eng-2015-0030.

[45] D. R. Clarke, M. Oechsner, and N. P. Padture, "Thermal-barrier coatings for more efficient gas-turbine engines," *MRS Bull.*, vol. 37, no. 10, pp. 891–898, 2012, doi: 10.1557/mrs.2012.232.

[46] Rolls Royce, " Pioneering intelligent innovation for our customers," 2021, [Online]. Available: https://www.rolls-royce.com/products-and-services/civil-aerospace/future-products.aspx#section-related-stories [Accessed: 10-Aug.-2021].

[47] National Aeronautics and Space Administration (NASA) – Edited by Nancy Hall, "Turbofan Engine," 2021, [Online]. Available: https://www.grc.nasa.gov/www/k-12/airplane/specth.html [Accessed: 10-Aug.-2021].

[48] F. Yin and A. Gangoli Rao, "Performance analysis of an aero engine with inter-stage turbine burner," *Aeronaut. J.*, vol. 121, no. 1245, pp. 1605–1626, 2017, doi: 10.1017/aer.2017.93.

[49] W. Pedrycz, A. Sillitti, and G. Succi, "Computational intelligence: An introduction," *Studies in Computational Intelligence*, vol. 617. pp. 13–31, 2016, doi: 10.1007/978-3-319-25964-2_2.

[50] MathWorks, "Genetic Algorithm," *Matlab Library*, 2021, [Online]. Available:

https://www.mathworks.com/discovery/genetic-algorithm.html [Accessed: 26-Aug.2021].

[51] C. A. García Montoya and S. Mendoza Toro, "Implementation of an evolutionary algorithm in planning investment in a power distribution system," *Ing. e Investig.*, vol. 31, no. 2, pp. 118–124, 2011.

[52] MathWorks, "Genetic Algorithm," *Matlab Library*, 2021, [Online]. Available: https://www.mathworks.com/help/gads/gamultiobj.html [Accessed: 28-Aug.-2021].